ARCHIVES OF ACOUSTICS
19, 3, 311–321 (1994)

LOUD MUSIC INDUCED THRESHOLDS SHIFTS AND DAMAGE RISK PREDICTION

A. JAROSZEWSKI and A. RAKOWSKI

Frederic Chopin Academy of Music
(00-368 Warszawa ul. Okólnik 2)

Temporary thresholds shifts in musicians using high power electronic equipment were measured immediately after performance. The danger of permanent hearing loss is predicted on the ground of Damage Risk Criteria.

1. Introduction

The danger of hearing loss in musicians exposed to high sound pressure levels produced by electronic equipment, has been discussed over the past three decades, not only in scientific papers [2, 3, 6, 7, 9, 11, 16, 17, 20, 21, 26, 27, 28, 31, 32, 33, 34, 37, 38, 39, 40, 48] but also in popular literature [19] and in news articles [1, 15]. However, the results of acoustical measurements, and the conclusions of various investigations are not in agreement with respect to the distribution of sound pressure levels with frequency and to the degree to which such exposures are dangerous.

RINTELMANN and BORUS [33] determined the octave band distributions of sound pressure levels in 44 musical selections performed by 6 American rock-and-roll groups. The overall sound pressure level amounted to 105 dB with the range from about 91 to 111 dB. The sound pressure levels in the octave bands between 63 Hz and 2.0 kHz were practically constant at 95–100 dB, and decreased to about 75 dB at 31 Hz and 8.0 kHz, respectively. According to the so-called Damage Risk Criteria (DRC) [4, 6, 7, 22] prolonged exposures to noise at approximately these sound pressure levels are recognized as leading to permanent hearing loss. However, audiometric tests in the experimental group of 42 musicians did not display significant differences in hearing level with respect to the control group. The experimental group had but relatively short professional careers of 2.9 years duration on the average. KRYTER's [22] and KRYTER's *et al.* [23] data suggest that permanent hearing loss from exposure to noise at levels comparable to those reported by RINTELMANN and BORUS [33], is usually observed only after 10 years of service if the exposure is repeated 5 times a week.

It should be also observed that audiometric test data given in the mentioned report refer to permanent hearing loss, because the measurements were taken at least 48 hours

after the performance. In another report, RINTELMANN *et al.* [34] had 20 subjects listen for an hour to rock-and-roll music and investigated temporary threshold shifts after 2, 30, 60 and 90 min. from the termination of the exposure. From hearing recovery patterns, it was concluded that daily exposures over an extended period would be hazardous to hearing.

FLUGRATH [15] measured the distribution of sound pressure levels in four octave bands for 10 music groups. In all groups investigated, the highest sound pressure levels of about 100 dB were observed only within the octave bands centered at 1 and 2 kHz and decreased to about 90 dB in the 0.5 kHz and 4 kHz octave bands. Flugrath formulated his conclusions using the data by KRYTER [22] and KRYTER *et al.* [23] based substantially on investigations by WARD *et al.* [41, 42, 44, 45], CARTER and KRYTER [8] and KRYTER's *et al.* [23] and by BOTSFORD [4]. With reference to these data, Flugrath stated that at a sound pressure level of 102 dB in the 2 kHz octave band, the permissible daily exposure should not exceed 12 minutes. It is quite obvious that in normal practice the daily exposure is significantly larger and should be regarded as potentially dangerous.

JERGER and JERGER [20] reported observations of the temporary thresholds shift in musicians from two music groups. They were exposed to sounds at sound pressure levels of 110 to 120 dB within the 600–1200 Hz octave band over a period of 4 hours. In one of the groups investigated, 30 to 50 dB temporary threshold shifts were observed 1 hour after the exposure. In the second group (comparatively younger), all musicians had TTS's ranging from 15 to 30 dB in at least one ear. Referring to KRYTER'S [22, 23] data, the authors estimated the permissible daily exposures in similar situations at only 9 to 22 min. for the 300 to 600 Hz band and from 5 to 11 min. for the 600 to 1200 Hz band. It should be emphasized, that in one of the groups permanent hearing losses of 30–70 dB in at least one ear were found in three musicians. Jerger and Jerger measured TTS only 1 hour after the performance. The TTS immediately after exposure may have been as much as 30 dB higher (KRYTER [22, 23]).

It is very important to note that both KRYTER's [22, 23] and BOTSFORD's [4] data on permissible exposures are based on the measurements of the impairment of speech recognition by 10%. This criterion was determined for industry employers. With regard to musicians, however, its direct application may not be quite proper.

The purpose of this study was to determine the distribution of sound pressure levels in octave bands in a typical rock music performance in Poland, to measure temporary thresholds shifts in the performing musicians immediately after the exposure, and to evaluate the danger of hearing loss. Control audiometric measurements of hearing loss one year after the first measurements were made to find out if the impairment of hearing can be detected, inasmuch as it can be predicted from the results published by ROBINSON [35] and WARD [47].

2. Subjects

The group of musicians tested were four members of one of the recognized music groups, aged 22 to 29, all graduates of music schools. Two of them played two instruments, i.e. saxophone and flute, saxophone and piano, two others — percussion and bass guitar. The experience in musical performance with high power electronic equipment differed

among individuals from 2 to 8 years and averaged 3.5 years. Usually the group gave three performances a week, lasting about 4 hours each, including 10 min. break after each three music pieces. The total playing time of the group including public performance and rehearsal amounted to 20 hours weekly.

3. Sound pressure level measurements

The measurements of sound pressure levels were made at the students' club dance hall. Direct sound pressure level indications oscillated between 90 and 120 dB. A routine musical performance was recorded on magnetic tape. The microphone was placed 2 m above the floor at a distance 1.5 m from the orchestra on the geometrical axis of the hall. With this arrangement a reference signal (horn sound) was recorded at the beginning of each tape reel. The sound pressure level of this reference signal, measured directly at the microphone location was 120 dB SPL. Twelve musical selections representative of the performance of the group were recorded. The material obtained was analyzed for the distributions of sound pressure levels in the successive octave bands.

4. The analysis of sound pressure distribution

The LTAS (Long Term Average Spectra) analysis revealed that the sound pressure levels over the separate musical selections were substantially constant except for the beginning fractions lasting about 5 to 15 sec. each. Therefore, only short samples from each of the records were selected for the analysis. The first 15 seconds from each record were discarded and the subsequent 50 seconds were used for LTAS analysis.

Sound pressure levels in the successive octave bands centered at 0.5, 1.0, 2.0 and 4.0 Hz, overall linear L, overall A and C weighted (Bruel and Kjaer) were computed. Median values for the sound pressure levels L, A, C and the maximum deviations of these values are presented in Fig. 1A.

Median values of the sound pressure levels referring to the maximum and to the mean sound pressure levels in separate octave bands and maximum deviations of these values are presented in Fig. 1B. Median values and maximum deviations of the mean sound pressure levels computed for 10 American musical groups after FLUGRATH [16] as well as data published by RINTELMANN and BORUS [33] and FEARN [13] are presented in the same figure for comparison.

It can easily be seen that sound levels produced by the music group used in the present investigation are within the limits determined by Flugrath except for the 0.5 kHz octave band. Even in this case, however, the difference is not substantial. In general, the group used in present investigations produced slightly higher- over-all sound pressure levels than those studied by Flugrath, but not so much different from the data of BOHNE *et al.* [3], FEARN [11, 12, 13] and LEBO and OLIFANT [26].

In all cases, sound pressure levels measured in this study for the rock music performances are higher than those permissible in industrial plants. According to BOTSFORD [4], the permissible daily exposure under the conditions presented in this analysis should not exceed 15 min. Thus, the daily dose of 4 hours exposure is 16 times larger than permissible.

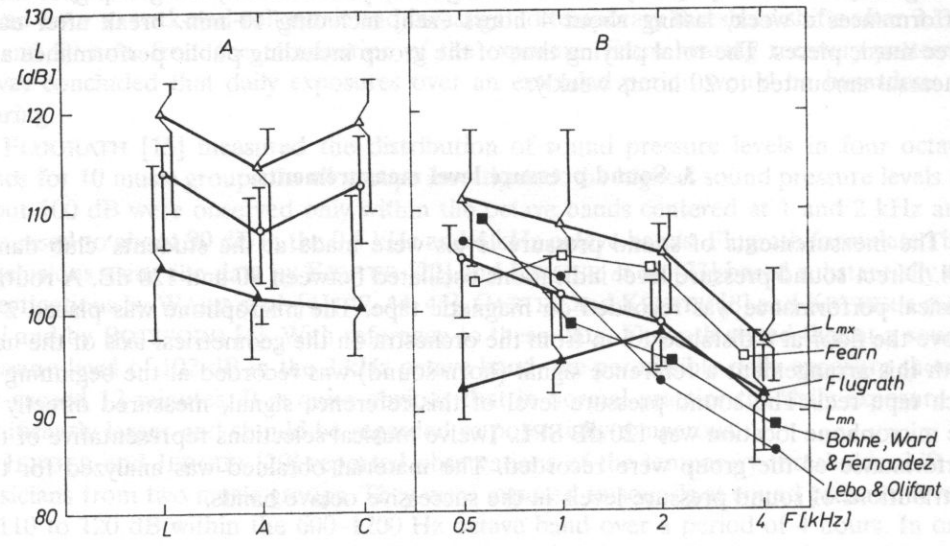

FIG. 1. A):. Median values and interquartiles of maximum (open triangles) and mean (open circles) sound pressure levels. Closed triangles — data from FLUGRATH. L-linear, A — A weighted, C — C weighted; B): Median values and interquartiles of maximum (L_{mx} — open triangles) and mean (L_{mn} — open circles) sound pressure levels in successive octave bands. Data from other authors indicated.

5. Hearing thresholds measurements

Threshold measurements in performers of rock music were made using a clinical audiometer at 10 frequencies within the range from 125 Hz to 100 kHZ. The audiometer was calibrated to audiometric zero level for the 18 to 25 years of age category.

The measurements were made 48 hours after the exposure (resting hearing level) and almost immediately after the exposure. Temporary thresholds shifts for the four musicians were determined as differences between resting hearing levels and hearing levels after 5, 9, 11 and 14 min. after termination of the exposure respectively. The determined values of TTS_t (TTS_5, TTS_9, TTS_{11} and TTS_{14}) were next used to find TTS_2 values (TTS that would be 2 min after the termination of the exposure). This procedure, introduced by KRYTER [22] and KRYTER *et al.* [23], is based on the time dependence of the magnitude of TTS which was investigated thoroughly by NIXON and GLORIG [29], KRYTER [22], BOTSFORD [4] and others.

The graphs in Figs. 2 to 5 present resting hearing levels measured and hearing levels two minutes after the exposure estimated. The difference of these two levels corresponds to the amount of TTS_2 i.e. temporary threshold shift 2 min after termination of the exposure.

Intersubjects median values of the temporary and permanent hearing losses and the maximum deviations of these values are presented in Figs. 6 and 7 for the right and left ears of all subjects. Median temporary thresholds shifts in Figs. 6 and 7 reach 30 dB at 1 kHz and slightly over 40 dB at 4 and 6 kHz for both ears. However, individual TTS_2

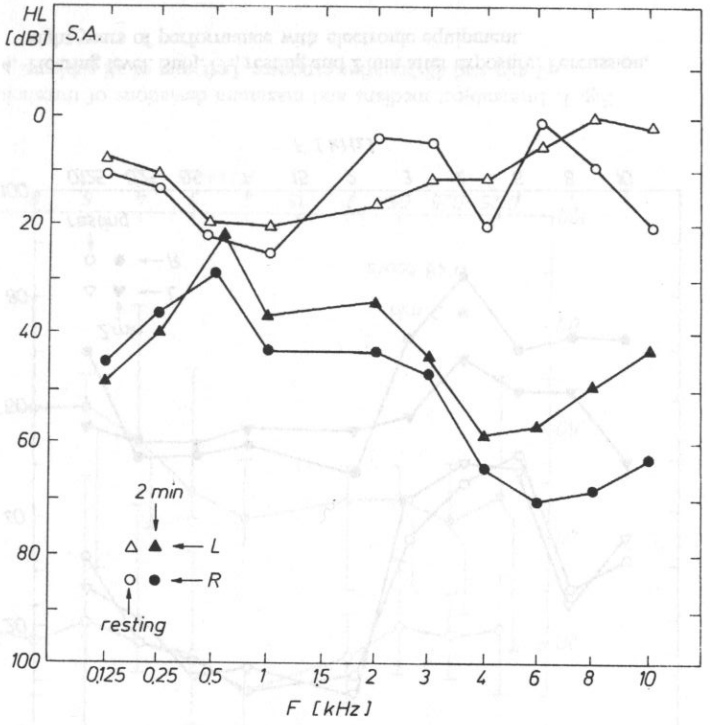

Fig. 2. Hearing level. Subj. *A*., resting and 2 min after exposure. Sax and flute, two years of performance with electronic equipment.

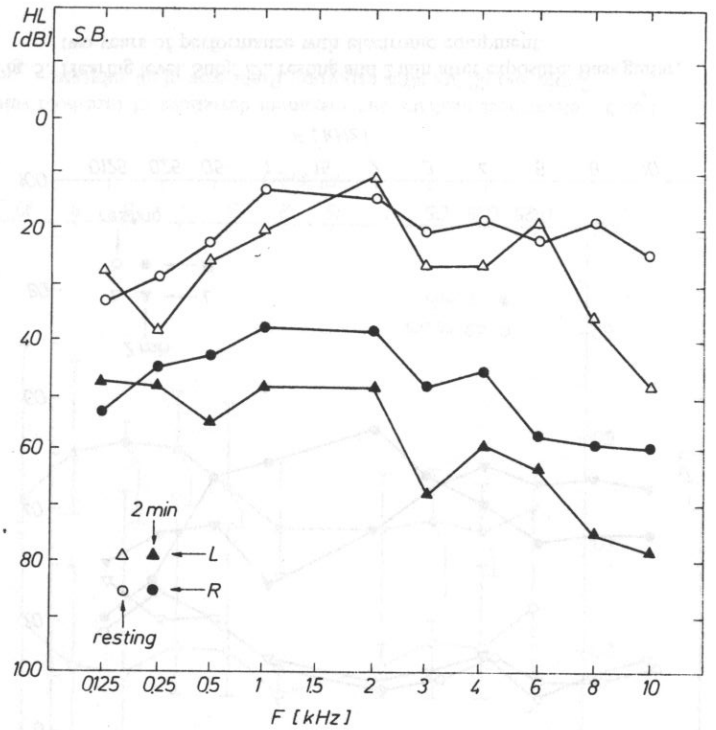

Fig. 3. Hearing level. Subj. *B*., resting and 2 min after exposure. Sax and piano, two years of performance with electronic equipment.

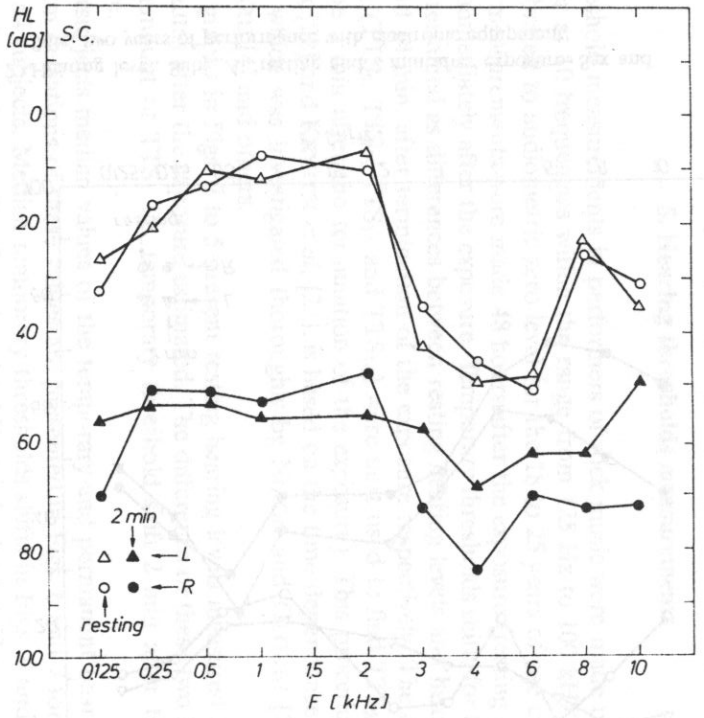

Fig. 4. Hearing level. Subj. $C.$, resting and 2 min after exposure. Percussion, eight years of performance with electronic equipment.

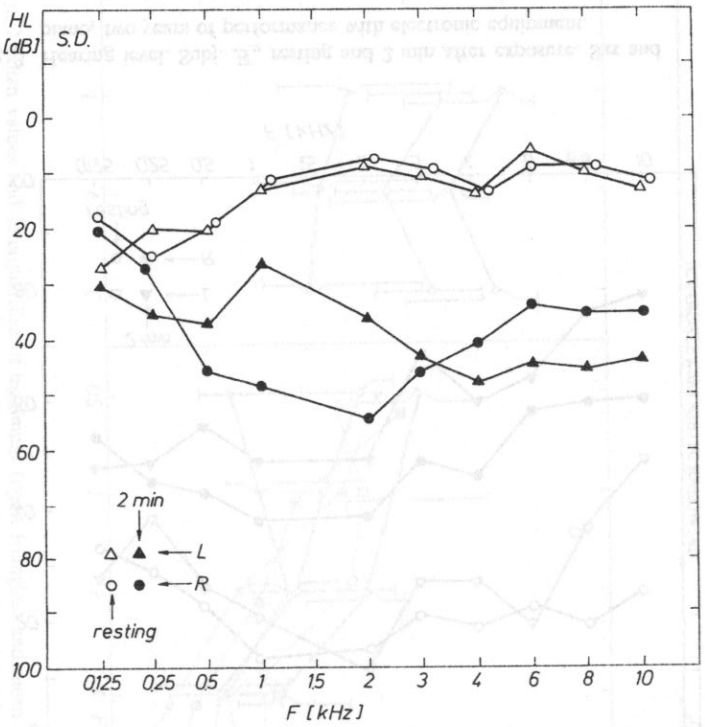

Fig. 5. Hearing level. Subj. $D.$, resting and 2 min after exposure. Bass guitar, two years of performance with electronic equipment.

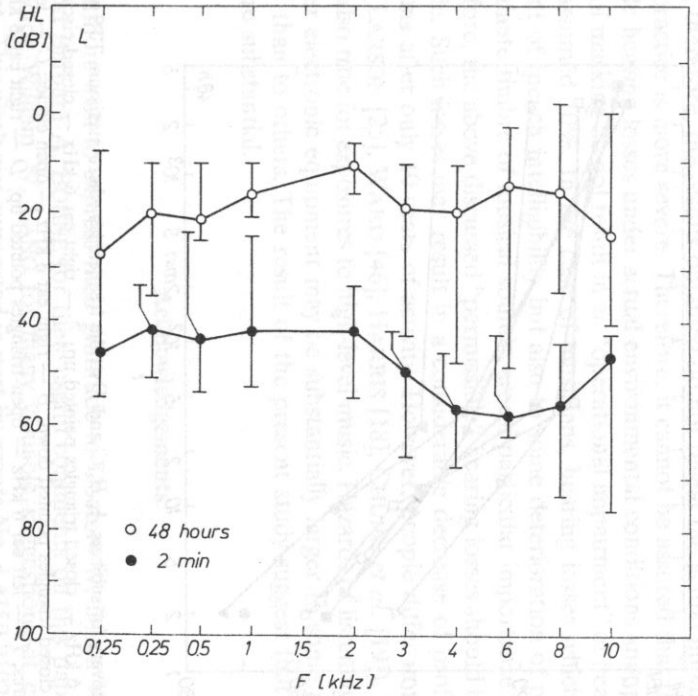

Fig. 6. Intersubject medians and maximum deviations of threshold values, 2 min and 48 hrs after exposure. Right ears of all subjects.

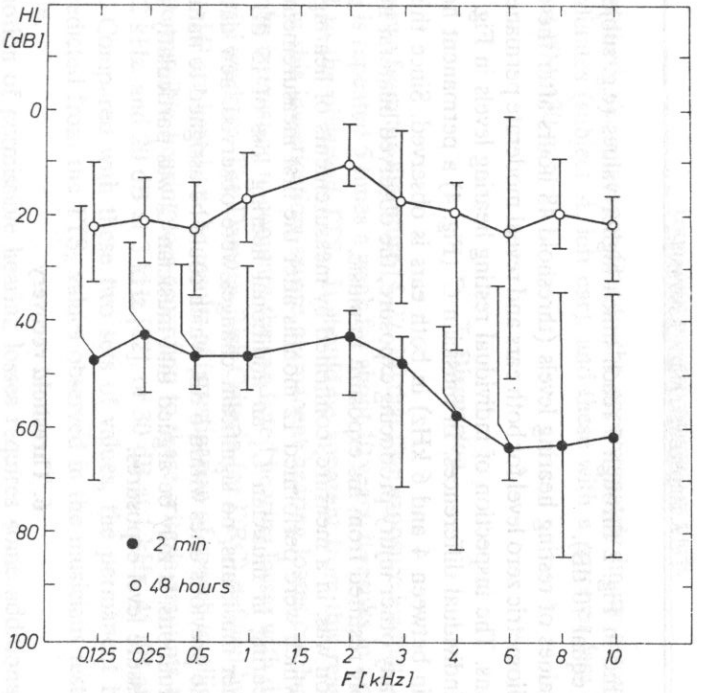

Fig. 7. Intersubject medians and maximum deviations of threshold values, 2 min and 48 hrs after exposure. Left ears of all subjects.

which may be found in Fig. 2 through 5 reach much higher values (e.g. subject A right ear, 6 kHz: TTS_2 equal 70 dB).

The median values of resting hearing levels (threshold 48 hours after the exposures) reach 20 dB reaudiometric zero level for both ears and reveal moderate permanent hearing loss in all musicians. The inspection of individual resting hearing levels in Fig. 2 through 5 shows marked individual differences. In musician C (Fig. 4) a permanent hearing loss of about 50 dB (in between 4 and 6 kHz) in both ears is observed. Since this musician had no record of any other injury-producing exposure, the observed bilateral hearing loss have most probably resulted from his exposure to music.

This supposition was, in a measure, confirmed by measurements of hearing threshold in all musicians, which were performed 12 months after the first measurements. Further impairment of hearing in musician C, an additional hearing loss of 15 dB at 2 kHz was found. In other musicians, no significant changes were observed, new data being in agreement with the previous ones within 6 dB, which could be assigned to natural resting hearing level fluctuations. It may be argued that musician C was particularly susceptible to high sound pressure level exposures.

6. Threshold recovery

The examination of threshold recovery (Fig. 8) shows that most of the recovery process takes place within about 30 min of the end of exposure. Two types of recovery curves can

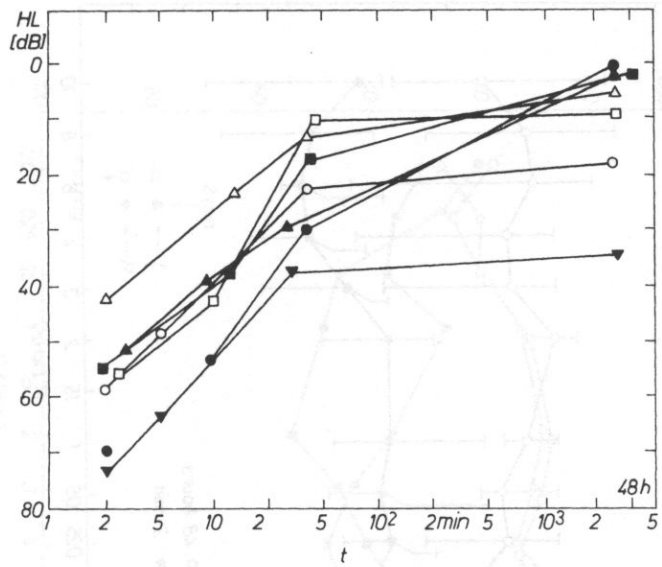

FIG. 8. Threshold recovery for subjects A, B, C and D at the frequencies where maximum TTS was observed. A — left ear 6 kHz — closed triangles pointed up, A — right ear 6 kHz — closed circles; B — left ear 8 kHz — closed triangles pointed down, B — right ear 8 kHz — open circles; C — left ear 2 kHz — open squares; D — left ear 6 kHz — open triangles pointed up, D — right ear 6 kHz — closed squares.

be distinguished, i.e. corresponding to the approximately linear recovery in logarithmic time coordinates (subject *A*, left ear), and these with a more or less distinct change of the slope at 20 to 30 min.

7. Discussion

It is known from the literature [4, 22, 29] that if an exposure leading to a given threshold shift TTS_2 is repeated 5 times a weak for about 10 years, it results in a permanent hearing loss equal to the observed TTS_2. It should be apparent from this reasoning that, in the musicians in this investigation, severe permanent hearing losses can be predicted.

It may be interesting to compare the predicted hearing losses with damage risk criteria for industrial workers. The Damage Risk Criteria (or DRC) defined by KRYTER [22] and BOTSFORD [4] are based on the results of investigation of speech intelligibility impairment by 10%. Permissible hearing loss according to these criteria amounts to 10 dB at 1 kHz, 15 dB at 2 kHz, and 20 dB at 3 kHz [22], or 30 dB at 1 kHz, 45 dB at 2 kHz and 60 dB at 3 kHz. Compared with these two sets of values, the permanent hearing losses that can be predicted from the TTS_2 values observed in the musicians tested are larger than permissible.

The notion of permissible hearing losses requires some additional consideration. It should be noted that no general agreement has been achieved concerning the sound pressure level at which a speech intelligibility test for establishing the DRC should be performed. Also, the speech intelligibility tests are often run without masking of any kind, and, therefore, the results obtained do not reveal the actual impairment of hearing, which in practice is more severe. Therefore, it cannot be assured that the above specified permissible hearing losses under actual environmental conditions and, particularly, in the presence of masking do not result in an "operational impairment" of hearing ability higher that the assumed 10%. In the case of musicians, hearing losses which lead only to the impairment of speech intelligibility but also to some deterioration of professional ability to discriminate timbre of musical sounds, are of particular importance.

Therefore, the above discussed "permissible" hearing losses should be regarded as not permissible. Such losses may result in a considerable decrease of professional efficiency in musicians after only 10 years of activity. However, people differ in their susceptibility to noise (LARSON [25], WARD [46], HARRIS [18], CHUNG *et al.* [19]). The same is most probably also true for exposures to high-level music. Hazards of listening to music through high-power electronic equipment may be substantially larger to some musicians e.g. one subject *C* than to others. The result of the present study suggest that in any case these hazards are substantial.

Acknowledgements

The authors wish to express their gratitude to Doctors W. Dixon WARD, William W. CLARC and Barbara A. BOHNE for their useful comments on this paper. Special thanks go to Doctor William W. LANG for many valuable suggestions at early stages of the experiment. This work was supported in part by grants No. 4 4159 9102 and 4 4075 92 03.

References

[1] Annon. Going deaf from rock'n'roll. Time 47, Aug. 9 (1968).

[2] A. AXELSSON and F. LINDGREN, *Hearing in classical musician*, Acta Oto-laryngological, Supplement 337 1981.

[3] B.A. BOHNE, P.H. WARD and C. FERNANDEZ, *Irreversible inner ear damage from rock music*, Trans. Amer. Acad. Phtalm. Otolaryng., 50–59 (1976).

[4] J.H. BOTSFORD, *Simple method for identifying acceptable noise exposure*, J. Acoust. Soc. Amer., **42**, 810–819 (1967).

[5] J.H. BOTSFORD, *Theory of temporary threshold shift*, J. Acoust. Soc. Amer., **49**, 440–446 (1971).

[6] A. BURD, *Hearing damage from music -UK experience*, J. Audio Eng. Soc., Sept. 1974.

[7] W. BURNS and D.D. ROBINSON, *Hearing and noise in industry*, HMSO 1970.

[8] R. CARTER and K.D. KRYTER, *Equinoxius contours for pure tones and some data on the critical band for TTS*, Bolt Beranek and Newman Inc., Rept. No 948 (1960).

[9] D.Y. CHUNG, G.N. WILLSON, R.P. GANNON and K. MASON, *Individual susceptibility to noise*, in: R.P. Hamernick, D. Henderson and R. Salvi Eds, New perspectives on noise-induced hearing loss, Raven Press, New York 1982.

[10] H. DAVIS, G.T. MORGAN, J.E. HAWKINS, R. GALAMBOS and F.W. SMITH, *Temporary deafness following exposure to loud tones and noise*, Acta Oto-Laryngol., Suppl. 88 (1950).

[11] R.W. FEARN, *Noise level in youths clubs*, J. Sound Vib., **22**, 126–128 (1972).

[12] R.W. FEARN, *Pop music and hearing damage*, J. Sound Vib., **29**, 396–397 (1973).

[13] R.W. FEARN, *Level limits on pop music*, J. Sound Vib., **38**, 501–502 (1975).

[14] R.W. FEARN, *Level measurements of music*, J. Sound Vib., **43**, 588–591 (1975).

[15] J.M. FLUGRATH, *Modern-day rock-and-roll music and damage risk criteria*, J. Accoust. Soc. Amer., **45**, 704–711 (1969).

[16] J.M. FLUGRATH, *Temporary threshold shift and permanent threshold shift due to rock-and-roll music*, J. Acoust. Soc. Amer., **51**, 151A (1972).

[17] H.J.H. FRY, *Overuse syndrome in musicians — 100 years ago: an historical review*, The Medical Journal of Australia, **145**, 620–625 (1986).

[18] J.D. HARRIS, *Hearing loss trend curves and the damage-risk criterion in Diesel-engineering personnel*, J. Acoust. Soc. Amer., **37**, 444–452 (1965).

[19] A. HOPE, *Hearing damage*, Studio Sound, Aug. **48** (1975).

[20] S. JERGER and J. JERGER, *Temporary threshold shift in rock-and-roll musicians*, J. Speech Hear. Res., **13**, 221–224 (1970).

[21] D.W. JOHANSON, R.E. SHERMAN, J. ALDRIGE and A. LORAINE, *Effects of instrument type and orchestral position on hearing sensitivity for* 0.25 *to* 20 kHz *in the orchestral musician*, Scandinavian Audiology, **14**, 215–221 (1985).

[22] K.D. KRYTER, *Exposure to steady-state noise and impairment of hearing*, J. Acoust. Soc. Amer., **35**, 1515–1525 (1963).

[23] K.D. KRYTER, W.D. WARD, J.D. MILLER and D.H. ELDREDGE, *Hazardous exposure to intermittent and steady-state noise*, J. Acoust. Soc. Amer., **39**, 451–464 (1966).

[24] K.D. KRYTER, *The effect of noise on man*, Academic Press, New York, London 1970.

[25] B. LARSEN, *Occupational deafness*, Acta Ot-Laryngol., **41**, 139–157 (1952).

[26] C.P. LEBO, K.S. OLIPHANT and J. GARRET, *Acoustic trauma from rock-and-roll music*, Calif. Med., **107**, 378–380 (1967).

[27] C.P. LEBO and K.S. OLIPHANT, *Music as a source of acoustic trauma*, Laryngoscope, **78**, 1211–1218 (1968).

[28] D.M. LIPSCOMB, *Ear damage from exposure to rock-and-roll music*, Arch. Otolaryng., **90**, 545–555 (1969).

[29] J.C. NIXON and A. GLORIG, *Noise-induced permanent threshold shift at* 2000 *cps and* 4000 *cps*, J. Acoust. Soc. Amer., **33**, 904–908 (1961).

[30] J.C. NIXON and A. GLORIG, *Noise-induced permanent threshold shift vs. hearing level in four industrial samples*, J. Audit. Res., **2**, 125–138 (1962).

[31] J. RABINOWITZ, R. HANSLER, G. BRISTOWN and P. RAY, *Study of the effects of loud music on musicians of the Suisse Romande Orchestra*, Journal de Medicine et Hygiene, **19**, 1909–1921 (1982).

[32] C.G. RICE, J.B. AYLEY, R. BARTLETT, W. BEDFORD, W. GREGORY and G. HALLAM, *A pilot study on the effects of pop group music on hearing*, J.S.U.R. Memo 266, Southampton: Univ. of Southampton Press (1968).

[33] W.F. RINTELMANN and J.F. BORUS, *Noise-induced hearing loss and rock-and-roll music*, Arch. Otolaryngol., **88**, 377–385 (1968).

[34] W.F. RINTELMANN, R.F. LINDBERG and E.K. SMITTEY, *Temporary threshold shift and recovery patterns from two types of rock-and-roll music presentation*, J. Acoust. Soc. Amer., **51**, 1249–1255 (1972).

[35] D.W. ROBINSON, *The relationship between hearing loss and noise exposure*, National Physical Lab. Report AC 32, Teddington, England (1968).

[36] G.T. SINGLETON, *Jet noise peak challneged by rock-and-roll*, Chicago Daily News, 22, March 12 (1968).

[37] E. SMITLEY and W.F. RINTELMANN, *Effect at continuous versus intemittent exposure to rock-and-roll music upon temporary threshold shift*, Arch. Envir. Health, **22**, 413–420 (1971).

[38] C. SPEAKS and D.A. NELSON, *TTS following exposure to rock-and-roll music*, J. Acoust. Soc. Amer., **45**, 342A (1969).

[39] C. SPEAKS, D.A. NELSON and W.D. WARD, *Hearing loss in rock-and-roll musicians*, J. Occup. Med., **12**, 216–219 (1970).

[40] R.F. ULRICH and M.L. PINHEIRO, *Temporary hearing loss in teen-agers attending repeated rock-and-roll sessions*, Acta Otolaryng., **77**, 51–55 (1974).

[41] W.D. WARD, A, GLORIG and D.L. SKLAR, *Dependence of temporary threshold shift at* 4 *kc on intensity and time*, J. Acoust. Soc. Amer., **30**, 944–954 (1958).

[42] W.D. WARD, A, GLORIG and D.L. SKLAR, *Temporary threshold shift from octave-band noise: applications to Damage Risk Criteria*, J. Acoust. Soc. Amer., **31**, 522–528 (1959).

[43] W.D. WARD, A, GLORIG and D.L. SKLAR, *Relation between recovery from temporary threshold shift and duration of exposure*, J. Acoust. Soc. Amer., **31**, 600–602 (1959).

[44] W.D. WARD, *Studies in the aural reflex. II. Reduction of temporary threshold shift from intermittent noise by reflex activity: implications for damage risk criteria*, J. Acoust. Soc. Amer., **34**, 234–241 (1962).

[45] W.D. WARD, *The use of TTS in the derivation of Damage Risk Criteria for noise exposure*, Int. Audiol., **5**, 309–313 (1966).

[46] W.D. WARD, *Susceptibility to TTS and PTS*, Proceedings of the International Congress on Noise as Public Health Problem, Dubrownik, Yugoslavia 1973.

[47] W.D. WARD, *The "safe" workday noise dose*, Noise, Shock and Vibration Conference 1974, Monash University, Melbourne, Australia 1974.

[48] D.H. WOOLFORD, *Hearing impairment among Orchestral Musicians*, Music Perception **5**, 261–284 (1988).

ARCHIVES OF ACOUSTICS
19, 3, 323–331 (1994)

PERCEPTION OF SOME INTONATIONAL DEVIATIONS IN MELODIES

J. FYK

Institute of Music Education
Pedagogical University
(65-610 Zielona Góra)

The aim of the experimental research was to determine sensitivity to intonational deviations in melodies. The following intervals were investigated: prime, minor second, major second, perfect, fourth, augmented fourth, diminished fifth and octave, as they appear in both tonal and atonal contexts. Subjects were music education students from Pedagogical University in Zielona Góra (Group One) and students from Chopin Academy of Music, Warsaw (Group Two). Each group consisted of 22 subjects. During each experimental trial the subjects listen to two versions of a short melody played on the piano. The second version of the melody was a transposition of the first one by a major second upwards. Moreover, in fifty per cent of the cases, the last tone of the second version was intonationally deviant either upwards or downwards. The subjects' task was to judge whether the last tone in the second version was an intonational deviant or not. Raw material from the research is presented in the form of psychometric functions. Tolerance zones of intonational deviations have been determined. The obtained results partially support the research findings on principles of tonal gravitation by other investigators, but some of the results are new.

1. Introduction

For a long time, theoreticians and musicologists have been busy arguing for the existence of pure musical systems in music practice. Therefore, even the slightest deviations from pure systems have been considered to be undesirable. The first experimental investigations in that area concerned the evaluation of purity of scales practised in the course of music instruction. DELEZENNE initiated such investigations in 1827 and continued them through many years that followed. He has established the Pythagorean scale as a standard pattern for intonational accuracy (ESBROECK&MONFORT, [2]). The view shared by Delezenne was later supported by other investigators such as RITTER (1861), CORNU and MERCADIER (1869), STEINER (1891), and JONQUIER (1898).

An experiment by GREENE [6] seems to have brought about some partial solutions as far as the problem of intonational purity is concerned. ESBROECK and MONFORT [2] published a study aimed at verifying the hypothesis of priority given to the Pythagorean scale. To a large extant, their findings supported the equally tempered system. In his theoretical considerations, HINDEMITH [8] also threw doubt upon the purity of a melody performed in a natural scale.

It was a research by GARBUZOV [5], however, which marked the starting point in establishing a new concept of intonational purity. Garbuzov maintained that the twelve-zone system was one in which vocal as well as instrumental pieces were performed. It also concerned the instruments tuned in the non-equally tempered system. He also held that the defined degree of tone system, theoretically established as a point on the frequency scale, determined the pitch zone of certain width from psychological point of view. Hence, many intonational variants of the same interval may function in accordance with the principle of intonational deviations of a given interval from the conventionally established standard pattern. Consequently, in recent research, the intonational deviations in intervals are considered in purely musical terms (FRANCÈS [3]; RAGS [10]; SAKHALTUYEVA [13, 14]; SHACKFORD [15]; CUDDY [1]; FYK [4]). Despite the above, the idea of a very close interrelationship between perfect intonation and numerical parameters seems still to prevail.

Most of the recent research on the musical intonation concerned vocal music and the music performed on instruments tuned in a non-fixed way. The perception of intonational deviations in melodies with respect to sounds used in common music practice is, however, the problem that is by no means solved (FRANCÈS [3]; FYK [4]; HARAJDA & FYK [7]). Therefore, there is a pressing need to bridge some gaps in that field. The aim of the present study was to investigate perception of intonational deviations of different magnitudes from the following intervals: prime (1), minor second (m2), major second (M2), perfect fourth (4), augmented fourth (4#), diminished fifth (5b), and octave (8). Short tonal and atonal melodies composed specifically for this research, were performed on the piano, and recorder on tape.

The intention of this research was to determine the intonation tolerance zones, i.e., to establish the permissible size of pitch deviations that can still be tolerated.

2. Method and Data Representation

Subjects were 22 students of music education from Pedagogical University in Zielona Góra (Group One) and 22 music students from Chopin Academy of Music in Warsaw (Group Two). To study the impact of musical education experience on the perception and tolerance of intonation deviations, the subjects selected for this experiment were divided into two groups. The first group members had 7–9 years of musical training and the second one — 14 years.

The test material was composed of 10 series comprising tonal and atonal melodies. Intervals under investigation appeared in two or three different melodic contexts and ended the melodies. The use of both tonal and atonal contexts allowed us to investigate the possible impact of tonality and movement direction of the interval on the perceptual tendencies. Each series of trials contained 20 pairs of a two-bar-long melody performed on the piano. The first tune in the pair was the standard melody whilst the other one was its transposition by a major second upwards. In the transposed melody the last tone was intonationally deviant in fifty per cent of the cases. The values for the intonational deviations, both upwards and downwards, were: 5, 10, 15, 25, and 50 cents where 1 octave = 1200 cents. The transposition of the second melody was introduced in order to eliminate the possibility of pitch comparisons of the last tones in two melodies rather than comparing the sizes of actual intervals. The order of individual pairs was randomized. The musical material of the test is presented in Fig. 1.

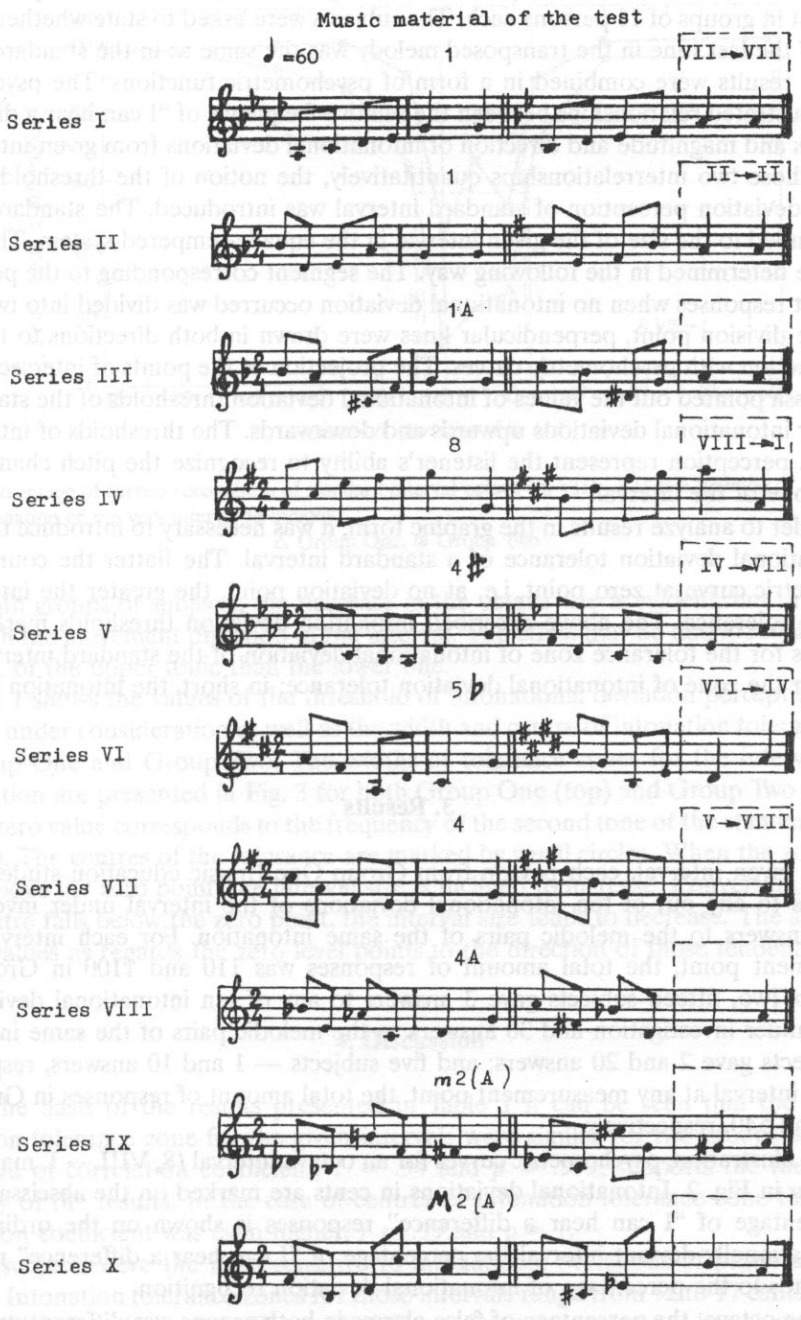

Fig. 1. Musical material of the test.
I, II. . .VIII — degrees of a major scale, A — interval in atonal context. In frames — interval intonationally deviant

Recorded test material was reproduced through a loudspeaker. The subjects listened to the test in groups of 11 persons each. The subjects were asked to state whether the intonation of the last tone in the transposed melody was the same as in the standard melody. Raw test results were combined in a form of psychometric functions. The psychometric graphs illustrated relationships between the relative frequency of "I can hear a difference" responses and magnitude and direction of intonational deviations from given intervals. To present those two interrelationships quantitatively, the notion of the thresholds of intonational deviation perception of standard interval was introduced. The standard interval corresponded to the size of the given interval in the equally-tempered system. The thresholds were determined in the following way. The segment corresponding to the percentage of correct responses when no intonational deviation occurred was divided into two halves. From the division point, perpendicular lines were drawn in both directions to the points of intersection with psychometric curves. The projection of the points of intersection onto the abscissa pointed out the values of intonational deviation thresholds of the standard interval for intonational deviations upwards and downwards. The thresholds of intonational deviation perception represent the listener's ability to recognize the pitch change in the second tone of the interval.

In order to analyze results in the graphic form, it was necessary to introduce the notion of intonational deviation tolerance of a standard interval. The flatter the course of the psychometric curve at zero point, i.e. at no deviation point, the greater the intonational deviation tolerance. The above described intonation deviation thresholds mark out the boundries for the tolerance zone of intonational deviation of the standard interval called thereafter the zone of intonational deviation tolerance; in short, the intonation tolerance zone.

3. Results

For a given interval, each person from Group One (music education students) gave 5 answers to any out of ten intonational deviations of the interval under investigation and 50 answers to the melodic pairs of the same intonation. For each interval at any measurement point, the total amount of responses was 110 and 1100 in Group One. In Group Two, fifteen subjects gave 3 answers to any of ten intonational deviations of interval under investigation and 30 answers to the melodic pairs of the same intonation. Two subjects gave 2 and 20 answers; and five subjects — 1 and 10 answers, respectively. For each interval at any measurement point, the total amount of responses in Group Two was 54 and 540, respectively.

As an illustration, psychometric curves for an octave interval (8, VIII → I, major scale) are shown in Fig. 2. Intonational deviations in cents are marked on the abscissa whereas the percentage of "I can hear a difference" responses is shown on the ordinate. For the intonationally deviant interval the percentage of "I can hear a difference" responses corresponds to the percentage of intonational deviation recognition.

For the octave, the percentage of false alarms in both groups was different: twelve per cent in Group One and forty-five per cent in Group Two. False alarms are understood as responses in which the subjects stated that they heard intonational deviations where there were none.

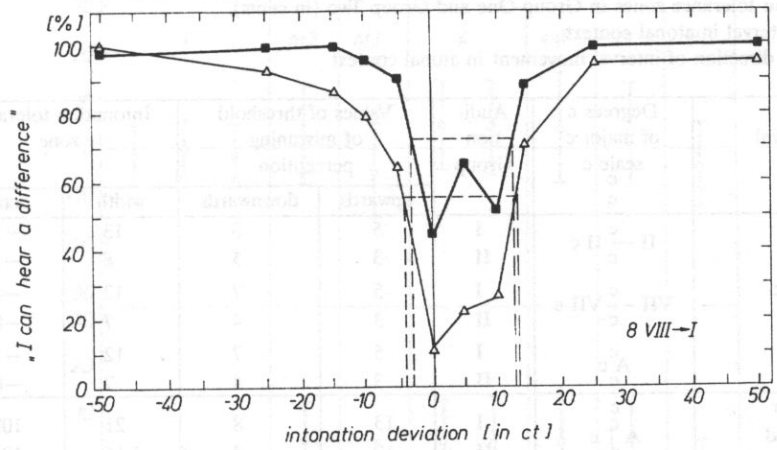

Fig. 2. Percentage of correct recognition of standard interval-octave (8, VIII → I) as a function of intonational deviation of the very interval in melody.
△ Group One, ■ Group Two

In both groups of subjects, the decrease in the octave size is evident, but in disagreement with the movement direction of the interval. The effect may be due to much stronger influence of the upper tonic than the lower one.

Table 1 shows the values of the threshold of intonational deviation perception for the intervals under consideration as well as the width and centre of intonation tolerance zones for Group One and Group Two. The widths of tolerance zones for the intervals under investigation are presented in Fig. 3 for both Group One (top) and Group Two (bottom). The zero value corresponds to the frequency of the second tone of the standard interval (440 Hz). The centres of the tolerance are marked by small circles. When the zone centre moves above the zero point, the interval size is inclined to increase. Conversely, when the zone centre falls below the zero point, the interval size tends to decrease. The shift of the central values as regards the zero level points to the direction of those tendencies.

4. Discussion

On the basis of the results presented in Table 1 it can be seen that the widths of intonation tolerance zone for the given intervals were similar for two groups of subjects. The value of correlation coefficient, $r = .94$ and $p = .999$, supports the thesis of the similarity of the results. In the case of centres of intonation tolerance zone the value of correlation coefficient was even higher, $r = .99$ and $p = 1$.

The subjects were the most sensitive to intonational deviations of prime and octave interval. Intonation tolerance zones for those intervals range from 12 to 17 cents in Group One and from 7 to 16 cents in Group Two. The widest tolerance zones have been obtained for augmented fourth, 23 cents in Group One and 22 cents in Group Two.

For prime, in both groups, there was a tendency to recognize intonation deviations of the second tone shifting down. As for minor second in an atonal context, there was

Table 1. Threshold values of intonational deviation perception. Width and centre of intonational deviation tolerance zones in Group One and Group Two (in cents).
A — interval in atonal context
↓, ↑ — direction of interval movement in atonal context

Interval	Degrees c of major c scale c	Audition Group	Values of threshold of mistuning perception		Intonation tolerance zone	
			upwards	downwards	width	centre
Prime /1/	II → II c	I	5	8	13	−1.5
		II	3	5	8	−1.0
	VII → VII c	I	5	7	12	−1.0
		II	3	4	7	−0.5
	A c	I	5	7	12	−1.0
		II	3	4	7	−0.5
Minor second /m2/	A ↓ c	I	13	8	21	102.5
		II	12	4	16	104.0
Major second /M2/	A ↑ c	I	15	5	20	195.0
		II	15	4	19	194.5
Perfect fourth /4/	V → VIII c	I	14	4	18	505.0
		II	12	4	16	504.0
	A ↓ c	I	14	6	20	504.0
		II	13	7	20	503.0
Augmented fourth /4#/	IV → VII c	I	15	8	23	603.5
		II	15	7	22	604.0
Diminished fifth /5b/	VII → IV c	I	14	8	22	603.0
		II	13	4	17	604.5
Octave /8/	VIII → I c	I	13	4	17	1195.5
		II	13	3	16	1195.0

a tendency to enlarge the interval size in agreement with the movement direction of the interval. The perception tendency for major second in atonal context was to decrease the size of the interval, which was in disagreement with the movement direction of the interval.

For perfect fourth, in both Group One and Group Two, there was a tendency to enlarge the interval size in accordance with the movement direction of that interval in both melodic contexts. As there were no data on the perception tendencies for the forth in the opposite direction, i.e. falling down, it was impossible to determine whether this tendency was caused by the movement direction of that interval only or not.

In augmented fourth, the second tone of that interval was commonly regarded as leading to the resolution. The result was the tendency to enlarge the interval size. Such perception tendencies were caused by tonal gravitation of the second tone in augmented fourth. As for diminished fifth, the presented data did not confirm the impact of tonal gravitation on decreasing the interval size. To the contrary, the tolerance to intonational

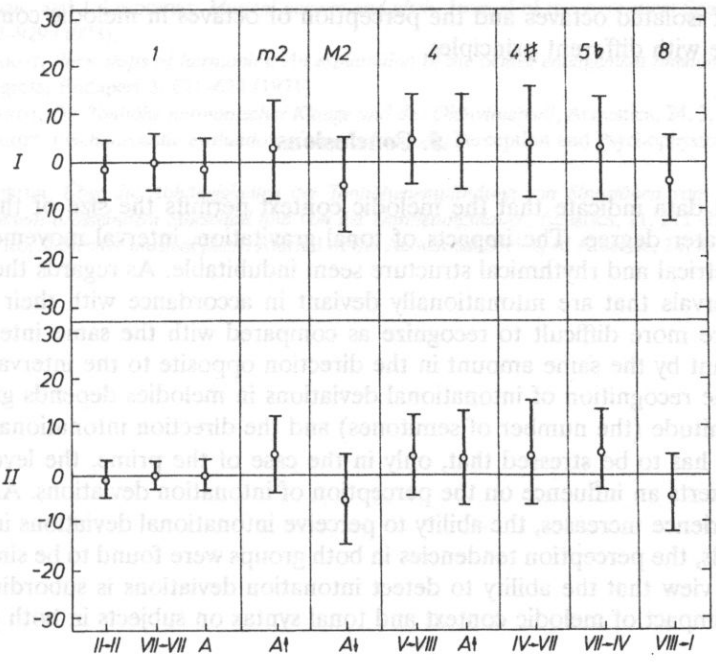

Fig. 3. Width of intonational deviation tolerance zones of the interval under investigation.
I, II. . .VIII — degrees of major scale, *A* — interval in atonal context, ↓, ↑ — direction of interval movement in atonal context, o — zone centres

deviations in the upward direction was greater. The latter finding is in agreement with the tendency to enlarge the interval size in diminished fifth, when the interval movement is in the upward direction.

The findings of this study that the octave tended to decrease in size did not provide a support for the previous hypothesis on the octave enlargement phenomenon raised by TERHARDT [17, 18, 19]. According to Terhardt, the phenomenon of octave enlargement is due to mutual interrelationship between the first and the second tone of the interval. Those two harmonic tones are assumed to affect each other. Kept in the memory, the size of the enlarged octave is thought to be reproduced afterwards in melodic sequences. Terhardt also maintains that the octave enlargement in pure tones is greater as compared with the same phenomenon in complex tones.

The tendency for the melodic octaves to be perceived as the physical interval smaller than 1 : 2 was also reported by other authors (WARD [21]; WALLISER [20]; SUNDBERG & LINDQVIST [16]; RAKOWSKI [11]; MIŚKIEWICZ [9]; RAKOWSKI & MIŚKIEWICZ [12]). All these studies were carried out on pure tones or harmonic sounds.

When discussing the discrepancy between the results of this research and the results obtained by the other authors, one must be aware of entirely different conditions in which those investigations were carried out. The present study was focused on the perception of octaves in melodic context while other researchers limited their investigations to isolated octaves only. It is noteworthy that the phenomenon of enlarged octaves emerged from the research on isolated octaves. The present research findings seem to suggest that the

perception of isolated octaves and the perception of octaves in melodic context function in accordance with different principles.

5. Conclusions

Presented data indicate that the melodic context permits the size of the interval to vary to a greater degree. The impacts of tonal gravitation, interval movement direction as well as metrical and rhythmical structure seem indubitable. As regards the atonal context, the intervals that are intonationally deviant in accordance with their direction of movement are more difficult to recognize as compared with the same intervals intonationally deviant by the same amount in the direction opposite to the interval movement. Moreover, the recognition of intonational deviations in melodies depends greatly on the interval magnitude (the number of semitones) and the direction intonational deviation.

In sum it has to be stressed that, only in the case of the prime, the level of musical experience exerts an influence on the perception of intonation deviations. As the level of musical experience increases, the ability to perceive intonational deviations improves. For other intervals, the perception tendencies in both groups were found to be similar and this supports the view that the ability to detect intonation deviations is subordinated mainly to the same impact of melodic context and tonal syntax on subjects in both groups.

References

[1] L.L. CUDDY, *Perception of structured melodic sequences*, L'Institut de la Recherche et de Coordination Acoustique/Musique, Paris 1977.

[2] G. ESBROECK and F. MONFORT, *Qu'est-ce que jouer juste*? Ed. Lumière, Bruxelles 1946.

[3] R. FRANCÈS, *La perception de la musique*, J.Vrin, Paris 1958.

[4] J. FYK, *Tolerance of intonational deviations in melodic intervals*, Unpublished Ph.D. dissertation (in Polish), Chopin Academy of Music, Warszawa 1980.

[5] N.A. GARBUZOV, *Zonal nature of sound pitch haering*, (in Russian), Academy of Science of USSR, Moscov–Leningrad 1948.

[6] P.C. GREENE, *Violin intonation*, Journal of the Accoustical Society of America, **9**, 43–44 (1937).

[7] H. HARAJDA and J. FYK, *The perceptibility of mistuned melodic intervals by school children*, Archives of Acoustics, **6**, 4, 371–384 (1981).

[8] P. HINDEMITH, *A composer's world; horizons and limitations*, Harvard University Press, Cambridge 1953.

[9] A. MIŚKIEWICZ, *Tuning intervals in harmonic spectrum sounds*, unpublished M.A. thesis (in Polish), Chopin Academy of Music, Warszawa 1980.

[10] Y. RAGS, *Intoning melodies with respect to some of their elements* (in Russian), Papers of the Theory of Music Department, Music National Publishing House, Moscov, 338–355 (1960).

[11] A. RAKOWSKI, *Categorical perception of pitch in music*, (in Polish), Chopin Academy of Music, Warsaw 1978.

[12] A. RAKOWSKI and A. MIŚKIEWICZ, *Deviations from equal temperament in tunning isolated musical intervals*, Archives of Acoustic **10**, 291–304 (1985).

[13] O. SAKHALTUYEVA, *On some principles of intoning in relation to form, dynamics and structure* (in Russian), Papers of the Theory of Music Department, Musical National Publishing House, Moscov, 356–378 (1960).

[14] O. SAKHALTUYEVA, *Intonation analysis of a performance of Mendelssohn's violin concerto the 1st movement; Application of acoustical research methods to music*, Moscov, 61–78 (1964).

[15] C. SHACKFORD, *Some aspects of perception*. Part I. Journal of Music Theory, **5**, 161–202 (1961) ; Part II. Journal of Music Theory, **6**, 66–90 (1962).

[16] J. SUNDBERG and J. LINDQVIST, *Musical octaves and pitch*, Journal of the Acoustical Society of America, **53**, 4, 922–929 (1973).

[17] E. TERHARDT, *Pitch shifts of harmonics; An explanation of the octave enlargement phenomenon*, Proc. 7th ICA Congress, Budapest **3**, 621–624 (1971).

[18] E. TERHARDT, *Die Tonhöhe harmonischer Klänge und das Oktavintervall*, Acoustica, 24, 3, 126–136 (1971).

[19] E. TERHARDT, *Psychoacoustic evaluation of musical sounds*, Perception and Psychophysics, **23**, 6, 483–492 (1978).

[20] K. WALLISTER, *Über die Abhängigkeiten der Tonhöhenempfindung von Sinustönen vom Schallpegel, von übergelagertem drosselndem Störschall und von der Darbietungsdauer*, Acustica, **21**, 211–221 (1969).

[21] W.D. WARD, *Subjective musical pitch*, Journal of the Acoustical Society of America, **26**, 3, 369–380 (1954).

ARCHIVES OF ACOUSTICS
19, 3, 333–353 (1994)

ACOUSTIC INVESTIGATION OF THE CARILLONS IN POLAND

M. SANKIEWICZ, A. KACZMAREK and G. BUDZYŃSKI

Department of Sound Engineering Gdańsk Technical University
(80-952 Gdańsk)

The carillons existing in Poland are described. Three carillons have been recently investigated acoustically: that as Jasna Góra Sanctuary in Częstochowa, installed in 1905, that one at St. Catherine Church in Gdańsk, built in 1989, and the one at the Gdańsk Main-City town-Hall, rebuilt, yet unsatisfactorily, in 1970. Results of the computerized spectral sound analysis of those carillons are presented, compared and discussed.

1. Introduction

Carillons are specific musical instruments, composed of bells tuned to consecutive steps of a musical scale, serving as sound sources while excited into vibrations by hammer strokes. Thus carillons may be classified as percussional idiophones. The number of bells in a carillon should not be smaller than 23, i.e. its scale should reach at least two octaves. This condition comes from a definition accepted, among others, by the Carillon Guild in U.S.A. [6]. However, many carillons have 36 or more bells, thus reaching a scale of three or more chromatic octaves.

A less numerous set of bells, usually less than ten, playing a simple melody is called a chime. Hence, some ambiguity arises how to denominate instruments composed of e.g. sixteen or twenty bells. They may be denoted as big chimes or as incomplete carillons. The decision may depend on other features of an instrument. On the other hand, the word 'chime' is being used for denoting tubular bells rather [16] than traditional ones of a campanoidal shape [15]. Thus, those and other terminological problems are still not solved within the topic [12].

Acoustic investigation on a carillon should, obviously, contain investigations on particular bells of the instrument, and then on the entire instrument. A study of the bell sound is more difficult than that of other musical instruments, first, because bell-sounds are of transient type, second, because they have a very complex temporal and spectral nature, where harmonic relations among partials are only crude approximations, third, because the sound spectrum depends on the way of excitement i.e. on the force, the velocity, and on the place of hammer stroke, as well as, on the position of a recording micro-

phones within a belfry space. More detailed dependences are considered in the specialized literature [1], [2].

Bells were studied by many outstanding scientists including Lord RAYLEIGH [20]. Classical papers on bells were collected by Rossing in Benchmark edition [16]. Main interest was devoted to analyses of bell sound complexity and to interdependences between bell dimensions and its sound spectrum. Carillon bells were mostly investigated as examples. However, further comparative investigations on various carillons seem to be desirable now, when measurements followed by computerized methods of analysis, are quicker and easier to be compared. Thus, objective comparisons of various carillon sounds are justified. They may be supported by the subjective assessments of sound quality.

The investigations on carillons in Poland, reported below, were considered by the authors as particularly important, because the carillon built recently in Gdańsk attracts great public attention due to its historical role in German–Polish relations. Another Gdańsk carillon only partly saved from war destruction presents also an interesting example. The third carillon, existing in Poland since XVIII century and rebuilt in 1905, gives good opportunity for comparisons, being approximately of same size as the first one.

It should be added here that may be more carillons or chimes existed in the past within the Polish territory, however, most probably, they were destroyed during the wars. For the three carillons investigated, more detailed data are given below.

2. Carillon data

The three investigated carillons are characterized here according to information either contained in the literature or collected during measurements and recordings made by the authors in situ. The carillons are described in chronological order of their construction or reconstruction.

2.1. The Jasna Góra Carillon

Jasna Góra ("The Bright Mountain") is a traditional name of the famous Our Lady Church and Monastery in Częstochowa. This Sanctuary numerously visited by pilgrims was outfitted in the XVIII century with a carillon situated in the upper part of the eminent main church tower.

The actually existing instrument was imported in the year 1905 from a Belgian enterprise Jos. Conthier et C-ie, Malines, and installed in the tower, rebuilt at that time after the big fire of 1900, which destroyed totally the old carillon together with the upper part of the XVIII-century tower [5].

The carillon has 36 bells, in chromatic scale ranging from C_4 to B_6. The bells are hung on supporting steel frames in the uppermost part of the tower in four floor-stages. The four biggest bells, provided with clappers are hung swinging, while all the bells have outside hammers. Some of the bells have double or triple hammers. The cabin with a keyboard is situated one floor below. Bells are played therefrom through a mechanical action with the use of transmission bars and levers.

2.2. The Town-Hall carillon

A chime in a Town-Hall tower of the Gdańsk Main-City existed already in XVI century. The chime had fourteen bells and a clock-bell [14]. The instrument was destroyed during the Second World War in 1944. Only three damaged bells were recovered after the destruction [21].

After the War, sixteen chime-bells dismounted from a former youth-center in a Gdańsk suburb, called Biskupia Górka (Bishop's Hill), have been installed in the rebuild Town-Hall tower in 1970 [3]. A seventeenth bell installed later on, came from those recovered from the old pre-war instrument. A XVI century clock-bell coming from the ruined St. John's Church nearby [4], is also installed in the tower as a present clock-bell [10].

The existing carillon, though incomplete, may serve, due to its automated driving mechanism, to play melodies. Actually, only one melody (part of Nowowiejski's "Rota") is repeated every hour, following the beats of the clock-bell. The sound quality of the carillon is not satisfactory, because of numerous bullets and splinter damages to bells, and due to difficulties in retuning the bells.

The carillon now has seventeen bells ranging at not fully chromatic scale from $A\#_4$ to E_6.

2.3. The St Catherine carillon

St. Catherine carillon is the newest and the best from such instruments existing in Poland. Its history is noteworthy in the past period, and especially in recent years. The first chime in St. Catherine Church was built in XVI century. In 1738 it was replaced by a big carillon having 35 bells. It was destroyed in a big fire in 1905. The next carillon, with 37 bells, was installed in 1910. It existed until the Second World War, when in 1942 its bells, except one, have been dismounted and sent to be melt down as material for armaments. Two years later the St Catherine Church and its characteristic belfry-tower were almost totally destroyed. After the War the 28 luckily saved bells of the dismounted carillon have been found in Germany, and later on, in 1954, installed in Our Lady Cathedral in Lübeck [10].

Thank to the initiative of a pre-war Gdańsk citizen Mr Hans Eggebrecht, a foundation was created in order to rebuild the St. Catherine carillon [9]. The main idea of the foundation was to reconcile German and Polish nations after the tragedy of War. The new set of 37 bells was ordered by German foundators from the renowned Dutch foundry Koninklijke Eisbout in Asten, which mounted the carillon in St. Catherine Church [11]. Earlier, Polish foundators rebuilt the monumental belfry-tower, see Fig. 1.

The new St. Catherine carillon has been solemnly installed at the belfry-tower in 1989. Since that time it plays melodies every hour automatically, thanks to a digital steering system and electromagnetic hammers. Up to 99 melodies can be stored in digital memory of the system. The instrument may be played from an electronic keyboard through a MIDI system interface. A foreseen mechanical keyboard and action has not yet been installed, so far.

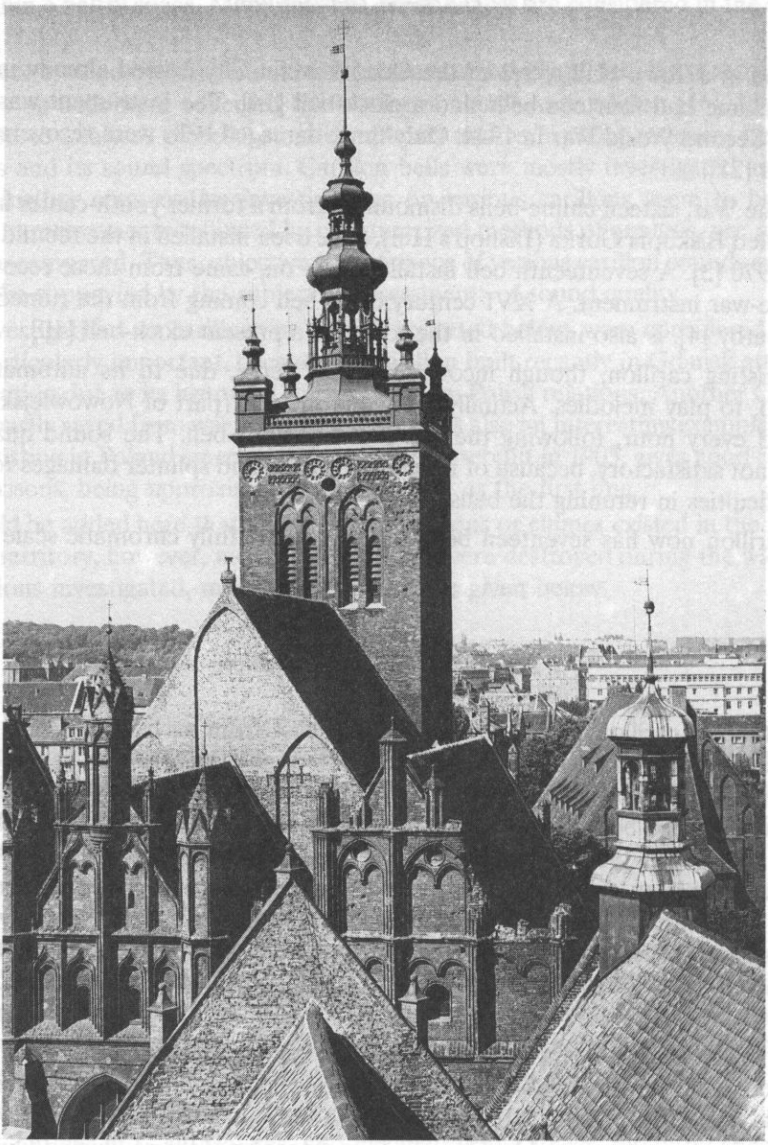

FIG. 1. The St. Catherine belfry-tower in Gdańsk.

The four low-note bells can be pealed either by clappers, when swung by wheel mechanisms, or by hammers, as are all remaining bells hung fixed. The largest of the bells serves also for striking hours. A part of the carillon bells mounted on a steel rack situated in the middle of the upper part of the rectangular, spacious, made of brick, belfry-tower is shown in Fig. 2.

The bells are tuned to chromatic scale reaching from C_4 to C_7.

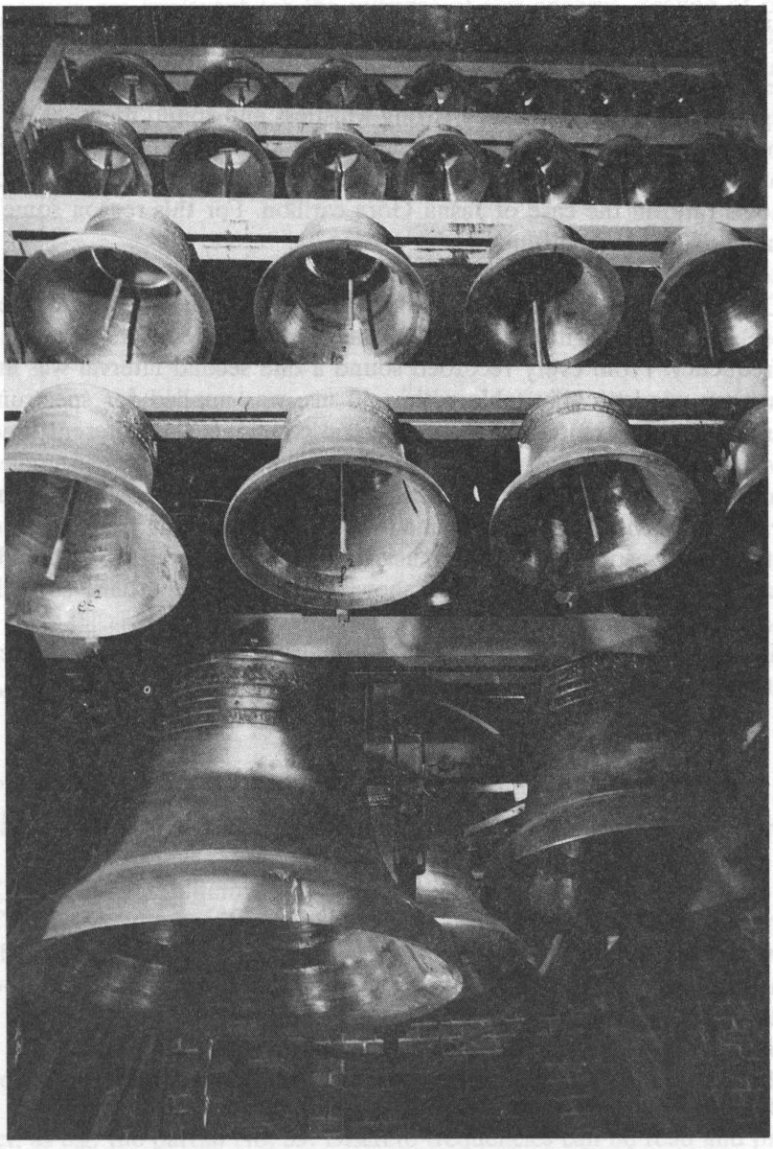

FIG. 2. A part of the St. Catherine carillon.

3. Acoustic investigation

Sounds of all carillon bells were recorded, using Nagra IV tape recorder with Neumann condenser microphone. Microphone distance varied for particular bells, which was inevitable because of difficulties in access to proper microphone positioning inside a belfry. However, the acoustic field at microphone positions although near to sound source was reverberant, especially in case of St. Catherine, due to sound reflections from inner belfry

walls. To suppress excessive field irregularities sounds were recorded also stereophonically with a pair of microphones and then the sum of those recordings analyzed.

Bad weather conditions were pungent difficulties encountered at recording carillon sounds. High force gusty wind caused strong whistless and sound impulses at both cases of recording made in the Town-Hall tower and in St. Catherine belfry-tower. Heavy rain pattering on the tin roof of the tower-helmet, caused noise interference, which diminished signal to noise ratio in the case of Jasna Góra carillon. For this reason some particular results of analysis had to be disqualified.

Recorded sounds were analyzed at the laboratory by means of a system composed of an IBM PC AT computer outfitted with a special board card and a software elaborated for that purpose. The 12 bit digital presentation was due to A/D conversion made at 24 kHz sampling frequency. From every recorded sound a one second interval was analyzed. A rectangular time window, adjustable within 40 ms, was applied for spectrum analysis. Multiple analyses were excuted for every spectral component at different time intervals adjusted with resampling, in order to achieve an integral number of samples within a chosen time window length. Its final selection depended on the choice of the most stable phase characteristics within a selected time interval. The resulting frequencies of spectral components were transposed onto the musical, equally tempered scale, based on A_4 = 440 Hz diapason. Spectra for every bell showing subsequent partials, as well as tables displaying relative tuning in cents, were printed as results.

The printed short-time spectra, taken at maximum sound power, have discrete spectral components numbered along the abscissa scale. The component number N, shown in Fig. 3 to 6 above locally maximum ray values, stems from the ratio:

$$N = \frac{f_{\text{sampling}}}{2^n} = \frac{24000}{1024} \cong 23.4 \text{ Hz} \quad \text{per ray}$$

The whole process of analyses for a carillon including the printing of results lasted about two hours.

A part of the recordings was analyzed using a NeXT computer, with an A/C converter AD64x, where sounds were introduced at 44.1 kHz sampling frequency. NeXT software programs were also applied to digital editing of sound samples. Resulting duration of analyses in time-domain, filtered for chosen sound partials, was limited to about 1.3 s, in order to eliminate components due to unwanted sounds.

Replaying of the recorded bell sounds allowed to assess subjectively the quality of particular bells and compare them in favourable listening conditions at the laboratory.

4. Results

As a full presentation of all resulting spectral diagrams and tables would take too much volume, so only selected results given as examples are quoted here.

4.1 Jasna Góra carillon

Fig. 3 depicts the short-time spectrum of the largest bell, i.e. C_4. Abscissae scale in Hertz is linear for easier search of harmonic relations; only a range to 3 kHz is shown,

as higher partials are irrelevant for the purpose of this analysis. Scaling of ordinates is relative, as amplitudes depend much on the selected moment of the time window, and also on the signal to noise ratio of the sound recording. Partials numbered are those of local maximum amplitude.

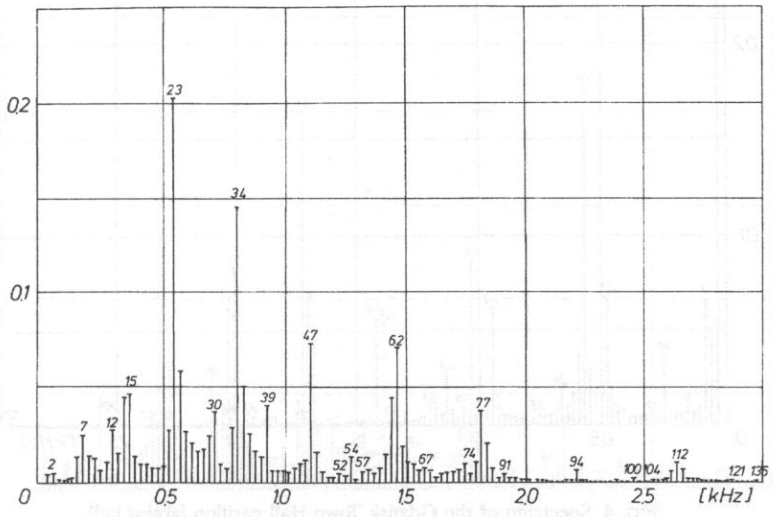

FIG. 3. Spectrum of the largest bell from Jasna Góra carillon.

The following partials among the numbered ones may be easily identified as relevant to the inner tuning harmony of the bell:

No. 7 — the Lower Octave (Hum tone),
12 — the Prime,
15 — the Minor Third,
23 — the Octave,
30 — the Tenth (Octave + Major Third),
34 — the Twelfth (Octave + Fifth),
47 — the Double Octave.

The Fifth and the Eleventh are missing in this case, while some irrelevant frequencies are distinct, as e.g. the partial No. 39. Discrete frequencies can be read and printed from analyses with the precision better than 10–4, where from relative tuning deviations are calculated. Appropriate results are listed in Tables shown in next section.

4.2 Town-Hall carillon

Figure 4 gives the short-time spectrum of the largest bell ($A\#_4$), while the Fig. 5 shows that one of the clock bell. The last example may be interesting because of the lower than usual height to diameter ratio of that old bell, and noticeable difference in timbre.

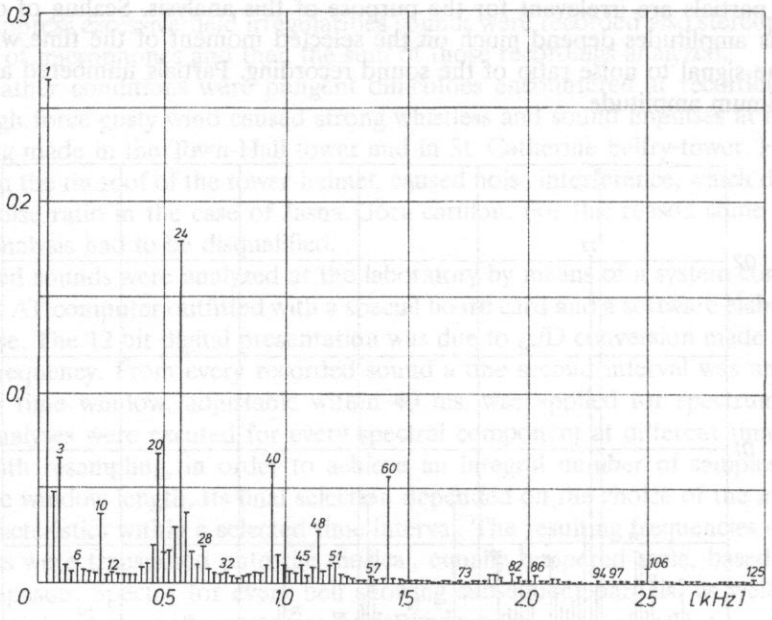

FIG. 4. Spectrum of the Gdańsk Town-Hall carillon largest bell.

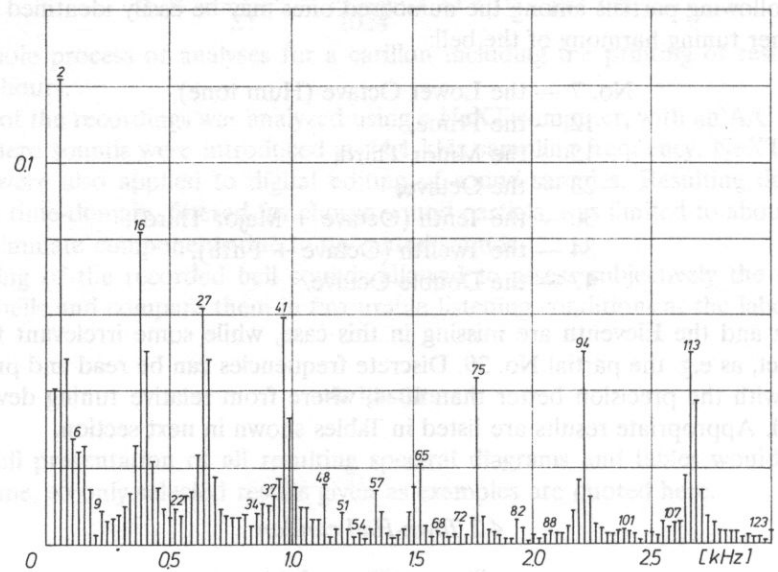

FIG. 5. Spectrum of the Gdańsk Town-Hall tower clock bell.

4.3. St. Catherine carillon

Figure 6 shows the short-time spectrum of the largest bell (C_4) when pealed with its clapper. Hammer excitation gives similar result; only amplitudes of partials differ slightly.

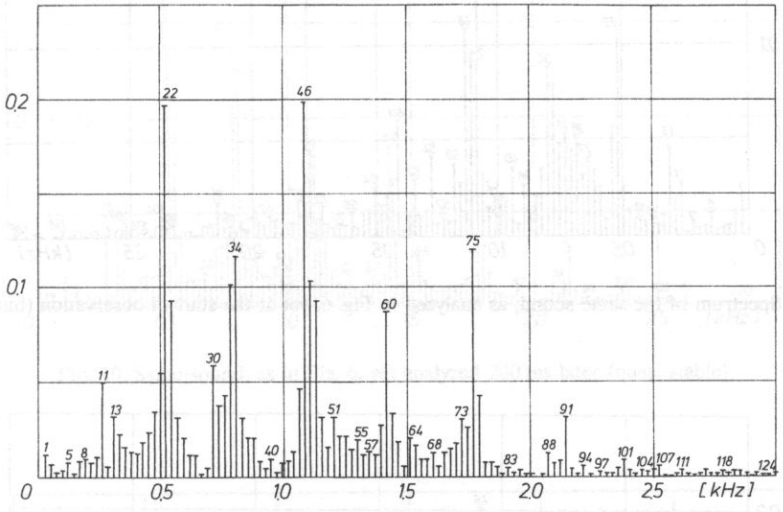

FIG. 6. Spectrum of the St. Catherine largest bell sound (analyzed at the moment of maximum sound power).

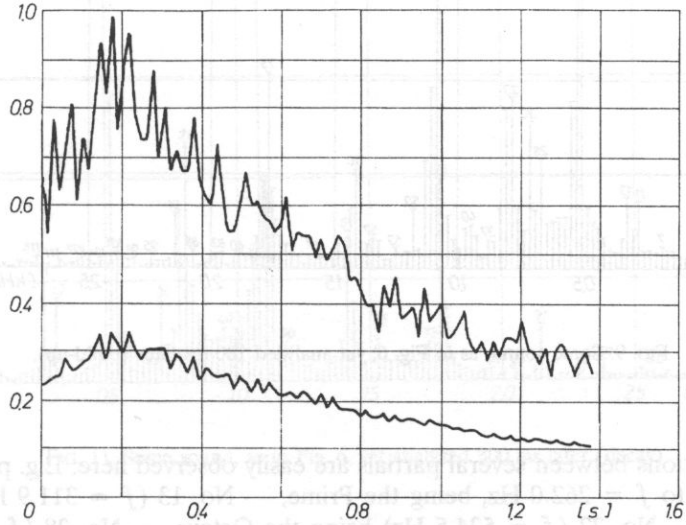

FIG. 7. Sound waveform of the St. Catherine largest bell (upper trace — peak values, lower trace — rms values).

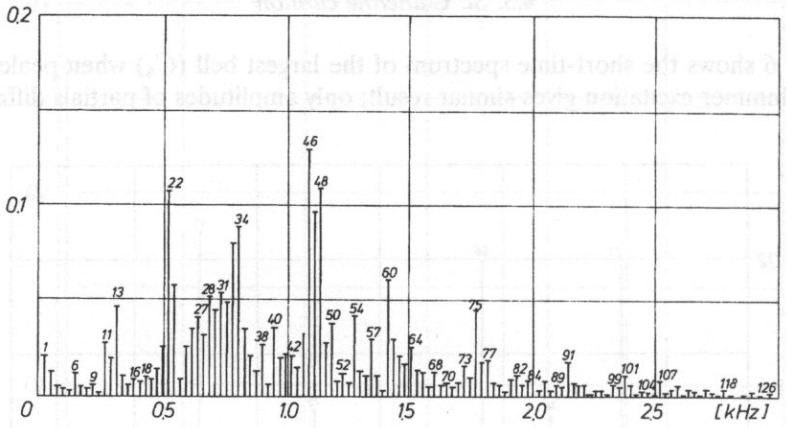

FIG. 8. Spectrum of the same sound, as analyzed in Fig. 6, yet at the start of observation (build-up).

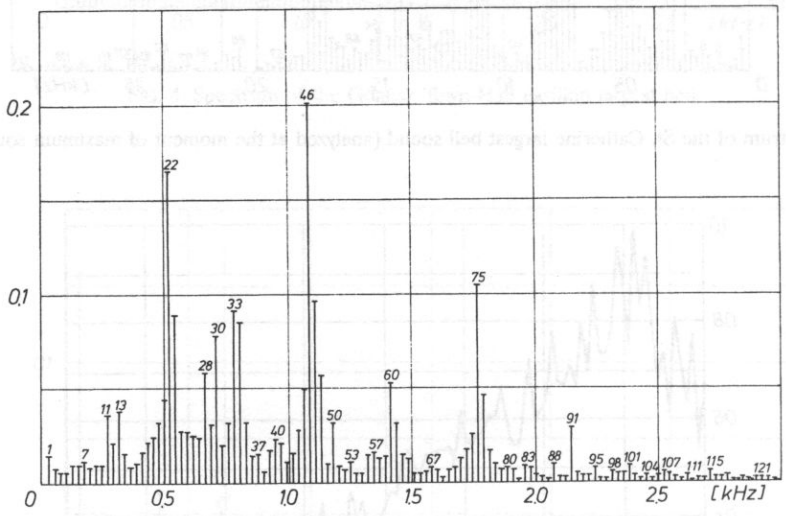

FIG. 9. Some sound, as in Fig. 6, yet analyzed 100 ms later (build-up).

Harmonic relations between several partials are easily observed here. E.g. partial No. 11, corresponding to f = 262.0 Hz, being the Prime, — No. 13 (f = 311.9 Hz) being the Minor Third, — No. 22 (f = 524.5 Hz) being the Octave, — No. 28 (f = 655.8 Hz) being the Tenth, — etc. However, some discrepancies from the perfect inner harmony are noticeable. Besides, some partials are unstable within the observation period and their values depend on the selected time interval for analysis.

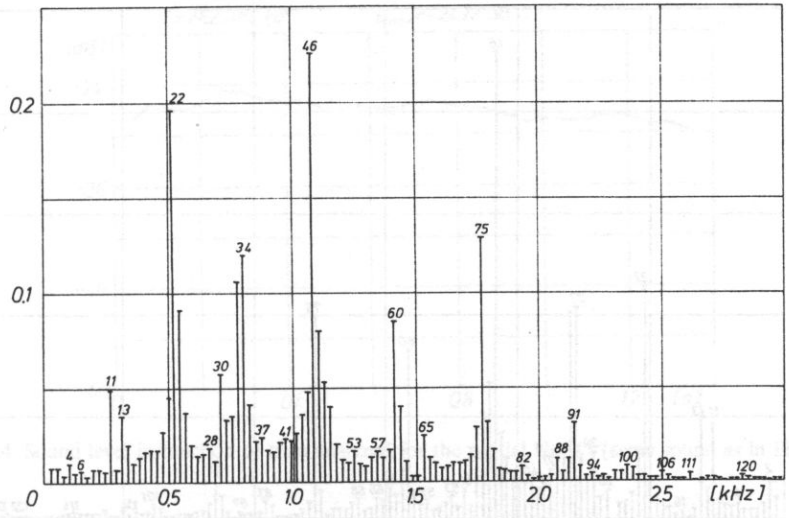

FIG. 10. Same sound, as in Fig. 6, yet analyzed 200 ms later (quasi-stable).

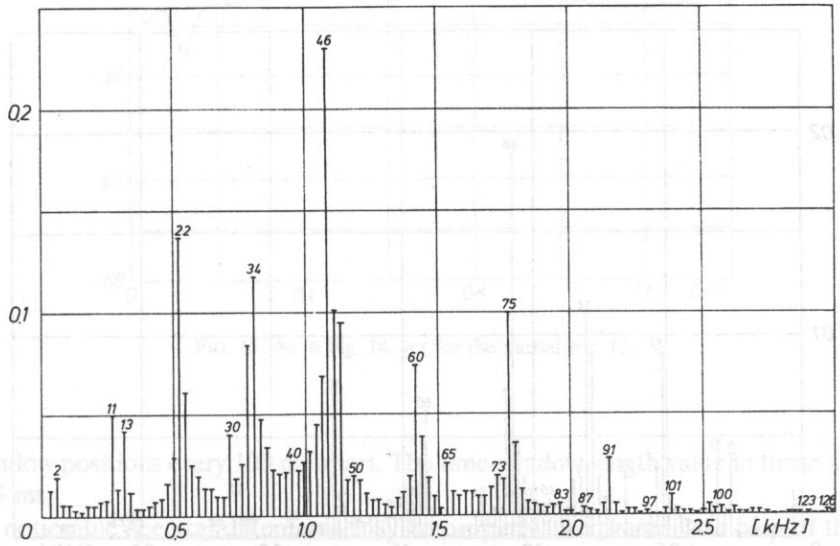

FIG. 11. Some sound, as in Fig. 6, yet analyzed 300 ms later (decay).

The diagram in Fig. 7 shows the build-up and decay of the analyzed sound as function of time. The upper trace presents peak-values while the lower one rms-values of the

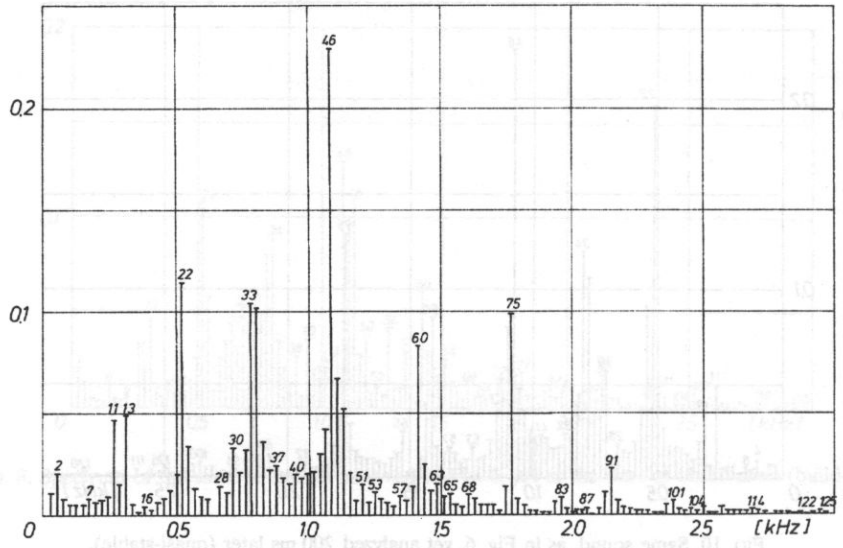

FIG. 12. Same sound, as in Fig. 6, yet analyzed 400 ms later (decay).

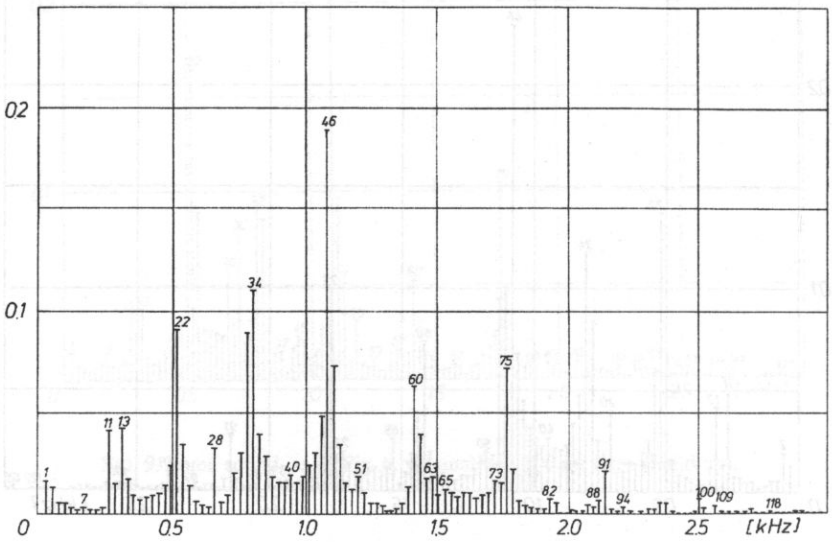

FIG. 13. Some sound, as in Fig. 6, yet analyzed 500 ms later (distinct decay).

function. In order to show the dependence of the short-time spectral on the selected observation time the following six spectrograms are presented, see Figs 8 to 13, taken at

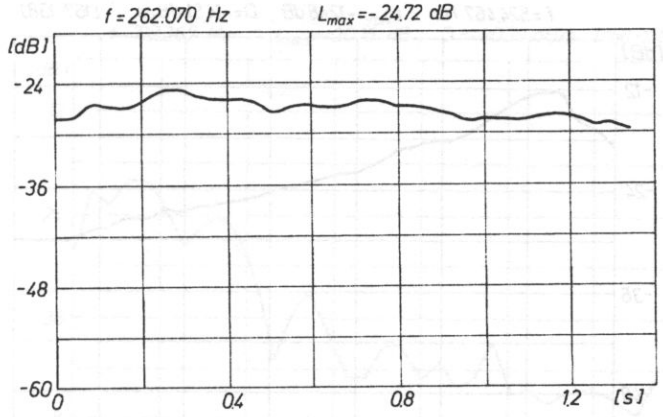

FIG. 14. Sound level in function of time analyzed for the partial No. 11 (same sound as in Fig. 6).

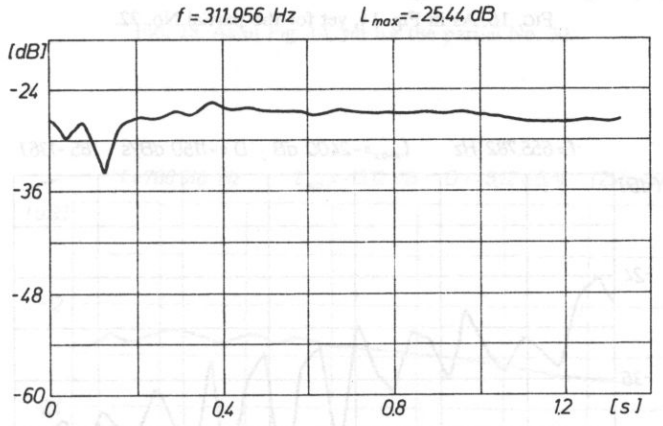

FIG. 15. As in Fig. 14, yet for the partial No. 13.

time-window positions every 100 ms apart. The time-window length value in those analyses was 42.5 ms.

The noticeable spectral differences may be properly interpreted with help of the time domain analysis results computed for the eight selected partials, see Figs. 14 to 21. Hence it appears that e.g. the Minor Third (No. 28) component instability, see Fig. 17, is caused by warble beats at a frequency of about 8 Hz, produced between two close situated vibration modes of the bell. A similar instability shows the Eleventh (No. 30), see Fig. 18, although considerably out of tune. It is worth noticing that those two warbling partials are both decaying faster than the majority of other more stable component, e.g. the Prime (Fig. 14), the Third (Fig. 15), the Twelfth (Fig. 19), and the Double Octave (Fig. 20). Decay rates

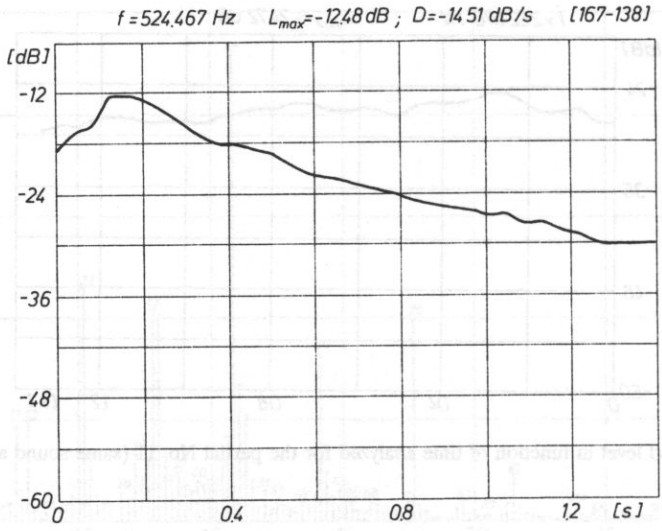

FIG. 16. As in Fig. 14, yet for the partial No. 22.

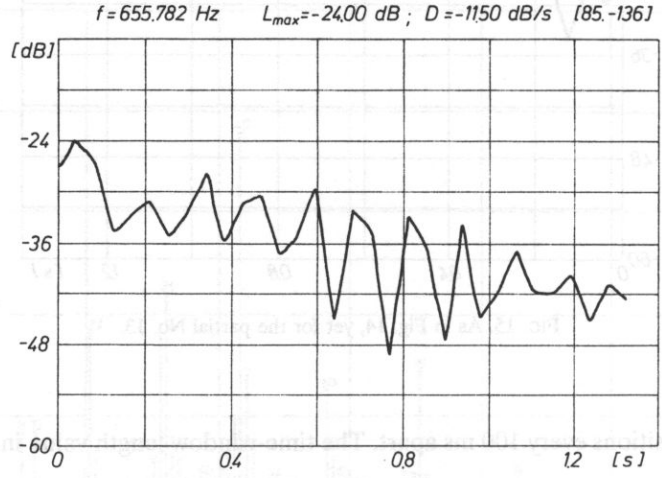

FIG. 17. As in Fig. 14, yet for the partial No. 28.

D [dB/s], averaged within the observed time interval, computed for every analyzed partial, are quoted above diagrams rim.

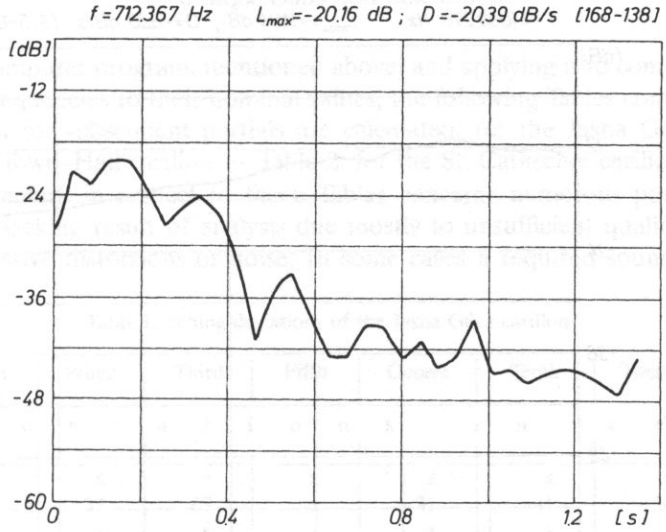

FIG. 18. As in Fig. 14, yet for the partial No. 30.

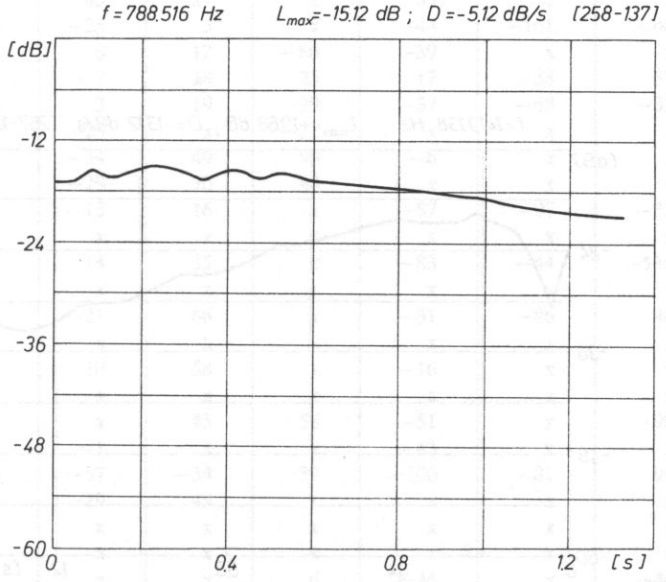

FIG. 19. As in Fig. 14, yet for the partial No. 33.

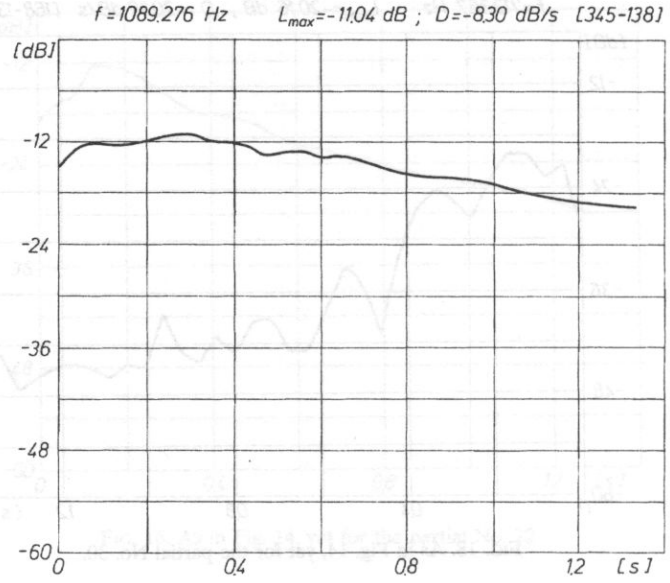

FIG. 20. As in Fig. 14, yet for the partial No. 46.

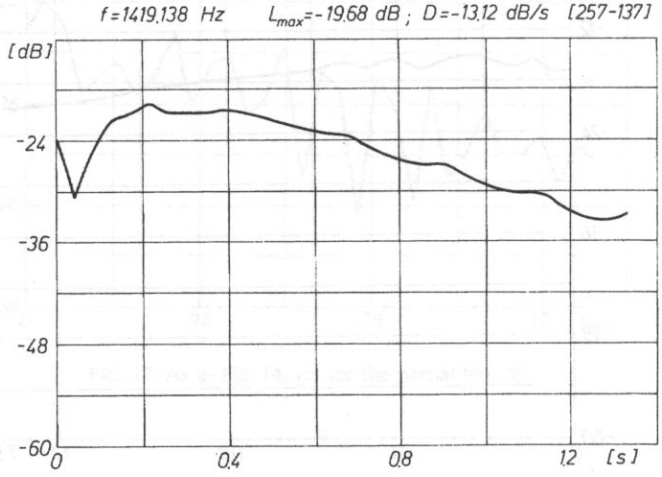

FIG. 21. As in Fig. 14, yet for the partial No. 60.

5. Comparisons and discussion

Using the computer program, mentioned above, and applying it to comparisons of analyzed partial frequencies to their nominal values, the following Tables containing relative tuning deviation for subsequent partials are calculated: for the Jasna Góra carillon — Table 1 for the Town–Hall carillon — Table 2, for the St. Catherine carillon — Table 3.

A general remark in respect to those Tables concerns numerous positions marked "x". It denotes lacking result of analysis due mostly to unsufficient quality of recording made with excessive distorsions or noise. In some cases a required sound could not be

Table 1. Tuning deviations of the Jasna Góra carillon

Partials:	Hum tone	Prime	Third	Fifth	Octave	Tenth	Twelfth	Upper Octave
	Deviations in cents							
Bell:								
C 4	x	x	x	x	x	x	x	x
C#4	x	37	67	x	−31	41	−56	−1
D 4	x	x	x	x	x	x	x	x
D#4	87	x	6	x	−18	24	144	46
E 4	76	84	64	x	−34	5	35	−24
F 4	81	x	2	−26	−18	−10	−27	27
F#4	58	−25	14	−66	−61	−8	34	−22
G 4	x	x	x	x	x	x	x	x
G#4	1	48	−24	x	85	x	x	x
A 4	30	−25	5	x	−44	−161	−48	x
A#4	23	6	12	−80	−39	x	x	x
B 4	102	−7	48	25	17	−38	32	x
C 5	6	3	19	−99	−37	−48	−33	31
C#5	7	−23	x	−21	x	x	x	x
D 5	x	−34	49	99	−6	x	x	x
D#5	89	−29	70	43	x	x	x	x
E 5	90	−13	16	x	−87	−97	−33	x
F 5	x	x	x	x	x	x	x	x
F#5	1	14	35	x	−83	−44	−116	x
G 5	x	x	x	x	x	x	x	x
G#5	31	−21	66	x	−31	−86	40	−44
A 5	x	x	x	x	x	x	x	x
A#5	45	10	58	x	−16	x	x	x
B 5	x	x	x	x	x	x	x	x
C 6	30	x	43	58	−51	x	−90	45
C#6	x	−1	x	x	−43	x	x	x
D 6	33	−57	−34	−39	−100	−81	94	42
D#6	38	−29	49	x	x	x	x	x
E 6	x	x	x	x	x	x	x	x
F 6	x	x	x	x	x	x	x	x
F#6	−32	x	x	6	−34	x	−44	x
G 6	x	−4	−19	x	−126	−118	x	x
G#6	x	x	x	x	x	x	x	x
A 6	−66	9	−15	x	−67	x	x	x
A#6	15	65	−22	x	−126	x	x	x
B 6	−6	−55	51	x	17	x	x	x

recorded due e.g. to a damaged hammer etc., so a few bells were passed over. However, the number of positively made analyses seems being sufficient to discuss the tuning quality of the investigated carillons.

It may be noticed, by inspection of the figures and comparisons among the Tables, that the new St. Catherine carillon is the best tuned. Deviations with negative values denote frequencies lower than nominal values.

The listed deviations are mostly within the limits calculated theoretically by SCHAD [18] and those found empirically by other investigators [6], [19]. Only values at a few positions in the Table 3 require verification, namely concerning the bells D_4, $F\#_4$, and B_5. A human error can not be excluded as the process of time interval selection for the analysis depends, as mentioned above, on operator's skill. At any rate, the most important five partials which decide upon strike note and upon tonal sound sensation are tuned so well that their deviation are unnoticeable for the listener. Next four partials are more deviated, e.g. for double octave deviations are more than half of semi tone, however, levels of those partials is mostly very low, so if theoretically audible they do not influence the sound quality. Besides, there are no available data from the literature, giving opportunity to compare respective deviations to those at other carillons of quality.

Table 2. Tuning deviations of the Town-Hall carillon

Partials: / Bell:	Hum tone	Prime	Third	Fifth	Octave	Tenth	Twelfth	Upper Octave
	Deviations in cents							
A#4	14	−3	47	−107	26	−74	20	−15
B 4	0	1	22	−98	−10	−63	−25	19
C 5	−83	18	17	−58	−15	−93	−22	26
C#5	−15	−41	3	−131	−28	0	−32	11
D 5	−40	18	17	−48	−23	−65	−36	7
D#5	−51	4	22	17	−4	21	2	45
E 5	−34	−11	7	−125	−23	35	−33	7
F 5	x	x	x	x	x	x	x	x
F#5	−43	80	5	x	−19	−12	−17	19
G 5	−7	−15	0	−88	−37	−62	−54	−16
G#5	−55	33	−25	−115	−55	−69	−85	−22
A 5	−18	−7	4	x	−26	27	−36	7
A#5	−54	32	41	x	7	22	−12	30
B 5	−56	9	6	x	−29	−62	−39	6
C 6	−36	−22	−91	−44	49	−21	35	89
D#6	−18	12	−54	−16	24	x	x	x
G 6	−83	15	29	−6	−36	x	−69	x

The Table 2 shows the most values of deviation negative, in particular for Upper Ocatve partials in nine bells, their average value is — 27,2 cents. It shows clearly that those bells were tuned to diapason $A_4 = 435$ Hz, which is 19.8 cents below the actual diapason of 440 Hz. Higher values of deviation found for that carillon are easy to explain, because of the aforesaid war damages to bells, and because of their provenience from different instruments. Those deviations are audible as distinct mistuning when listening to a played melody.

Table 3. Tuning deviations of the St. Catherine carillon

Partials:	Hum tone	Prime	Third	Fifth	Octave	Tenth	Twelfth	Upper Octave
Bell:	Deviations in cents							
C_4	7	1	3	−2	1	−10	9	68
$C\#_4$	−2	2	4	23	4	−21	11	73
D_4	14	0	3	50	3	21	12	75
$D\#_4$	x	6	x	29	4	−28	9	75
E_4	1	5	5	4	−9	−19	16	80
F_4	x	5	0	7	8	−60	16	82
$F\#_4$	9	1	4	−42	3	6	10	73
G_4	−1	3	5	−63	3	−41	18	86
$G\#_4$	−3	−1	4	17	3	43	14	72
A_4	x	x	4	26	3	43	14	78
$A\#_4$	5	x	6	17	5	49	18	86
B_4	x	7	4	12	3	x	18	86
C_5	4	3	5	13	4	47	12	55
$C\#_5$	3	3	3	19	4	62	9	67
D_5	3	x	4	x	4	62	14	77
$D\#_5$	2	4	2	5	5	−31	13	75
E_5	5	4	5	−2	6	−58	13	74
F_5	x	3	5	13	4	−14	10	70
$F\#_5$	x	4	4	x	3	−26	7	64
G_5	4	7	6	0	6	x	11	67
$G\#_5$	x	3	3	4	5	−27	14	77
A_5	2	4	5	16	5	−36	12	72
$A\#_5$	x	4	6	x	6	−29	13	82
B_5	x	x	x	x	x	x	x	x
C_6	2	3	3	x	4	x	−1	11
$C\#_6$	3	4	9	27	5	15	1	52
D_6	4	3	4	x	6	27	2	79
$D\#_6$	3	4	4	x	6	−35	−6	40
E_6	3	6	5	x	6	42	−3	x
F_6	3	4	6	x	4	−10	−10	32
$F\#_6$	3	4	−7	x	2	−66	−26	x
G_6	5	4	6	x	6	x	−14	21
$G\#_6$	6	3	11	x	4	44	−23	3
A_6	5	5	6	x	−4	x	−22	3
$A\#_6$	5	6	8	x	4	x	x	x
B_6	5	4	15	x	4	6	−36	76
C_7	3	2	14	x	5	x	x	x

The large deviations found for Jasna Góra carillon require further investigation. A possible explanation lays in the fact that due to then damaged mechanical system of excitation the bells were excited with their hammers raised by hand, so hammer travels might have been inadequate to excite properly bell partials, and were at any rate unequal. Most of measured deviations being negative, they show that the carillon was also tuned to the old diapason value, what is evident considering the year of its founding.

It may be added, that recordings at Jasna Góra were made only once, while those at Town-Hall and St. Catherine were repeated, after earlier investigations [8], [17], so an eventual error probability is far less for those last carillons.

Beside of the examples shown in presented Figures and Tables the elaborated software permits to compute, show, and print several other kinds of characteristics e.g. quasi-threedimensional evolutive spectra, time characteristics for selected partial, their decay time, etc. It may be added that the employed method is developed from a similar one employed earlier at Gdańsk Sound Engineering Department for investigation of organ sounds.

Following the results obtained further investigations are planned. Among others a psychophysiological study of listeners' preference between carillons with the Minor- versus Major-Third bells [13]. Such evaluation made recently by HOUTSMA and THOLEN [7] should be followed by many others executed in various conditions, before any initiative to build a whole "Major Third" carillon could be undertaken.

6. Conclusions

The abridged report on carillon investigations, presented here, is rather a preliminary attempt to gain a full information concerning those unique musical instruments in Poland. A dedicated software for IBM AT computer was elaborated and a complete method of investigation implemented, using also NeXT computers. It permits for easy and quick repeating and verifying measurements. Thus, comparison to other carillons in the World, well known and precisely investigated and described in the literature, will be possible. Besides, it may be expected that thanks to the discussion on methods of computerized bell sounds analysis among interested acousticians and sound engineers, a degree of standarization of such methods will be achieved, which will facilitate an exchange of information and accelerate fruitful comparisons.

7. Acknowledgements

Authors express their thanks and gratitude to Professor Andrzej RAKOWSKI from the Chopin's Academy of Music, Warsaw, for his advices concerning presentation of results. They are also much indebted to Fathers Paulites from Jasna Góra, as well as to Doctor Grzegorz SZYCHLIŃSKI from Gdańsk, for their help in recordings of carillon sounds. A permission for publishing photographs by Mr. K. JAKUBOWSKI is gratefully acknowledged.

References

[1] H. BAGOT, *Bells. Their design and tuning*, Acoustics Australia, **14**, 2, 35–41 (1986).

[2] A.L. BIGELOW, *The acoustically balanced carillon*, Princeton University, Princeton, N.J. 1961 reprint in Acoustics of bells, Ed. T. Rossing, Van Nostrand, N.Y. 1984.

[3] T. DOMAGAŁA, *Gdańsk — The Main City hall* (in Polish), KAW, Gdańsk 1981.

[4] W. DROST, *Kunstdenkmäler der Stadt Danzing — St. Johann, Bd.1, T.2: Glocken*, W. Kohlhammer, Stuttgart 1957.

[5] J. GOLONKA, *Bells, carillon bells and balfries* (in Polish), Jasna Góra, 26–30, 8, 1986.

[6] E.W. VAN HEUVEN, *Acoustical measurements on church bells and carillons*, De Gebr. van Cleef, The Hague, Netherlands 1949 in: Acoustics of bells [Ed.] T. Rossing, V. Nostrand, N.Y. 1984.

[7] A.J. HOUTSMA and H. THOLEN, *A carillon of major-third bells: a perceptual evaluation*, Music Perception **4**, 255–256. (1987).

[8] M. ISZORA and M. SANKIEWICZ, *Acoustical investigation of St. Catherine Carillon bells* in Polish, 37 Open Seminar on Acoustics, 2, 177–180, Gdańsk 1990.
[9] A. JANUSZAJTIS, *The St. Catherine church in Gdańsk* [in Polish]. OO.Karmelici, Gdańsk 1989.
[10] A. JANUSZAJTIS, *The music of the Gdańsk bells* (in Polish) KMPZP-3 Akademia Muzyczna im. St. Moniuszki, Gdańsk 1989.
[11] KÖNIGLICHE EIJSBOUTS *"Glockenliste für das spielbare Glockenspiel der St. Katharinenkirche in Danzig-Gdańsk*.
[12] E. LEIPP, *Aspects technologique et acoustiques du carillon*, Bull. du G.A.M., Université Paris VI, No. 66, 1973.
[13] I.A. MURRA and G.M.L. GLADWELL, *On a search for a major-third and other non-standard bells*, J. of Sound and Vibration, **149**, 2, 330–340 (1991).
[14] H. PAWŁOWSKI, *Das Glockenspiel auf dem Rechstädtischen Rathause zu Danzig*, Ostdeutsche Monatshefte, IX, 6, 1928.
[15] R. PERRIN, T. CHARNLEY and J.H. SAMSON, *The Campanoid: an equation for the church bell profile*, J. of Sound and Vibration, **151**, 1, 163–167 (1991).
[16] T.D. ROSSING, *Acoustic of bells*, Part VI, Van Nostrand Reinhold Co., New York 1984.
[17] M. SANKIEWICZ, *Acoustic investigations of bells and carillons* [in Polish] Inżynieria i Reżyseria Dźwięku, 166–187, AGH Kraków 1989.
[18] C.R. SCHAD, *Form-Klang-Rechnungen an Glocken*, Acustica, **64**, 272–285 1987.
[19] F.H. SLAYMAKER and W.F. MEEKER, *Measurements of the tonal characteristics of carillon bells*, J. of Acoust. Soc. Am., **26**, 515–522 (1954).
[20] J.W. STRUTT–RAYLEIGH, *The theory of sound*, vol. 1, Dover Publ., New York 1945.
[21] G. SZYCHLIŃSKI, *The tower clock of the St. Catherine Church* and *The tower clock of the Main-City Hall* [in Polish], Kartoteka konserwatora M. Gdańska 1991.

ARCHIVES OF ACOUSTICS
19, 3, 355–365 (1994)

INITIAL MODAL TESTING OF A CANTILEVER BEAM

E. SKRODZKA and E. HOJAN

Institute of Acoustic A. Mickiewicz University
(60-769 Poznań, ul. Matejki 48/49)

This paper is devoted to modal testing and to the problem of contactless measurements of a system response signal. The aim of investigation was to establish the best, contactless method for obtaining experimental data used in the process of modal analysis of vibrating objects. Measurements were carried out for a cantilever beam. The beam was excited manually by a small/large impact hammer with a force transducer. The response signal was measured by a microphone probe and a condenser microphone. For comparison, the response signal was also measured by an accelerometer. The spectra of both the exciting and the response signals were delivered to a dual channel analyzer from which the Frequency Response Function (FRF) was obtained. On the basis of FRFs, modal parameters (modal frequencies and mode shapes) were established. A comparison was made between experimental results and theoretical calculations.

1. Introduction

Some measurements were carried out for a cantilever beam. Modal parameters (modal frequencies and mode shapes) were extracted from a set of frequency response functions (FRFs).

By the definition [1], the Frequency Response Function (FRF) is a ratio between a displacement response spectrum and a force spectrum (in this case the FRF is called *receptance*); or a ratio between a velocity response spectrum and a force spectrum (*mobility*). When the "output" quantity is an acceleration, the FRF is called *inertiance* or *accelerance*.

Modal analysis is a technique applied in vibration analysis to describe the dynamic behaviour of structures. The analytical modal analysis [7] is an analysis of the structural mathematical model in order to find modal parameters of the structure. Mathematically it can be considered as the eigenvalue problem. Modal analysis has some limitations and imposes some assumptions on the object under investigation. The first assumption is that the structure is a linear system whose dynamics may be represented by a set of linear, second order differential equations. The second assumption is that the structure obeys Maxwell's reciprocity theorem. Maxwell's reciprocity theorem in terms of the frequency

response function measurements implies that the FRF measured between points i and j is identical with the FRF measured between points i and j. The third assumption is that the structure can be considered as a time-invariant system during the test. This assumption implies that the coefficients in linear, second order differential equations are constant and do not vary with time. The fourth assumption is that the dumping is small or proportional to the mass or stiffness. The last assumption states that excitation and response are measured at a point exactly.

Experimental modal analysis is a synthesis of the modal model on the basis of experimental data. Actually the mathematical structural model can be obtained. Experimental modal analysis is based on measurements of the set of Frequency Response Functions. Modal parameters like modal frequencies, modal dumping and mode shapes are extracted from these FRFs. Modal frequency is the system resonant frequency. Modal dumping is a dumping at a resonant frequency. A mode shape is a vibration pattern in a modal frequency.

When the set of modal parameters is found, curve fitting can be performed and mathematical modal model is obtained.

2. Aim

The main goals of investigation were:

a) Setting modal frequencies using two methods. According to the first of them (called the X-method), modal frequencies were those frequencies for which in the FRF modulus maxima appeared. In the second method (called the Y-method) modal frequencies were found as those for which a real part of an accelerance was zero and imaginary part reached an extremum [2];

b) An attempt to answer the question: is it possible to perform modal testing when the "response signal" is measured in a non-contact way by using a condenser microphone or a microphone probe?

Additional questions were those of the object linearity, mode shapes and choice of the best exciting tool (either a small impact hammer or a big impact hammer) for objects of medium mass.

Results were compared to theoretical calculations.

3. Measurements and theoretical calculations

The cantilever beam was an object under investigation. Physical parameters of the beam were: dimension $364 \times 45 \times 6.3$ mm, Young modulus of elasticity $E = 21 \cdot 10^{10}$ N/m^2, volume density $\varrho = 7850$ kg/m^3. There were chosen 6 measuring points, 2 cm, 8 cm, 13 cm, 20 cm, 28 cm and 34 cm distant from the rigid fixation point. In the first part of measurements the beam was excited in the point number 2 using either the BK 8202 big impact hammer (its mass was equal to about 209 g) or the BK 8203 small impact hammer (its mass was equal to about 4 g). In the second part of investigation the point number 4 was the excitation point. A response signal was measured either by an accelerometer or by a condenser microphone for free field measurements or by a microphone probe. The

microphone and the probe were 0.4 cm distant from the beam surface. Both the exciting and response signals were delivered to a dual channel analyzer. From the analyzer, the FRFs were obtained. The frequency range of measurements was of 0–4500 Hz.

Theoretically calculated frequencies [3] in the frequency range of interest for the above beam should be: 38 Hz, 239 Hz, 670 Hz, 1310 Hz, 2170 Hz, 3200 Hz and 4400 Hz. For these frequencies theoretical nodal points should be distant from the rigid fixation point of the cantilever as is listed in the Table 1.

Table 1. Distances of nodal points from the rigid fixation point of the cantilever

	x_0 [m]	x_1 [m]	x_2 [m]	x_3 [m]	x_4 [m]
f_1 = 38 Hz	0.0	—	—	—	—
f_2 = 239 Hz	0.0	0.282	—	—	—
f_3 = 670 Hz	0.0	0.182	0.316	—	—
f_4 = 1310 Hz	0.0	0.130	0.234	0.330	—
f_5 = 2170 Hz	0.0	0.101	0.182	0.263	0.337

4. Results

From the FRFs modal frequencies were extracted for the following pairs of measuring devices:

- the accelerometer — the big impact hammer,
- the accelerometer — the small impact hammer,
- the condenser microphone — the big impact hammer,
- the condenser microphone — the small impact hammer,
- the microphone probe — the big impact hammer,
- the microphone probe — the small impact hammer,

Examples of measured FRFs (point no. 2 — excitation, point no. 4 — response) for each pair of measuring devices are shown in Fig. 1–3.

For each pair of measuring devices frequencies "suspected" to be the modal frequencies should appear in 6 FRFs because of 6 measuring points at least 5 times. Distributions of theoretical nodal points and measuring points show that a measuring point can be placed in a nodal point at most once for each modal frequency. Another important parameter in the process of modal frequency extraction was a coherence function. "Suspected" frequencies for which the coherence function was less than 0.8 were neglected. For each pair of the measuring devices modal frequencies were found either as frequencies of the FRF modulus maximum (X-method) or as frequencies for which the FRF real part was zero and the FRF imaginary part had extreme value (Y-method). An assumption was made that the measured FRFs were accelerances. Because of the equipment accuracy it was impossible in Y-method to find the accurate frequency for which the FRF real component was equal to zero. In fact two frequencies were found for which the FRF real part had two different signs (positive-negative or negative-positive). From these two frequencies the one, corresponding to the greater value of the FRF imaginary part, was chosen as a "modal" frequency.

Using X-method and Y-method, there were found sets of 7 modal frequencies for the measurements that were carried out with the accelerometer in the response path (in the frequency range of interest there were also 7 natural frequencies!). When a response signal

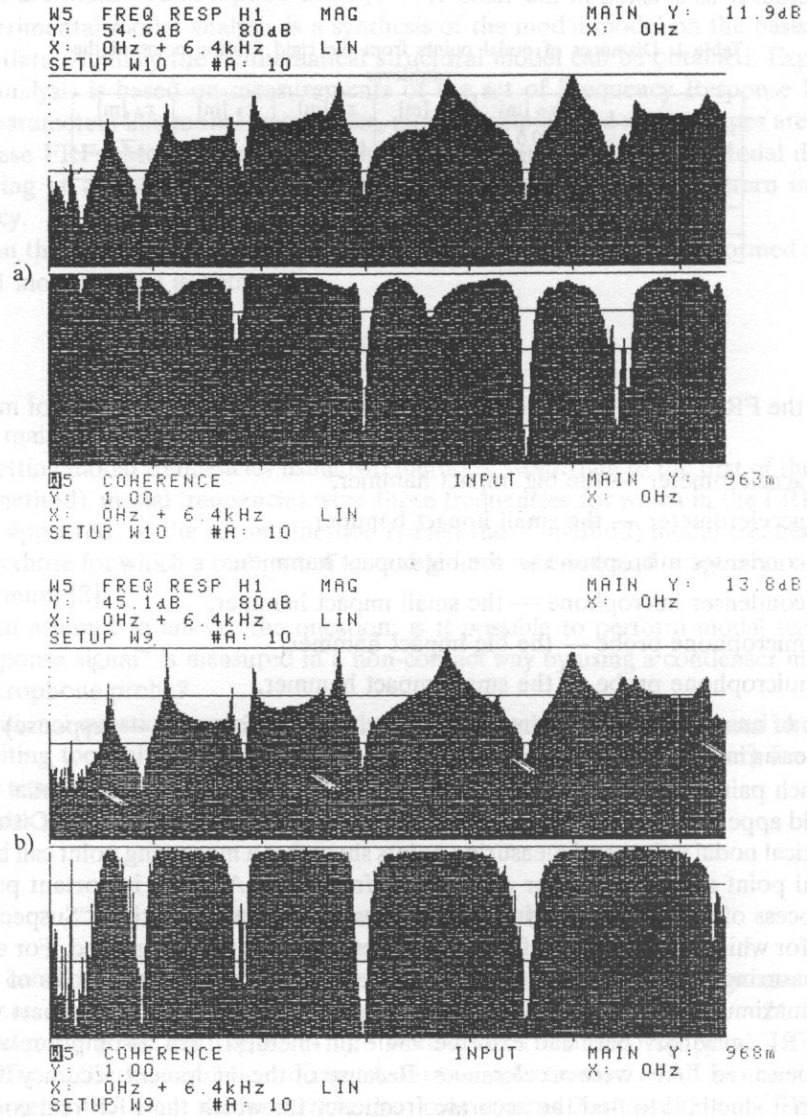

FIG. 1. Typical measured FRFs and coherence functions for
a) the accelerometer — the big hammer,
b) the accelerometer — the small hammer.

was measured by the microphone or the microphone probe, a sound pressure was a measured quantity. There is a limited range of frequency ($f < 1950$ Hz) in which the measured pressure is proportional to the acceleration of beams' vibrating point [6]. This leads to the

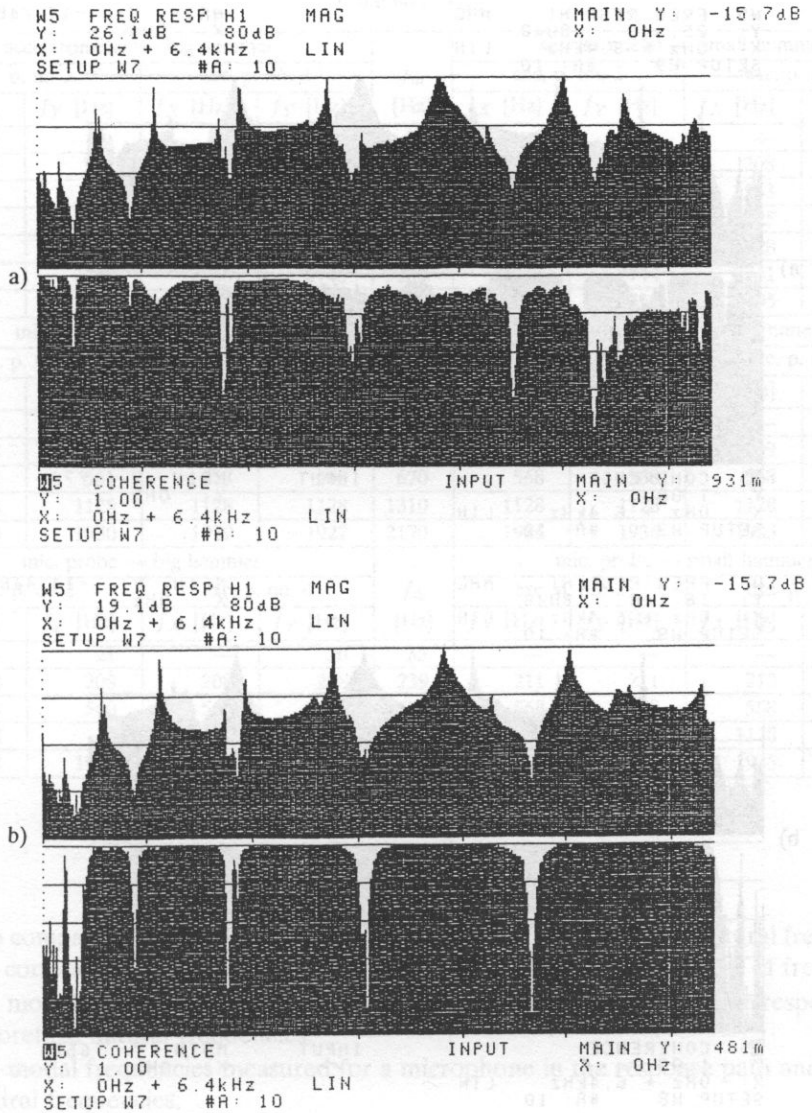

FIG. 2. Typical measured FRFs and coherence functions for
a) the condenser microphone — the big hammer,
b) the condenser microphone — the small hammer.

conclusion that only for frequencies less than 1950 Hz the measured FRF was the accelerance. This is the reason that only 5 modal frequencies measured by means of the condenser microphone probe were taken into account in further considerations.

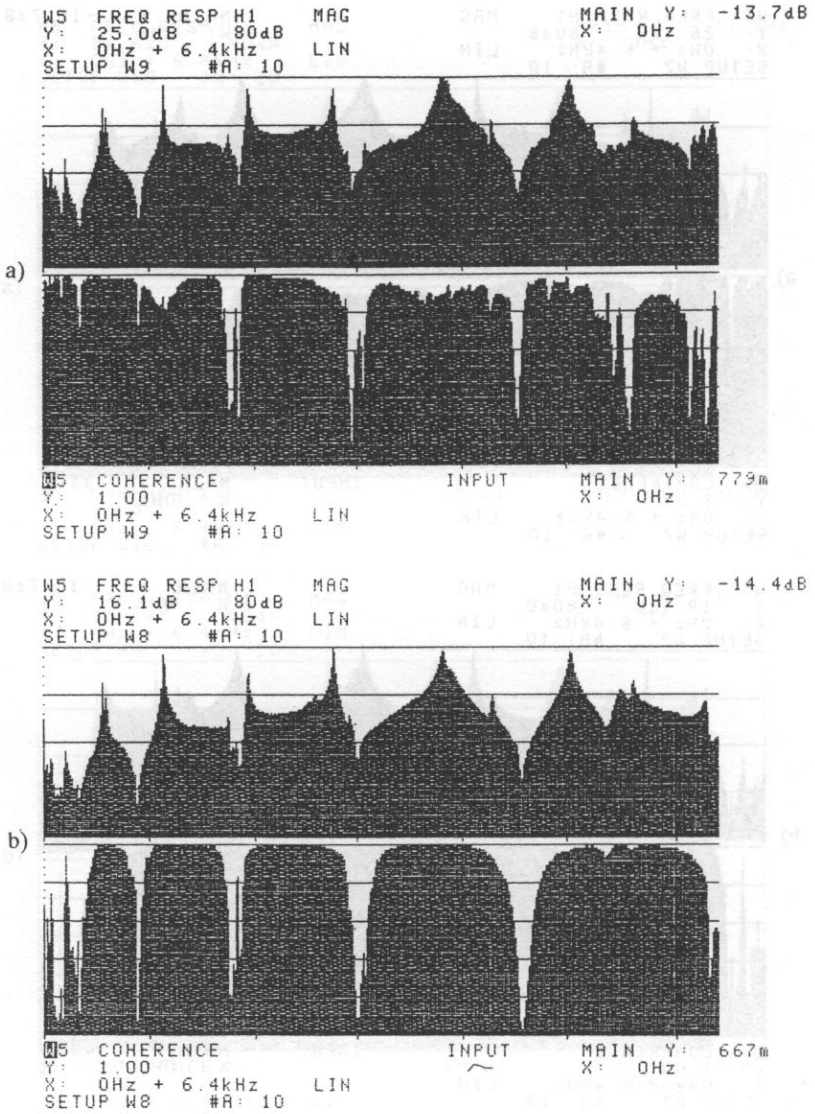

FIG. 3. Typical measured FRFs and coherence functions for
a) the microphone probe — the big hammer,
b) the microphone probe — the small hammer.

Some of these frequencies had not the same value for 6FRFs. They differed from each other by the value of measurement accuracy or more. In such cases the weighted mean value was calculated. The appropriate value of the coherence function was chosen as the weight. The results obtained are listed in the Table 2.

Table 2. Modal frequencies: theoretical — f_{th}, obtained using the X-method — f_X, obtained using the Y-method — f_Y

accelerometer — big hammer					accelerometer — small hammer			
exc. p. no 2		exc. p. no. 4		f_{th}	exc. p. no. 2		exc. p. no. 4	
f_X [Hz]	f_Y [Hz]	f_X [Hz]	f_Y [Hz]	[Hz]	f_X [Hz]	f_Y [Hz]	f_X [Hz]	f_Y [Hz]
28	—	35	16	38	—	—	—	—
209	208	208	208	239	208	208	208	208
561	560	563	568	670	561	565	563	563
1125	1125	1128	1128	1310	1128	1128	1125	1128
1928	1928	1928	1928	2170	1928	1928	1928	1928
2745	2740	2746	2746	3200	2743	2744	2741	2741
3809	3845	3802	3820	4400	3792	3796	3795	3801
microphone — big hammer					microphone — small hammer			
exc. p. no 2		exc. p. no. 4		f_{th}	exc. p. no. 2		exc. p. no. 4	
f_X [Hz]	f_Y [Hz]	f_X [Hz]	f_Y [Hz]	[Hz]	f_X [Hz]	f_Y [Hz]	f_X [Hz]	f_Y [Hz]
24	23	30	28	38	—	—	—	—
208	208	209	208	239	212	212	209	209
568	561	568	568	670	568	568	568	568
1128	1128	1128	1128	1310	1128	1128	1128	1128
1928	1930	1929	1922	2170	1936	1936	1933	1935
mic. probe — big hammer					mic. probe — small hammer			
exc. p. no 2		exc. p. no. 4		f_{th}	exc. p. no. 2		exc. p. no. 4	
f_X [Hz]	f_Y [Hz]	f_X [Hz]	f_Y [Hz]	[Hz]	f_X [Hz]	f_Y [Hz]	f_X [Hz]	f_Y [Hz]
—	21	—	30	38	—	—	—	—
208	208	208	208	239	211	211	212	208
568	560	568	560	670	568	568	568	568
1128	—	1128	—	1310	1128	1118	1128	1136
1928	1933	1928	1936	2170	1935	1935	1935	1935

5. Discussion

1. To compare the extracted modal frequencies and the theoretical natural frequencies, average correlation coefficients were calculated between the following sets of frequencies:

a) modal frequencies measured when there was accelerometer in the response path and theoretical natural frequencies.

b) modal frequencies measured for a microphone in the response path and theoretical natural frequencies,

c) modal frequencies measured for a microphone probe in the response path and theoretical natural frequencies,

d) modal frequencies measured for an accelerometer in the response path and modal frequencies measured for a microphone in the response path,

e) modal frequencies measured for a accelerometer in the response path and modal frequencies measured for a microphone probe in the response path.

Their values are shown on Fig. 4.

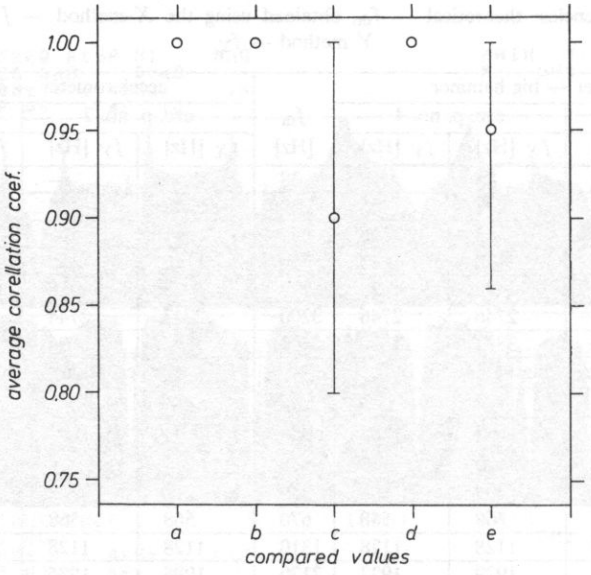

FIG. 4. Average correlation coefficients for results mentioned in 5.1.

It is clear that results obtained by means of the microphone probe in the response path are in a worse agreement with theoretical predictions and with the results obtained when there was the accelerometer in the response path. A good agreement between the results mentioned in b) and d) can be caused by the fact that the microphone was the free-field microphone, designed to compensate for the disturbance caused by its own presence in the sound field [5].

2. In order to compare the X-method and the Y-method of extracting modal frequencies, the following average correlation coefficients were calculated:

a) X-method results — theoretical predictions,

b) Y-method results — theoretical predictions,

c) X-method results — Y-method results,

d) X-method results with the accelerometer in the response channel — theoretical predictions,

e) Y-method results with the accelerometer in the response channel — theoretical predictions,

f) X-method results with the microphone in the response channel — theoretical predictions,

g) Y-method results with the microphone in the response channel — theoretical predictions,

h) X-method results with the microphone probe in the response channel — theoretical predictions,

i) Y-method results with the microphone probe in the response channel — theoretical predictions,

Their values are plotted on Fig. 5.

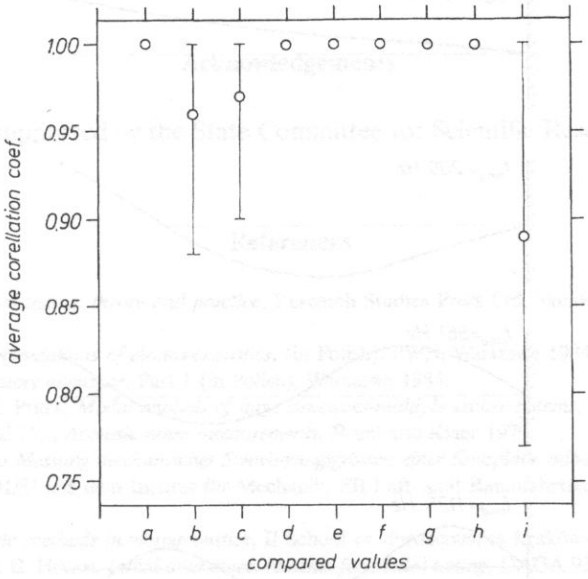

FIG. 5. Average correlation coefficients for results mentioned in 5.2.

It can be seen from Fig. 5 that the results obtained by the X-method correlate with theoretical values on the same level. The same can be seen for Y-method results except those for the microphone probe. This is the reason for slightly worse correlation between the X-method results and the Y-method results. Analysis of Fig. 5 leads to the conclusion that X-method and Y-method are of the same value. Poor results for the microphone probe are caused by a wrong definition of the FRF.

It seems to be worth pointing out that for frequencies extracted by the Y-method, FRF imaginary components reach extremes. It means that in same frequencies it is a maximum and in others — a minimum. It is caused by the fazor rotation of 180° for every next modal frequency.

3. Setting in order the average correlation coefficients considering excitation point no. 2 and no. 4 (without results for the microphone probe) leads to conclusions that the beam is the linear object. Object's linearity is one of the main assumptions of modal testing.

Taking into account Fig. 1–3 it can be seen that better coherence functions were obtained for the big impact hammer. It seems to be a rule using this tool for modal testing of all objects, except the cases when its high crest factor can cause damaging of the structure.

4. Examples of experimental mode shapes obtained from FRFs measurements for excitation by the big hammer and for the accelerometer in the response path are shown on Fig. 6. They are similar to those predicted by the theory.

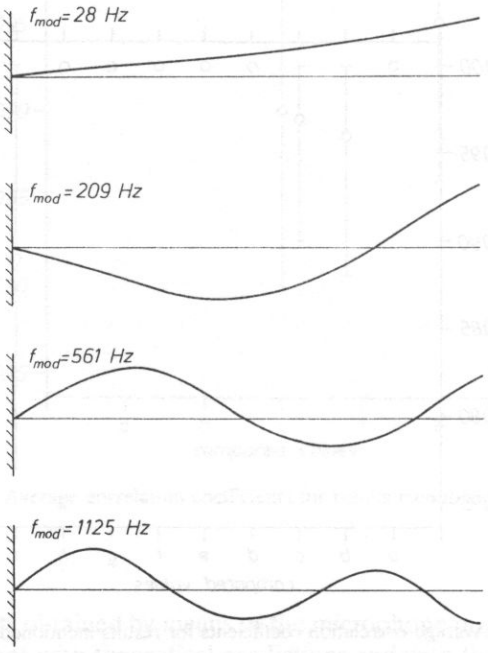

FIG. 6. Examples of measured mode shapes for the cantilever beam.

It should be pointed out that amplitudes of motion of measuring points are not envelopes of imaginary parts of FRFs.

These amplitudes were obtained by multiplication the FRF modulus by the cosine of a relative phase angle between points under investigation. Such procedure was caused, on one hand, by the fact that the extracted modal frequencies were close to real modal frequencies but not equal to them and, as a consequence, in the measured modal frequencies FRF real parts were not equal to zero. On another hand, modal dumping were in the range of 0.02–0.1. Both these facts gave their contribution to mode shapes.

6. General conclusions

• There is no difference between the X-method and the Y-method of extracting modal frequencies from FRFs. However, the Y-method seems to be more suitable, especially when experimental data are digitally processed.

• In a general case it is almost impossible to perform non-contact modal testing using in the response path a condenser microphone or a microphone probe. When a microphone is a condenser microphone for free field measurements, modal testing can be done but only in the narrow frequency range. The bigger is objects linear dimension the narrower is a frequency range.

• A big impact hammer with a force transducer should be used for every object under investigation providing it does not damage the structure.

• The cantilever beam under investigation was the linear object and its mode shapes were similar to those predicted be theory.

Acknowledgements

This work was supported by the State Committee for Scientific Research P.No 7 S101 053 4.

References

[1] D. J. Ewins, *Modal testing: theory and practice*, Research Studies Press Ltd, Taunton, Somerset, England 1988.

[2] Z. Żyszkowski, *Foundations of electro-acoustics*, (in Polish), PWN, Warszawa 1984.

[3] M. Kwiek, *Laboratory acoustics*, Part 1 (in Polish), Warszawa 1984.

[4] K. Zaveri and M. Phill, *Modal analysis of large structures-multiple exciter systems*, Bruel and Kjaer 1985.

[5] J. R. Hansall and Co., *Acoustic noise measurements*, Bruel and Kjaer 1979.

[6] H. Fleischer, *Zur Messung mechanischer Schwingungsgrössen einer Kreisplatte mittels Sondemikrofon*, Forschungsberichte 01/81 aus dem Institut für Mechanik, FB Luft- und Raumfahrttechnik, HBSw München 1981.

[7] T. Uhl, *Energetistic methods in vibroacoustics*, II School of vibroacoustics Kraków–Krynica, 51–58, 1992.

[8] E. Skrodzka and E. Hojan, *Initial data measurements for modal testing*, DAGA 93, Frankfurt amd Main, 1100–1103, 1993.

ARCHIVES OF ACOUSTICS
19, 3, 367–380 (1994)

THE FORMATION OF ONSET TRANSIENTS IN ROOMS MEASURED BY CROSSCORRELATION

J. ŻERA and M. DAROWSKA

Laboratory of Musical Acoustic Chopin Academy of Music
(00-368 Warszawa, ul. Okólnik 2)

A crosscorrelation measure for the degree of change in onset transients caused by reflections in a room was investigated. The measurements were based on a numerically modelled room. It was shown that the variability of the measure depends on the rise time of the source signal and on the delay of the measuring window from the beginning of the sound. The introduced measure is related to the early/late energy parameters of a room, and is associated with a subjective evaluation of the transients.

1. Introduction

The formation of transients in the acoustic signal appears to be an important effect of strong early reflections during the propagation of sound in rooms. Under certain conditions the change in the onset transient may be responsible for the perceived quality of the propagated sound. An acoustic transient may affect the intelligibility of speech. The intelligibility decreases when a delayed single reflection is added [13]. An acoustic transient may also affect the timbre of musical instruments. It is well known from the manipulations of onset transients in modern electronic music that onset plays a substantial role in timbre perception. A change in the onset influences the ability to identify correctly musical instruments [14]. Therefore, the nature and degree of the onset transient change in the transmission of the acoustic waveform through a room should be investigated to determine its influence on the subjective impression of the acoustic qualities of sound.

The formation of transients in the acoustic signals in rooms has received relatively little attention in the literature. The only work to which we may refer is that of CZARNECKI [6] who undertook a detailed analysis of amplitude and shape variations during the onset of sound for a relatively simple case with a limited number of sound reflections. He defined two independent sources of amplitude disturbances: "amplitude irregularity" and "phase irregularity". Czarnecki's study indicated that the amplitude irregularity depends only on the character of an impulse response of a room. This holds for signals with no specific phase across such frequency components as Gaussian noise. Phase irregularity appears for periodic signals and results from the interaction of the delays of reflected waveforms and the frequency of the propagated signal. The irregularity of the total waveform depends on the specific phases of superimposed reflections.

In the present work we are interested in how the source signal differs from the signal recorded at some observation point in a room and whether this difference is perceivable by a listener. A normalized crosscorrelation coefficient is used as a measure of this difference. The crosscorrelation function has been used primarily to study the spaciousness and diffuseness of sound fields in rooms [1–5, 11, 12, 15, 16]. These studies have focussed on the role of lateral reflections for binaural difference cues in creating the spatial impression of sound. The major finding was that the decrease of the crosscorrelation between lateral signals is related to the growth of the subjective impression of spaciousness. In the present study the crosscorrelation function is used to measure the degree to which the onset transient of a sound transmitted in a room remains similar to its origin, that is to the onset transient of the source signal. A similar approach has recently been used by CZYŻEWSKI [7] to compare the input and output signals of digital reverberators.

Measurements were made in the monophonic condition to simplify the analysis. The monophonic condition does not reflect all of the complexities of spatial impression involved in onset transient perception but is justified by the preliminary character of this investigation. Nevertheless, this investigation includes an analysis of a multiple set of reflections in three-dimensional space. This is a more realistic approach than that of CZARNECKI [6] who calculated patterns of transient buildups using the one-dimensional model.

The present research was designed to address the following questions:

a) What is the range of the predefined correlation between signals recorded at various observation and source points in a room.

b) How does this parameter depend on the impulse character of the source signal, and

c) What is the relation between the correlation coefficient and other parameters often used in room acoustics: reverberation time, early reverberation time, delay of first reflection, definition, clarity.

2. The crosscorrelation criterion for monophonic comparison of sound in a room

We seek a simple numerical parameter based on the CrossCorrelation function which would represent the similarity between the onset transient of the source waveform and the onset transient of the waveform received in a room. The source and the observation points are both located somewhere inside a room. This parameter, called the Maximum CrossCorrelation (MCC), is defined as the maximum absolute value of the crosscorrelation function determined over a specific observation time T:

$$\mathrm{MCC} = \max |R_{\mathrm{sr}}(\tau)|,$$

where

$$0 < \tau < T$$

$$R_{\mathrm{sr}}(\tau) = \int_{t}^{t+\Delta t} p_s(t) p_r(t+\tau)\, dt$$

MCC — maximum absolute value of the crosscorrelation function, $p_s(t)$ — source signal, $p_r(t)$ — signal recorder in a room, Δt — averaging time, $\langle 0, T \rangle$ — interval over which the crosscorrelation function is defined.

By calculating the maximum value of a correlation function, we can ignore the time delay between the signals p_s and p_r resulting from the distance between their respective locations. The MCC is simply a measure of the similarity between the signals $p_s(t)$ and $p_r(t)$ because they are compared with the relative delay revealing their best similarity.

The crosscorrelation function is, in a simple way, related to the autocorrelation function of the source signal because a recorder signal is obtained by convolving the source signal with the impulse response of a room. This relation may be used as an alternative way to calculate the crosscorrelation function. The MCC depends both upon the impulse response of a room and the source signal. In this study we concentrate on the investigation of the variability of the MCC for simple source signals, sinusoids of various frequencies.

3. Testing material

The calculation of the acoustical parameters and the synthesis of stimuli for the listening tests were based on a numerically modelled concert hall. In the model we adopted a geometrical shape and wall absorption coefficients similar to those existing in the chamber-music concert hall at the Chopin Academy of Music in Warsaw whose volume is about 800 m^3 (Fig. 1a).

The ray tracing method was used to obtain the impulse response of the room (KULOWSKI [9]). The impulse response of the room was calculated for octave-frequency bands at 250, 500, and 1000 Hz. Four source positions on the stage and twenty observation points in the audience space were investigated (Fig. 1b). We assumed that eighty echograms ($4 \times 20 = 80$) constituted a sufficient statistical representation of the possible reflection patterns in the modelled room. Each observation point was represented by a sphere of 0.5-m radius. For each combination of source and observation point, a total of 32.000 rays were emitted in random directions with equal probability to calculate the impulse response. Each ray was traced until the energy level became — 40 dB re its initial-value.

In typical application the impulse response of the room is obtained by cumulating energy arriving at the observation point in predefined time bins. This calculation, characteristic of a ray tracing method, is especially designed for calculating the energy of the room (e.g., reverberation time or energy arriving in specified time intervals) because the phase relations between reflected sounds are not preserved. The method is not sufficient, however, when it is necessary to obtain an amplitude response in which exact delays between wavefronts approaching the observer should be preserved. Those are essential to compute correctly the signal waveform at the observation point.

The following procedure was used to obtain correct estimation of the amplitude impulse response without forfeiting the phase relations. Each group of N rays moving in the same general direction, that is reflecting from the same set of walls, was separated. Then, this group was treated as representing a single equiphase surface propagating in a room. The energy associated with this surface was calculated as $E = \sum_1^N E_i$ (where E_i is the energy represented by a single ray) and its mean time of moving from the source to the observer as $\tau = (\sum_1^N \tau_i)/N$. Finally, the amplitude of a single peak in the amplitude impulse response was calculated as $A = \sqrt{E}$, and it was located at the time delay of τ.

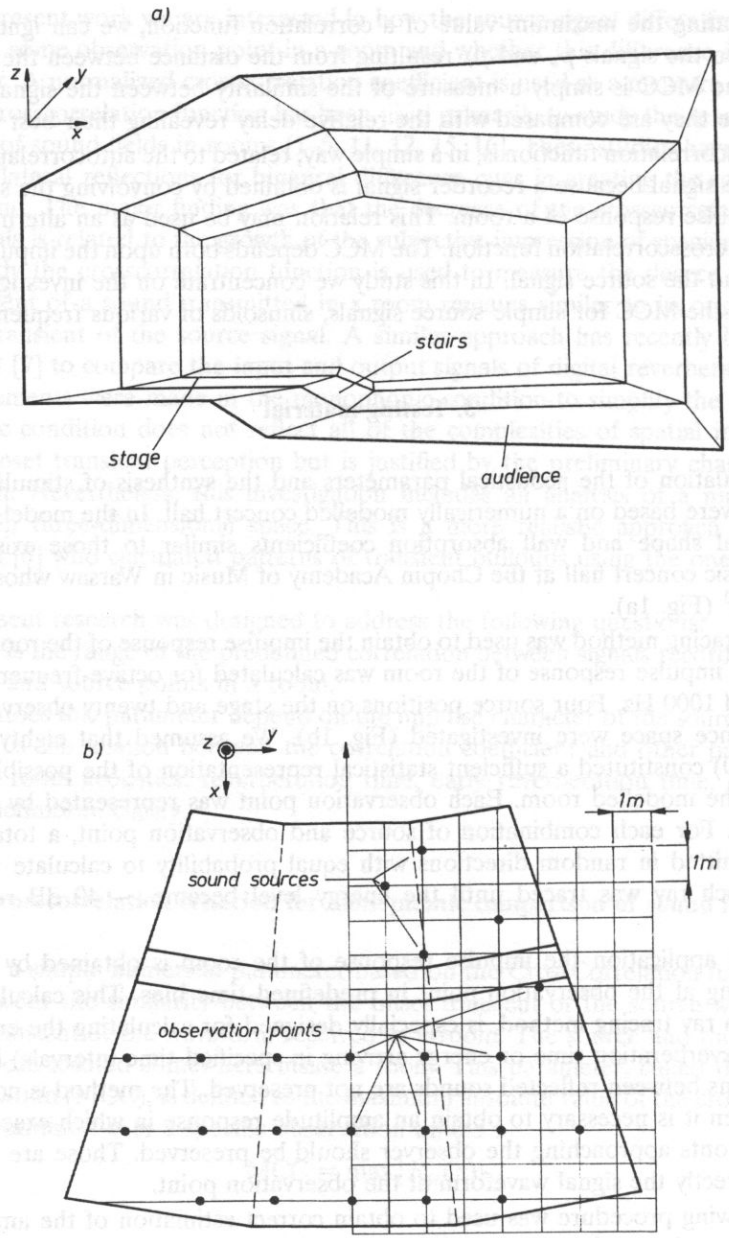

FIG. 1.
a) A three-dimensional view of the modelled room.
b) Horizontal view. Sound sources are positioned 1.2 m above the stage floor. Observation points are 1.3 m above the audience floor.

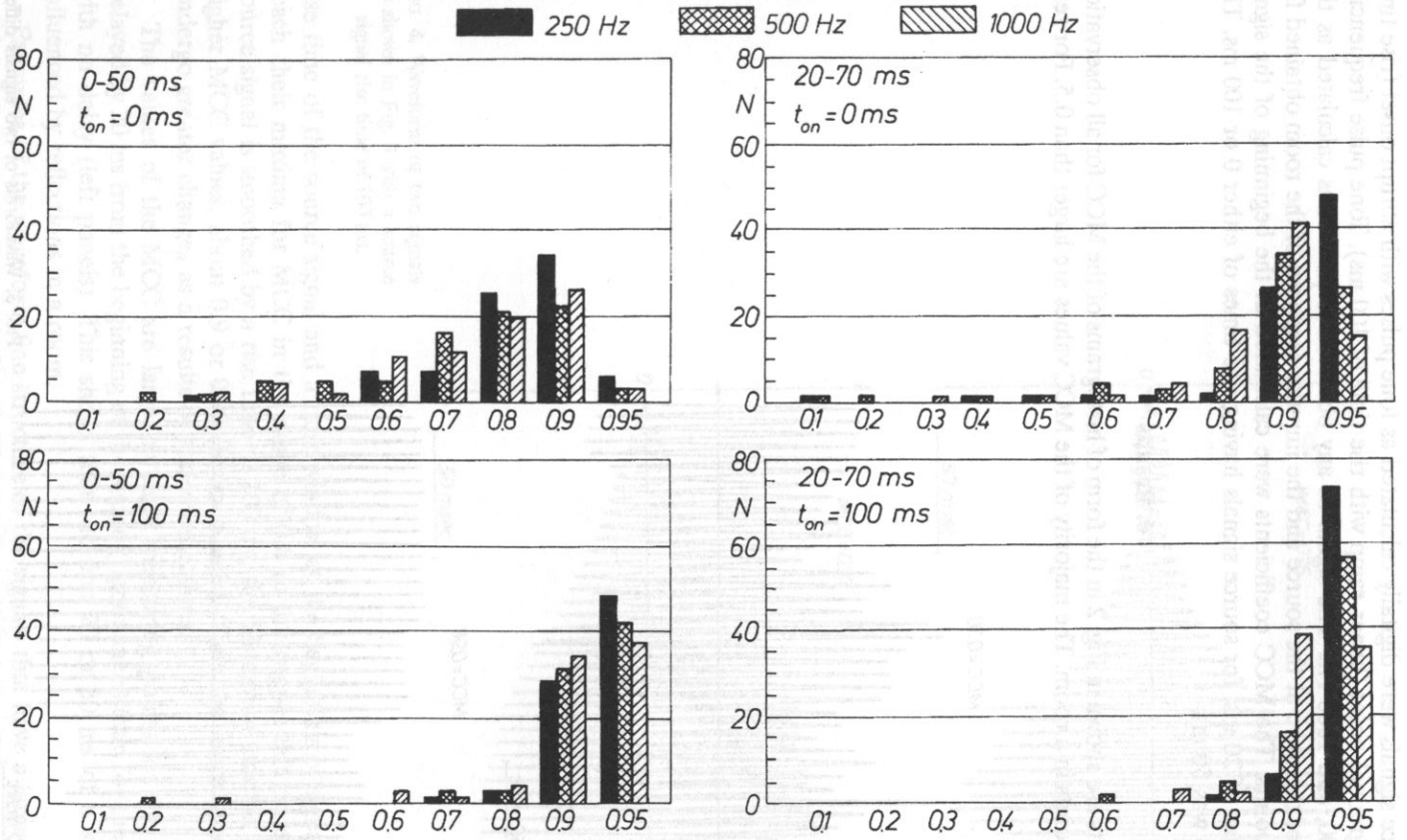

FIG. 2. Histograms of the Maximum CrossCorrelation coefficients (MCC) for pairs of source signals and signals received at observation points. The MCC values are calculated for the intervals 0–50 ms and 20–70 ms from the beginning of the sound. The source-signal rise time, T_{on}, is 0 or 100 ms. The source-signal frequency is 250, 500, or 1000 Hz.

The source signals were digitally calculated as tone pulses with abrupt onset (rise time of 0 ms) or gradual onset (linear ramp with rise time of 100 ms). Tone pulse frequencies were 250, 500, and 1000 Hz. The signal at any observation point was calculated as the convolution of the wave at the source and the impulse response of the room obtained for this pair of points. The MCC coefficients were calculated at the beginning of the signal or with a delay of 20 ms, for source signals having rise times of either 0 or 100 ms. The time window was 50 ms.

4. Results

The results are shown in Fig. 2 in the form of histograms of the MCC for all observation and source points in a room. The majority of the MCC values are larger than 0.5. For zero

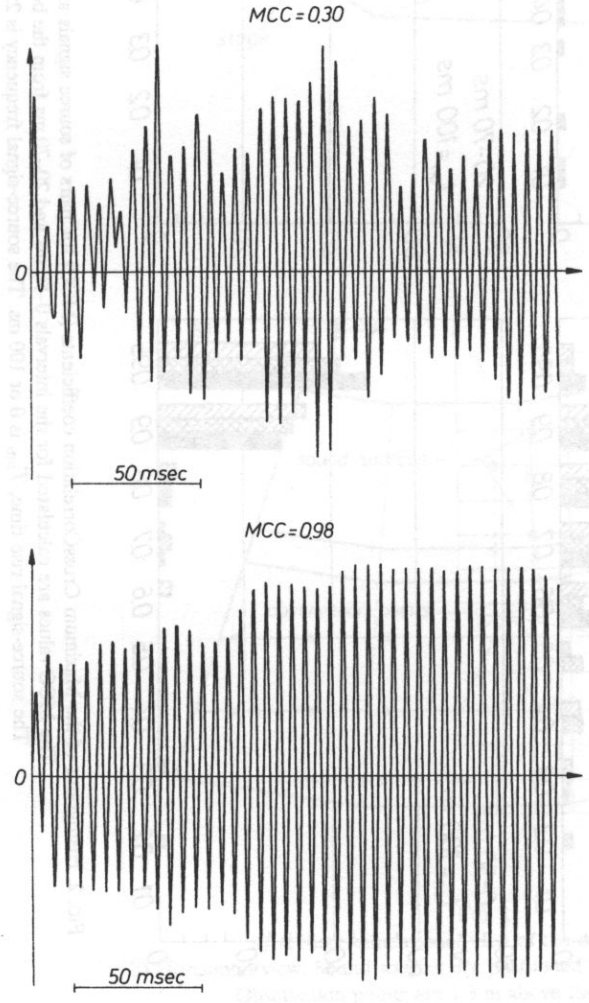

FIG. 3. Waveforms of two signals differing in MCC values. The rise time of the source signal is 0 ms.

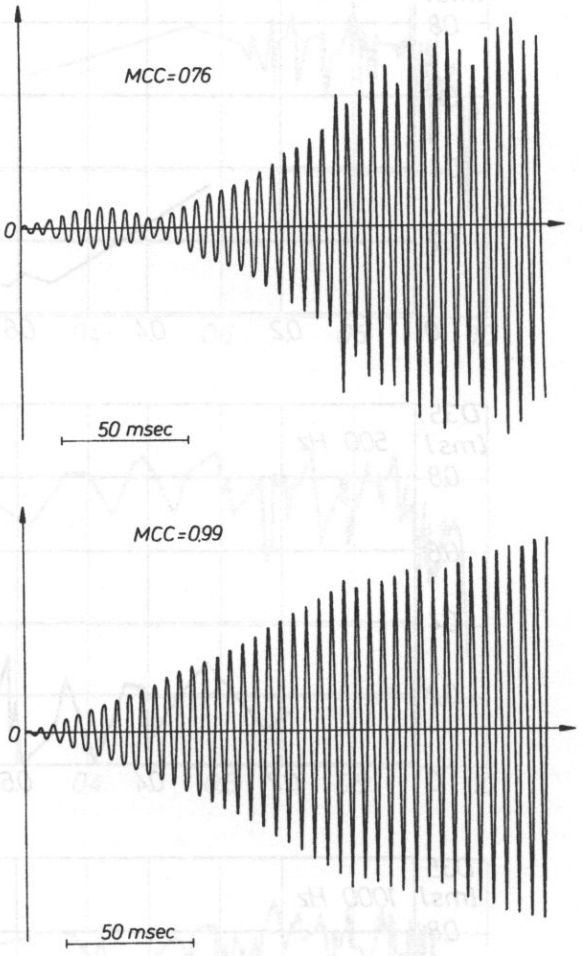

FIG. 4. Waveform of two signals as shown in Fig. 3 with a source signal rise time of 100 ms.

rise time of the source signal and a time window at the beginning of signal, histograms reach their maxima for MCC in the range of 0.8 to 0.9 (upper left panel). When the source signal is smoothed by a rise time of 100 ms, the histogram maxima are shifted to higher MCC values, about 0.9 or 0.95 (lower panels). Thus the more impulsive signals undergo greater changes as a results of added reflections.

The values of the MCC are larger at most measuring points for the time window delayed by 20 ms from the beginning of the sound (right panels) than for the time window with no delay (left panels). This shows that the first 20 or 30 ms of a signal is most influenced by reflections in a room.

Examples of the waveform fine structure of the signals that have a large difference in MCC coefficients are shown in Fig. 3. The amplitude envelope of the signal with MCC = 0.98 is relatively smooth and rises gradually to its steady state value (lower panel).

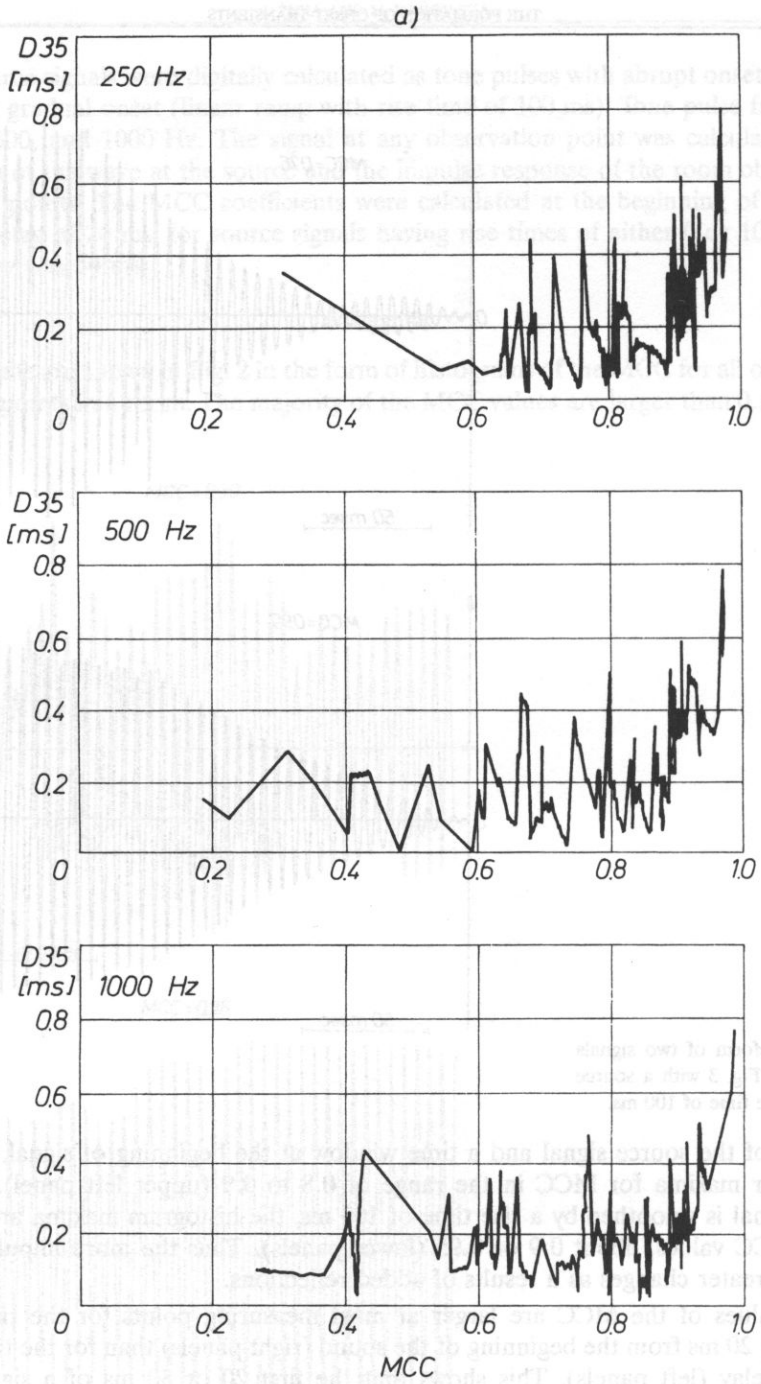

FIG. 5a. The relation between the MCC coefficient and the ratio of energy arriving in the first 35 ms, D35, of the echogram for the three signal frequencies.

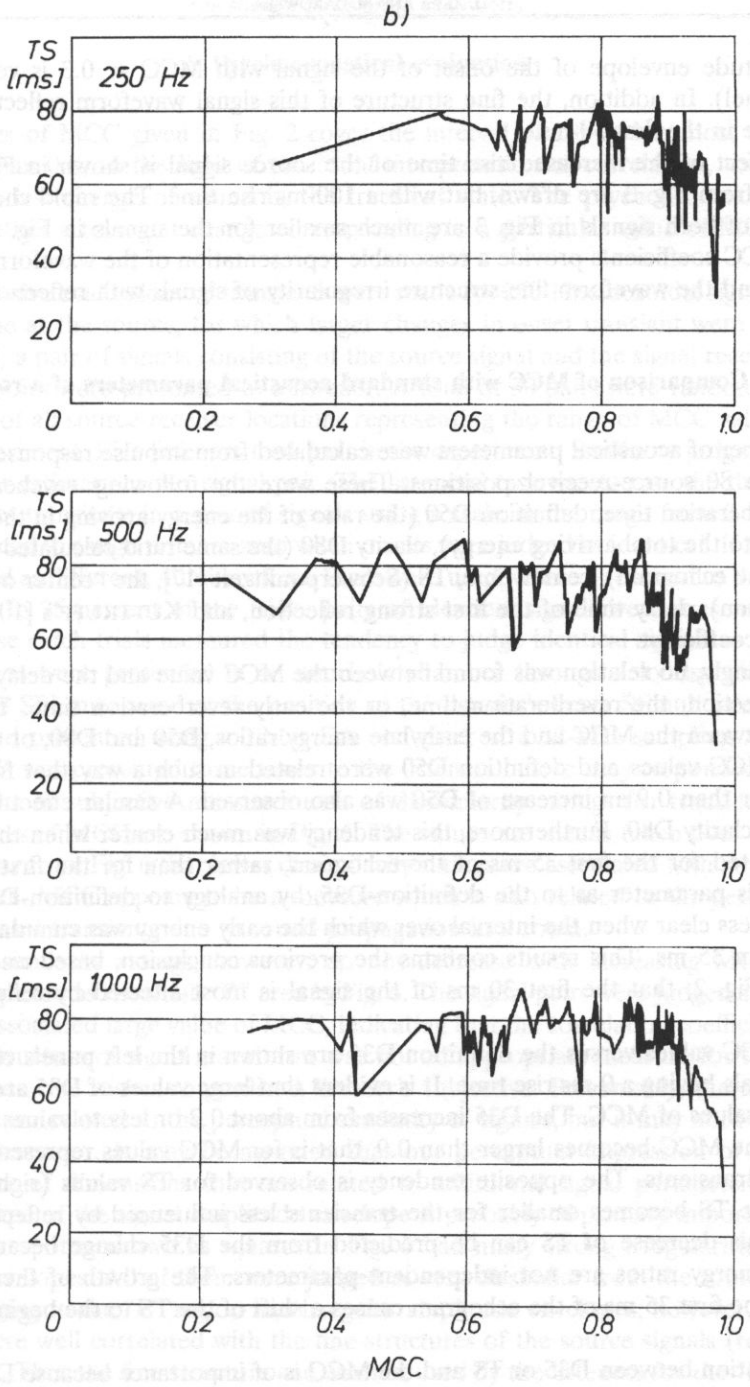

FIG. 5b. The relation between the MCC coefficient and center time, TS, of the echogram.

The amplitude envelope of the onset of the signal with MCC = 0.3 is very irregular (upper panel). In addition, the fine structure of this signal waveform reflects the phase disturbance in the first 50 ms.

The effect of the increased rise time of the source signal is shown in Fig. 4, where the signal from Fig. 3 are drawn, but with a 100-ms rise time. The rapid changes in the amplitude of both signals in Fig. 3 are much smaller for the signals in Fig. 4. Summing up, the MCC coefficients provide a reasonable representation of the waveform amplitude envelope and the waveform fine-structure irregularity of signals with reflections added.

5. Comparison of MCC with standard acoustical parameters of a room

A number of acoustical parameters were calculated from impulse responses of a room taken from 80 source-receiver positions. These were the following: reveberation time, early reverberation time, definition D50 (the ratio of the energy arriving in the first 50 ms of a signal to the total arriving energy), clarity D80 (the same ratio calculated for the first 80 ms of the echogram), center time, TS (Schwerpunktzeit [17], the "center of gravity" of the echogram), delay time of the first strong reflection, and KUTTRUFF's [10] "temporal diffusion" coefficient.

Surprisingly, no relation was found between the MCC value and the delay of the first strong reflection, the reverberation time, or the early reverberation time. There was a relation between the MCC and the early/late energy ratios, D50 and D80, or center time, TS. The MCC values and definition D50 were related in such a way that for values of MCC larger than 0.9 an increase of D50 was also observed. A similar effect was less apparent for clarity D80. Furthermore, this tendency was much clearer when the definition was calculated for the first 35 ms of the echogram, rather than for the first 50 ms. We refer to this parameter as to the definition-D35, by analogy to definition-D50. The results were less clear when the interval over which the early energy was cumulated became smaller than 35 ms. This results confirms the previous conclusion, based on histograms shown in Fig. 2, that the first 30 ms of the signal is most affected by reflections in a room.

The MCC values versus the definition D35 are shown in the left panels of Fig. 5, for source signals having a 0-ms rise time. It is evident that large values of D35 are associated with large values of MCC. The D35 increases from about 0.2 or less to values larger than 0.4 when the MCC becomes larger than 0.9, that is for MCC values representing a little change of transients. The opposite tendency is observed for TS values (right panels of Fig. 5). The TS becomes smaller for the transients less influenced by reflections (large MCCs). This decrease of TS can be predicted from the D35 change because TS and early/late energy ratios are not independent parameters. The growth of the amount of energy in the first 35 ms of the echogram causes a shift of the TS to the beginning of the echogram.

The relation between D35 or TS and the MCC is of importance because D35 (usually calculated as D50) and TS are parameters applied in room acoustic. Thus the present results show that these standard parameters are useful in estimating the size of the change in the onset of the signal after a transmission through the room. Only a small change in transients should be expected when the value of D35 is greater than 0.4.

6. Psychoacoustical evaluation

The values of MCC given in Fig. 2 cover the interval of 2.0 to 1.0, most values being greater than 0.8. In the light of the usual interpretation of correlation, these values suggest a modest change of sound in the transient state. The psychoacoustic data will establish whether a transient change corresponding to a particular value of MCC is perceptible.

The subjective evaluations of transients were made for 250-Hz sinusoidal signals having 0-ms rise time at the source, for which larger changes in onset transient were observed. On each trial, a pair of signals consisting of the source signal and the signal received at an observation point were presented to a listener. A total of 30 pairs were randomly chosen from the set of all source-receiver locations representing the range of MCC values in the previous experiment. Five listeners took part in the experiment. Similarity judgments were based on four estimations per signal pair. The listeners' task was to rate the dissimilarity between onset transients in a pair of signals using a scale in the range from 0 to 6. They were introduced to assign number zero when onsets were judged as identical. If the signals were regarded as different, numbers from 1 to 6 were used, where 6 referred to the greatest dissimilarity. In 25 percent of the trials, pairs of identical signals were presented to the listener. These catch trials measured the tendency to judge identical signals as different.

The sounds were presented in an anechoic chamber through a loudspeaker (Alton 140) at 60 dB SPL measured at the position of the listener's head. Stimuli were digitally calculated and presented using a 12-bit DA converter at a 32-kHz sampling rate. Each pair of signals was presented three times to the listeners before they responded.

The results of subjective measurements of dissimilarity ratings for transients having different values of MCC are shown in Fig. 6. The values are means taken over three subjects. It is clear from Fig. 6 that lower dissimilarity ratings are associated with larger values of MCC. Then, MCC appears to be a measure which is also related to the perception of changes in onset transients due to sound propagation in a room.

Some dissimilarity ratings, however, do not decrease with increasing MCC. These points are depicted as the small "B" area in Fig. 6. The signal pairs were judged as different despite the associated large value of MCC, indicating that the correlation coefficient based on the fine structure of signal waveforms was not an appropriate measure for these pairs of signals when one wishes to predict a listener's subjective. Presumably, the correlation is a major factor related to the perceptual similarity of signals, but it may not be the only important parameter. It may be assumed that our perceptual impression of transients has a number of dimensions that are related to additional signal parameters. Among them, the shape of the signal amplitude envelope is probably of primary importance. The signals with response shown as squares in Fig. 6 had many strong irregularities in their amplitude envelopes. All of them were judged as very dissimilar from the source signals. Those belonging to the "B" region had irregular amplitude envelopes; however, their fine structures were well correlated with the fine structures of the source signals (resulting in large MCCs). Thus the fine structure cue was not used by the listeners for the "B" region. It is possible that the envelope cue was used.

Finally, it should be stressed that pairs of signals with the highest correlation (MCC > 0.99) were clearly recognized as different by the listeners. There is no critical value of MCC in Fig. 6 above which the stimuli taken at observation points would become

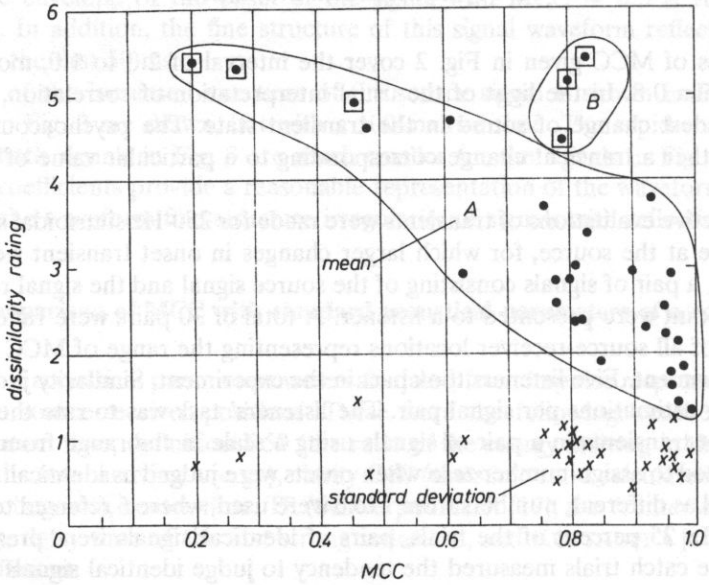

FIG. 6. Dissimilarity ratings for pairs of source signals and signals received at observation points. "A" — the set of results showing a decrease in dissimilarity as MCC increases. "B" — points showing no such relation. Circles within boxes show the results for stimuli of with onsets having many irregularities. The stimulus frequency is 250 Hz.

indistinguishable from the source signals. Due to the fact that all signals in the control catch trials were correctly judged as identical, it is clear that the subject's responses were not biased toward a judgement.

7. Conclusions

It was shown that the maximum value of the crosscorrelation function (MCC) between the source waveform and waveform corresponding to an observation point in a room calculated over the first 50 ms of signal durations is a parameter that describes well transient changes due to reflections in a room. This parameter is sufficiently sensitive to differentiate numerically between pairs of signals at different locations in a room. In our model of a room MCC values ranged from 0.2 to 1.0.

Relations of MCC to two well recognized parameters in room acoustic, the definition D35 and TS, were obtained. These relations predict that for values of D35 greater than 0.5, reflections will have a very small influence on onset transients.

Finally, dissimilarity ratings from human observers show that the MCC parameter is related to the subjective evaluation of the transients. The ear appears to be rather sensitive to transient build up associated with room reflections, as the transients were easily distinguished from their sources even for MCC larger than 0.99.

These conclusions should be treated with some caution as the data presented in this work were calculated for only one model room, a medium size chamber concert hall. This model hall corresponds to an existing hall with good acoustical characteristics. Rooms of different sizes and having different subjective evaluations are to be examined in future work.

As a final note, some musical interpretation may be made basing on the obtained results. The data shown in Fig. 2 suggested that the influence of reflections is the strongest during approximately the first 30 ms of a signal and for signals having short onset times. The sounds of many instruments have onset times shorter than 50 ms. It has been reported [8] that guitars subjectively rated as having superior sound quality have rise times in the range of 30 to 70 ms, with quality ratings diminishing for shorter rise times (e.g., less than 20 ms). This would be consistent with the notion that the sound produced by instruments judged as having superior sound quality are less disturbed by room reflections than the sound of instruments judged as having poor sound quality. Quality ratings for the sound of such instruments should be less dependent on the sound field in a room, including the listener and performer position.

Acknowledgments

The authors are very indebted Dr Andrzej KULOWSKI for his computer program of the ray tracing method, which he made available. We thank Mr. David EDDINS, Dr Antoni Jaroszewski and Dr Beverly WRIGHT for their comments on the earlier draft. We also thank Dr Witold STRASZEWICZ for his helpful criticism and discussions. This work was supported by the grant number CPBP 02.03.VIII.8.2 from the Polish Academy of Sciences.

References

[1] Y. ANDO, *Subjective preference in relation to objective parameters of music sound fields with a single echo*, J. Acoust. Soc. Am. **62**, 1436–1441 (1977).

[2] Y. ANDO, K. KAGAYAMA, *Subjective preference of sound with a single early reflection*, Acoustica **37**, 111–117 (1977).

[3] Y. ANDO, D. GOTTLOB, *Effects of early multiple reflections on subjective preference judgements of music sound fields*, J. Acoust. Soc. Am. **65**, 524–527 (1979).

[4] Y. ANDO, M. IMMAMURA, *Subjective preference tests for sound fields in concert halls simulated by the aid of computer*, J. Sound Vib. **65**, 228–239 (1979).

[5] Y. ANDO, Y. KURIHARA, *Nonlinear response in evaluating the subjective diffuseness of sound fields*, J. Acoust. Soc. Am. **80**, 833–836 (1986).

[6] S. CZARNECKI, *Irregularities in acoustic signals in rooms*, Doctoral thesis, Institute of Fundamental Technological Research, Polish Academy of Sciences, (1958) (in Polish).

[7] A. CZYŻEWSKI, *A method of artificial reverberation quality testing*, J. Audio End. Soc. **38**, 129–140 (1990).

[8] A. JAROSZEWSKI, A. RAKOWSKI, J. ŻERA, *Opening transients and the quality of classic guitars*, Archives of Acoustic **3**, 79–84 (1978).

[9] A. KULOWSKI, *Computer modelling of acoustic field in rooms*, Scientific report CPBP 02.03. VIII.8.6 (1989) (in Polish).

[10] H. KUTTRUFF, *Uber Aotukorrelationmessungen in der Raumakustik*, Acustica **16**, 166–174 (1965/66).

[11] J. P. A. LOCHNER, J. F. BURGER, *The subjective masking of short time delayed echoes by their primary sounds and their contribution to the intelligibility of sounds*, Acustica **8**, 1–10 (1958).

[12] R. W. MUNCLEY, A. F. B. NICKSON, P. DUBONT, *The acceptability of speech and music with a single artifical echo*, Acustica **3**, 168–173 (1953).

[13] T. NAKAJIMA and Y. ANDO, *Effects of a single reflection with varied horizontal angle and time delay on speech intelligibility*, J. Acoust. Soc. Am. **90**, 3173–3179 (1991).

[14] P. SCHAEFFER, *Traité des objets musicaux*, Editions du Seuil, Paris 1974.

[15] M. R. SCHROEDER, D. GOTTLOB, K. F. SIEBRASSE, *Comparativestudy of European concert halls: correlation of subjective preference with geometric and acoustic parameters*, J. Acoust. Soc. Am. **56**, 1195–1201 (1974).

[16] H. YANAGAWA, Y. YAMASAKI and T. ITOW, *Effect of transient signal length on cross-correlation functions in a room*, J. Soc. Acoust. Am. **84**, 1728–1733 (1988).

[17] M. VORLANDER, *Ein Strahlverfolgungs-verfahren zur Berechnung von Schallfeldern in Raumen*, Acustica **65**, 138–148 (1988).

ARCHIVES OF ACOUSTICS
19, 3, 381–393 (1994)

ON GENERATING ULTRASOUNDS BY LASER IN POLYMERS

L. RADZISZEWSKI

Chair of Mechanical Equipment
Kielce University of Technology
(25-314 Kielce, Al. 1000-lecia P.P. 7)

The paper reports an experimental investigation of the possibility of generating ultrasonic waves by a Q-switched Nd:YAG laser of small power in polymers by the example of polyvinyl chloride. The possibility of creating acoustic-point-sources in visco-elastic materials is confirmed. Explanation of the mechanism of generation of ultrasonic waves is proposed. Directivity amplitude patterns of the acoustic sources are determined using ultrasonic broadband of resonance frequencies: 1 MHz, 2.25 MHz, 5 MHz, and a head for acoustic emision. The directivity frequency pattern for a head 2.25 MHz is also determined.

1. Introduction

Although the idea of the research on the application of light to the generation of acoustic waves, which comes from BELL [1], appeared quite a long time ago (1881), intensive experimental investigations were started in the early 1960 s, after the invention of the laser. The present paper is a contribution to this research. However, in order to have a better understanding of the validity and purposefulness of the investigation presented in this paper, it will be probably to provide at the outset a brief historical overview of the research in question. Thus, quite an extensive introduction to the present article is motivated by the fact that it contains an approach to this research which is not often met in the literature.

The problem of thermally generated elastic impulses, which is always involved in the generation of ultrasound waves by laser radiation, was considered for the first time by DANILOVSKA [2], who employed equations of classical thermoelasticity to the description of the phenomenon. Appearance of new sources of intensive light, lasers, which make possible generation of a strong photo-acoustic effect, drew more interest to this phenomenon in recent years. Very accurate sensors (capacitance transducer, mode of PZT ceramic) have become available for the measurement of elastic waves. Application of lasers for generation of elastic waves in solids was described for the first time by WHITE in 1963 [3]. He considered the problem of the way in which the change in the temperature of the surface of an elastic half-space exerts an influence on stresses in the investigated point of

a half-space depending on time and distance from its surface. A theoretical description (one-dimensional model of wave generation in solid body by a laser) was given by READY in 1965 [4] and BUSHNELL and MCCLOSKEY in 1968 [5]. In the first experimental investigations lasers of a very high power (greater than 10 MW) were used. It always caused a significant damage of the metal surface. The metal surface on which the waves were generated was either not modified (e.g. PENNER and SHARMA — 1966 [6]) or modified (e.g. FELIX — 1974 [7]). A common feature of these first works was also the fact that not much attention was given to the kinds of waveform which could be generated. Although LEE and WHITE showed in 1968 [8] that Rayleigh's waves could also be generated by a Q-switched ruby laser, until 1979 there were no publications which dealt with simultaneous laser generation in metal of longitudinal, shear and Rayleigh's waves. It was LEDBETTER and MOULDER in 1979 [9] who showed that neodymium laser of high energy (0.3–1 J) and focused light beam could simultaneously generate volume and surface waves in metals. AINDOW *et al.* demonstrated in 1981 [10] that a Q-switched ND:YAG laser of a much lower energy (ca 30 mJ) could be used to generate ultrasound pulses, both in aluminium and in steel. He observed generation of pulses of volume and surface waves with densities of the power of laser beam both below and above the ablation threshold, after which damage of a metal surface follows. It was perhaps the first work in which the mechanisms of wave generation were divided into the thermoelastic and ablation mechanisms, and their relative efficiencies was determined. In that investigation a piezoelectric transducer was employed as the receiver. It distorted, to a certain degree, the output electric signal which was the image of the recorded wave. It is sufficient in many applications that a thermoelastic source of ultrasound can be treated as a point dipole and the ablation source- as a point force normal to the free surface SCRUBY *et al.* 1980 [11]. Equations of directivity patterns for the thermoelastic and ablations sources were presented by SCRUBY *et al.* in 1982 [12]. Theoretical calculations and experimental measurements of the shape of the impulse on the surface were presented by DEWHURST *et al.* in 1982 [13]. In 1980, Scruby proposed to use, as model of the thermoelastic source on free surface of metal pair of equivalent forces acting parallel to this surface (Fig. 1a). In 1984 [14] ROSE expounded Scruby's model basing on point temperature source acting on the metal surface, and provided a precise analytical solution. In 1984 [15] WADLEY showed that experimental measurements were in good agreement with the above models, with the exception for a small positive "precursor" in the epicenter, whose source of origin was not well-known. The calculated and experimental directivity patterns complied with each other, in particular if finite dimensions of both the acoustic source and the receiver were taken into consideration. In 1986 [16] DOYLE extended Rose's work by integrating Green's elastic function in the whole material volume in which temperature was growing. He showed that the finite dimensions of the source followed from thermal diffusion inside the plate and they were the main cause of the "precursor" occurring in the waveform in the epicenter. SCHLIECHERT [17] and AUSSEL [18], using different calculation methods, confirmed independently Doyle's results. In 1989 [19] CONANT and TELSCHOW applied the Hankel-Laplace transform to the calculation of laser-generated thermoelastic disturbance in a plate (they neglected thermal conductivity, but took into account finite depth where electromagnetic wave was absorbed). Those authors suggested that finite dimensions of the source in time and space could be the cause of the "precursor" to appear. In 1989 [20], MCDONALD provided a new description of the source of laser-generated ultrasounds. He

was basing on the generalized theory of thermoelasticity, and calculated numerically the inverse Henkel-Laplace transform. This author suggested that the "precursor" resulted from conversion of thermal wave to the acoustic one at the plate surface. An essentially new element resulting from the generalized theory of thermoelasticity is the adoption of the hyperbolic equation of heat transport, which causes finite velocity of heat propagation (normally a little higher than the velocity of longitudinal wave).

The ablation source of ultrasounds is described in a less precise way, but more intuitively. Physical phenomena occurring during that mode of laser work were described by READY in 1971 [21] and next by KREHL *et al.* in 1975 [22]. Directivity pattern of ablation source was provided by HUTCHINS *et al.* in 1981 [23] for longitudinal wave and COOPER in 1985 [24] for shear wave. The shape of ablation-generated waves in the epicenter was given by DEWHURST *et al.* in 1982 [13]. Approximate model calculations for ablation source were given by AUSSEL *et al.* in 1988 [18], as well as by SCRUBY and DRAIN in 1990 [25]. Problems of laser generation and ultrasound propagation were much less frequently analyzed for plastics and composite materials than for metals. In 1971 [21], READY determined the temperature distribution in non-metal (a one-dimensional model) after absorption of an electromagnetic wave sent from the laser. In 1985 [26], BOURKOFF and PALMER were perhaps the first to investigate the possibility of a small power laser generation (using visible light) of ultrasounds in non-metals (polyamid reinforced by glass fibres and epoxy reinforced by carbon fibres). They used a PZT transducer or interferometer as a receiver. In 1988 [27] BUTTLE applied a pulsed laser and point piezelectric transducer to investigate the propagation of elastic waves in composites of epoxy resin reinforced by glass or carbon fibers. In 1989 [28] CASTAGNEDE *et al.* investigated the elastic properties of polyester reinforced by glass fibers. A pulsed laser was the source of ultrasounds and a point transducer from PZT-ceramic was used as the receiver. In 1990 [29] TAYLOR *et al.* applied an industrial laser TEA CO_2 for ultrasounds generations in polymers. He obtained a good conformity of the results of the waveform measurements with Rose's theory [14], under the assumption that the ultrasound source is at a long distance ca 200 μm from the material surface. Taylor's results are confirmed by [19], in which an experimental and theoretical investigations was made on the effect of the position of the thermoelastic source of ultrasounds under the surface of material, up on the waveform. In 1993 [30] POUET and RASOLOFOSAON applied a laser to the generation and reception of ultrasound waves in different polymers, in order to measure internal friction and dispersion of the velocity of longitudinal wave. In 1993 [31] CORBEL *et al.* measured and calculated the directivity amplitude pattern of laser — generated waves in composites of various degrees of an isotropy, made from epoxy resin reinforced by carbon fibers.

The object of interest of the present Author is the propagation of laser-generated ultrasound waves in plastics, and therefore this paper refers to the investigations [19, 29, 30] and to some, degree, it is their continuation. The purpose of this work was to carry out experiments which would enable: 1) examination of the possibilities of a small power pulsed laser generation of ultrasound waves in non-metals of visco-elastic properties, on the example of isotropic polyvinyl chloride; 2) determination of the directivity patterns of the acoustic point source using commercial ultrasonic heads made from PZT-ceramic. There is a need to provide more precise interpretation of the results of acoustic measurements in non-metals and composite materials by the acousto-ultrasonic and acoustic emision methods. Therefore, the subject of this investigation will be the problems connected with

optical generation and propagation of elastic waves. It seems relevant to provide a short discussion in Section 2 of the basic mechanisms of this generation in order to familiarize the Reader with the description of experimental investigations provided in Section 3.

2. Basic mechanisms of optical generation of elastic waves

2.1. Thermoelastic excitation

A laser beam, incident on a free surface of a optically opaque solid body, is partly reflected and partly absorbed. In metals, absorption of an electromagnetic wave is mainly caused by interaction with its electrons and it occurs on the so-called skin layer of thickness of about 0.1 nm. A significant role is also played by heat diffusion during generation of an elastic wave. It causes the source of sounds to be "displaced" inside the material. In polymers the coefficient of absorption γ of the electromagnetic wave, caused by vibrations of atoms or group of atoms excited by the electromagnetic wave, is relatively small contrary to the case of metals. It causes the wave to penetrate inside the material to a significant depth ($d = 1/\gamma = 0.1$–1 mm). For polymers the phenomenon of heat diffusion can be negligible and heat conductivity is very small. As a result, heat flow from the area where the electromagnetic wave was absorbed is negligible (in the scale of the source time) and it is about 0.1 nm. The energy of laser radiation absorbed is transformed into heat. In this way the volume element in which absorption of electromagnetic radiation occurs becomes heated and deformed. Instantaneous spatial deformation of this volume element leads to radiation of the elastic waves (Fig. 1a). In the heated volume element a compressions wave (L) is initially created. Shear (S) and surface (R-Rayleigh) waves are created on the surface of a solid as a result of transformation of the compressions waves. The compression wave falls on the surface of a solid also generates a head wave (H), its front having the form of a spherically truncated cone and which is tangential, under a precisely defined angle, to the shear wave (Fig. 2). Volume waves generated in the isotropic medium are propagated approximately as spherical waves. The mechanism of thermoelasticity of generating acoustic wave occurs most frequently under densities of laser light powers smaller than 10 MW/cm^2. Increasing the power density over this value, we can trigger an additional mechanism which generates acoustic waves, the so-called ablation mechanism. Further growth of the power density up to about 1 GW/cm^2 will cause a continuous change of the signal structure and a systematic increase in its amplitude. Above this power value, the plasma formed on the surface of the sample screens the access of laser radiation to the material and the signal amplitude decreases.

2.2. Ablation excitation

Under the density of power specific for each material the ablation mechanism, which consists in rapid evaporation of a part of the material, leaves behind a small crater in the surface layer. It follows from the principle of conservation of momentum and impulse force that the above loss of material in the surface later is the cause of the effect of a certain instantaneous pressure exerted on the crater surface — in this way an acoustic

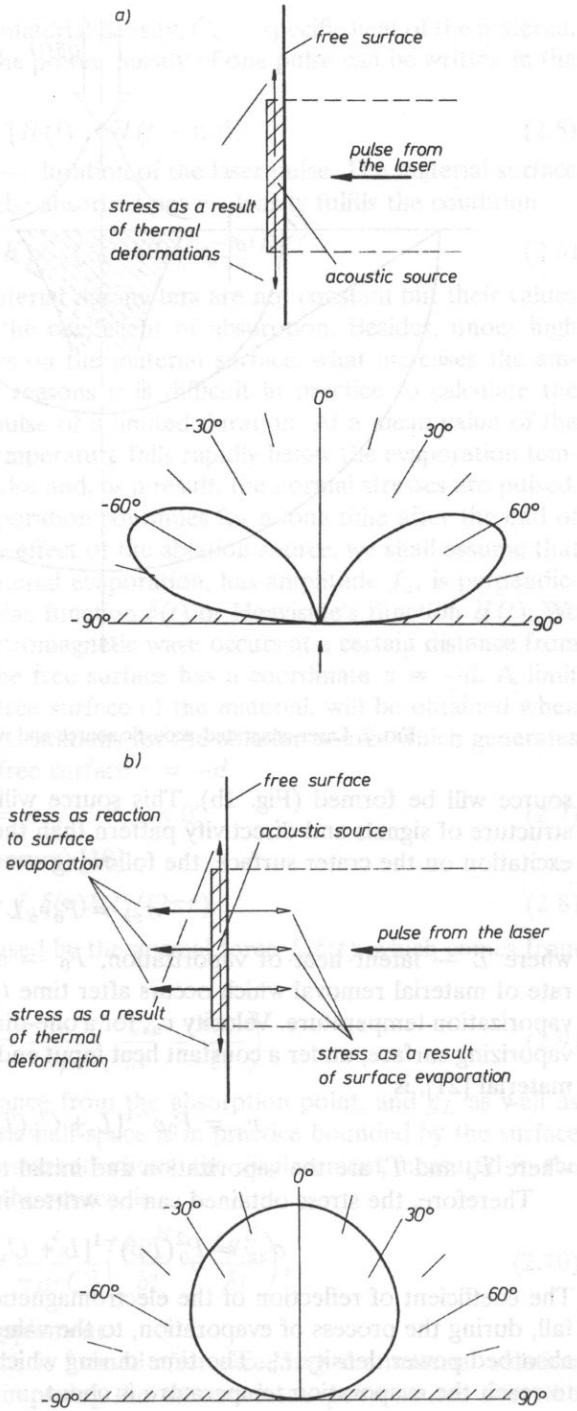

FIG. 1. Model of acoustic source and its directivity pattern for dilatation component of acoustic field according to [12] a) thermoelastic source, b) ablation source.

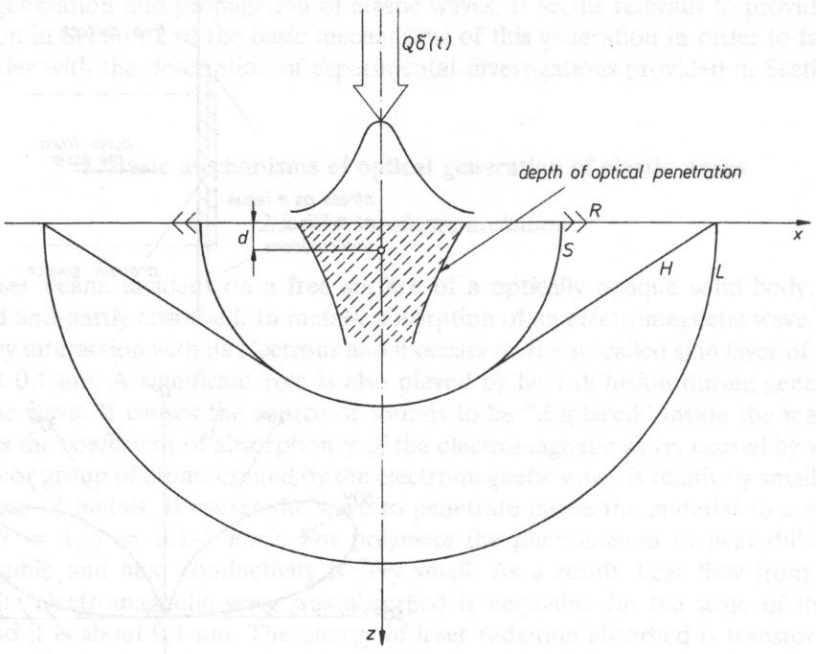

FIG. 2. Laser-generated acoustic source and wave-fronts of the wave formed.

source will be formed (Fig. 1b). This source will generate elastic waves of a different structure of signals and directivity pattern than the thermoelastic source. Under ablation excitation on the crater surface, the following stresses [32] are formed:

$$\sigma_{zz} = P_0 v_a L^{-1}, \tag{2.1}$$

where L — latent heat of vaporization, P_0 — absorbed power density and v_a is the rate of material removal which occurs after time t_v necessary to heat the material to the vaporization temperature. Velocity v_a, for a one-dimensional heat flow with a continuously vaporizing surface, under a constant heat input and a continuous removal of the vaporized material [21], is

$$v_a = P_0 \rho^{-1}[L + C_v(T_v - T_i)]^{-1}, \tag{2.2}$$

where T_v and T_i are the vaporization and initial temperature, respectively.

Therefore, the stress obtained can be written in the form

$$\sigma_{zz} = P_0^2 (L\rho)^{-1}[L + C_v(T_v - T_i)]^{-1} \tag{2.3}$$

The coefficient of reflection of the electromagnetic wave which initially is 0.7 to 0.9 may fall, during the process of evaporation, to the value of 0.1. This causes an increase of the absorbed power density P_0. The time during which the surface temperature will increase to reach the evaporation temperature is about

$$t_v = 0.25\pi K \rho C_v (T_v - T_i)^2 P_0^{-2}, \tag{2.4}$$

where K — thermal conductivity, ρ — material density, C_v — specific heat of the material. If the laser works in the pulse mode, the power density of one pulse can be written in the following way

$$p(t) = P[H(t) - H(t - \tau_0)], \tag{2.5}$$

where $H(t)$ — Heaviside unit step, τ_0 — duration of the laser pulse. The material surface will undergo rapid evaporation when the absorbed power density fulfils the condition

$$P_0 > 0.25\pi[K\rho C_v(T_v - T_i)^2\tau_0^{-1}]^{1/2}. \tag{2.6}$$

Under such conditions the thermal material parameters are not constant but their values depend on temperature, particularly the coefficient of absorption. Besides, under high power densities a liquid phase appears on the material surface, what increases the amplitude of normal stresses. For these reasons it is difficult in practice to calculate the amplitude of stresses δ_{zz} for a laser pulse of a limited duration. At a mean value of the incident power density, the material temperature falls rapidly below the evaporation temperature after the end of each laser pulse and, as a result, the normal stresses are pulsed. However, at high power densities evaporation continues for a long time after the end of each laser pulse. In order to model the effect of the ablation source, we shall assume that the power pulse, equivalent to the material evaporation, has amplitude f_a, is perpendicular to the surface, and varies as a Dirac function $\delta(t)$ or Heaviside's function $H(t)$. We can assume that absorption of the electromagnetic wave occurs at a certain distance from the material surface (Fig. 2). Then the free surface has a coordinate $z = -d$. A limit case, when absorption occurs on the free surface of the material, will be obtained when we assume that $d \to 0$. The boundary conditions for the ablation source which generates a normal force are the following: for free surface $z = -d$

$$\sigma_{zz} = \sigma_{rz} = \sigma_{rr} = 0, \tag{2.7}$$

for surface $z = 0$ (where absorption occurs) [18]

$$\sigma_{zz} = f_a\delta(r)\delta(t)/(2\pi r). \tag{2.8}$$

Displacement on the acoustic axes caused by the normal force $f_a\delta(t)$, which comes from the ablation source, is [23]

$$u_z(r, \theta, t) = \frac{f_a}{4\pi\mu r}\left(\frac{\delta g_L}{\delta t} + \frac{\delta g_S}{\delta t}\right), \tag{2.9}$$

where μ — Lamé constant, r — distance from the absorption point, and g_L as well as g_S are given in the Supplement. Elastic half-space is in practice bounded by the surface $z = r$; if we take into consideration wave reflections, the displacement measured in the epicenter, i.e. on the acoustic axes of the source, is

$$u_z^E(r, \theta, t) = \frac{f_a}{\pi\mu r C_s^2}\left(\frac{\delta g_L^E}{\delta t} + \frac{\delta g_S^E}{\delta t}\right), \tag{2.10}$$

where g_L^E and g_S^E are given in the Supplement.

In reality, the acoustic source which is formed after exceeding the material ablation threshold, can be modelled by superimposing the thermoelastic point source over the point normal force, as well as by an adequate selection of the form of the excitation pulse. In this way it is possible to build a model which enables us to recreate the results of

experimental investigations. However, the model does not provide any relations between the parameters of the electromagnetic wave and the material parameters.

3. Measuring stand and measurements

In Fig. 3 the diagram of the measuring stand is shown. In the investigations, for excitation of ultrasounds, a Q-switched ND:YAG laser with a built-in nonlinear crystal was used. The duration of a single pulse was 10 ns, the diameter of the laser beam was 1.5 mm, and its energy — 1.7 mJ. The frequency at which the pulses were emitted was 2 Hz. An electromagnetic wave of length $\lambda = 532$ nm and power density 10 MW cm^{-2} illuminated, at the point of intersection of diagonals, the flat surface of a semi-cylinder from polyvinyl chloride (PVC) of radius 45 mm and height 40 mm. This flat surface was free (one time it was constrained with glycerine and plexiglass plate). The wave power density was selected in such a way that the ablation threshold was only slightly exceeded and the PVC surface was slightly damaged. Piezolectric ultrasonic heads were used to measure the deformation caused by the ultrasound dilatation wave, in the direction normal to the cylinder surface. The measurements were made using the following ultrasonic heads; a head for the measurement of acoustic emision (EA) of resonance frequency 160 kHz, and the following ultrasound broadband heads; 5 MHz, 2.25 MHz, 1 MHz of bandwidth about 100%. The diameter of the transducers in all the heads was 12.7 mm. The medium which coupled the head with a semi-cylinder from PVC was an aqueous solution of glycerine. During the amplitude measurements of directivity patterns the head moved with a constant velocity on one plane along a parallel back and forth, in the angular range of $\pm 90°$, and it stopped at the measurements points. Measurement of the maximum amplitude of the first pulse of the dilatation wave performed every 1°, within 4 seconds. The mean value of amplitude calculated from eight measurements at one point was taken as a result. The plane of measurements intersected the epicenter of the acoustic source. Both the control of the head movement and recording of the results were performed by a PC 386 computer. In the first stage of the investigation using all the heads, the amplitude directivity patterns $A =$

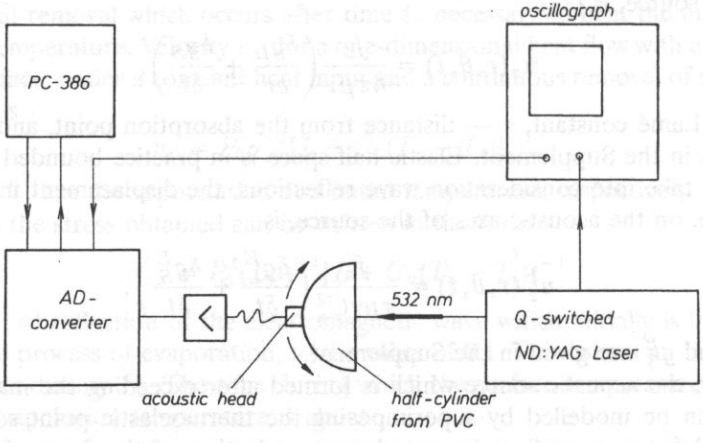

FIG. 3. Schematic diagram of the stand for measurements of laser-generate ultrasonic waves in PVC.

$f(\alpha)$, were measured, where α — angle of the head position with respect to the optical axis of laser beams radius. Four similar amplitude directivity patterns were obtained. They differ from each other mainly by absolute values of amplitudes. The highest amplitudes were obtained by the head 1 MHz ($A_{\max}$ = 11 V), and the smallest — by the head 5 MHz ($A_{\max}$ = 1 V). Amplitudes measured by the head 2.25 MHz ($A_{\max}$ = 9 V) were higher than those measured by the head for acoustic emission ($A_{\max}$ = 5.5 V). After an analysis of the results obtained, an ultrasound head 2.25 MHz of bandwidth 94.4% was selected for further investigation. Measurements of amplitude and frequency directivity patterns were performed using this head. During the measurements of frequency directivity patterns the head moved stepwise every 2.5° along a parallel line in the angle range ±90°, on the same plane where measurements of amplitude directivity patterns were performed. The first pulse of a dilatation wave was recorder at the points of measurement. Next a frequency spectrum was determined using a rapid Fourier transformer. The mean value (for two measurements made at one point) of frequency with the pulse of dilatation wave of maximum amplitude changes was taken as the result of measurements.

4. Result and discussion

The result of the measurements of maximum amplitude of the first pulse of the dilatation wave, depending on angle α, for different heads, are shown in Fig. 4. In order to compare the relations obtained $A_i = f(\alpha)$, where $i = 1, 2, 3, 4$, each curve was normalized to the form $A_{\text{norm}} = A_i / A_{i\,\max} = f(\alpha)$, and next they were represented in a system of polar coordinates. It follows from the directivity patterns that, using the head 1 MHz, 2.25 MHz and a head to EA, we obtain as a matter of fact the same relations. The maximum value of amplitude occurs in the direction 0°, i.e. in the direction of the laser beam. A systematic decrease in amplitude occurs with increasing angle to the value of about 50°. In the range from 50° to 90°, a slight relative amplitude increase with a local maximum for α = 68° can be observed. This slight amplitude increase in the range 50°–90° is the effect of the thermoelastic mechanism in the acoustic source, for which, according to the

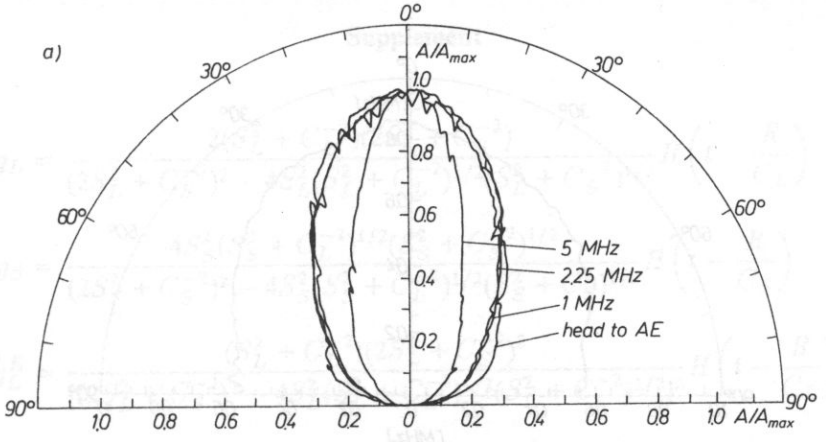

FIG. 4. Amplitude-normalized directivity pattern of laser-generated acoustic source in PVC determined by different heads; A — amplitude, $A_{\max}$ — maximum amplitude.

theory, maximum amplitude occurs for angle $\alpha = 64°$. As has been already stated, in Section 3, depending on the applied measurement head, we obtain different amplitude values, which results mainly from their different sensitivity. In the case of the head for the measurements of acoustic emission, its resonance frequency is 160 kHz and it is well below the frequency ca 1 MHz at which the maximum-amplitude disturbances occur. For this reason, the amplitude measured by this head is smaller than those measured by heads 1 MHz and 2.25 MHz.

A directivity amplitude pattern obtained from the second measurements made by the head 2.25 MHz, is represented in Fig. 5. It is evident from an analysis of the result obtained (in the case of the free surface) that the amplitude falls by 6 dB in the range of angle $\alpha = \pm 55°$, whereas in the range $\alpha = \pm 75°$, the amplitude falls by 12 dB. Such a form of the directivity pattern confirms that we have to do with an ablation mechanism.

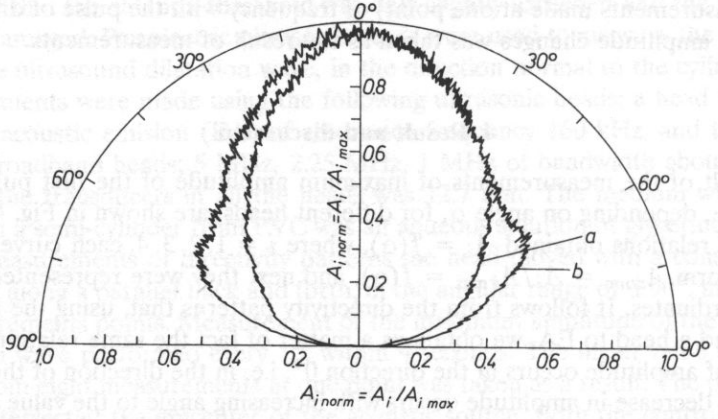

FIG 5. Amplitude-normalized directivity pattern of acoustic source in PVC measured by heads 2.25 MHz; A — amplitude, A_{max} — maximum amplitude a) with free surface; b) with constrained surface.

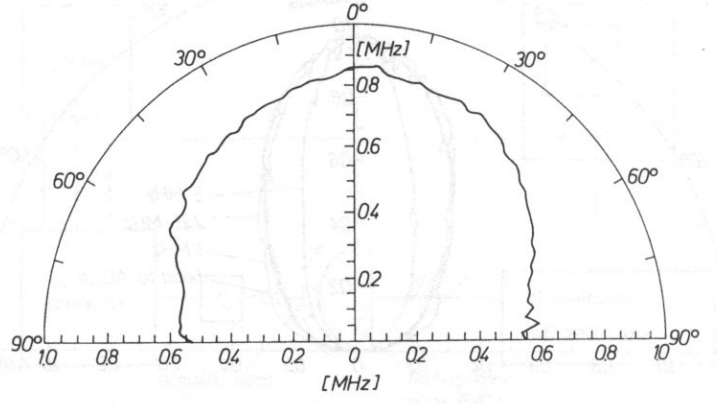

FIG 6. Frequency directivity pattern of laser-generated acoustic source in PVC determined by head 2.25 MHz MHz: f — frequency.

A directivity frequency pattern obtained from measurements by the head 2.25 MHz is represented in Fig. 6. It follows that the measured pulse of a dilatation wave of maximum amplitude varies with a frequency of about 0.85 MHz for $\alpha = 0°$. With an increasing value of this angle to $\alpha = 60°$, the frequency of changes of this pulse decreases systematically to the value of about 0.70 MHz. In the range of angles $\alpha = 60°$–$90°$, this frequency decreases more intensively than in the previous range, to the value of about 0.55 MHz for $\alpha = 90°$. Such a characteristic of the optically-generated acoustic source has not been known before. Variation in the vibration frequency, as a function of angle and PVC-viscoelasticity, is responsible for the form of the directivity amplitude pattern measured by the head 5 MHz. For his head, vibration amplitude is reduced by 6 dB in the range of angles $\alpha = \pm 20°$.

5. Conclusions

The investigation has shown applicability of the Q-switched Nd:YAG laser of wavelength $\lambda = 532$ nm, energy 1.7 mJ and duration of single pulse 10 ns, to the generation of ultrasounds in PVC. The investigation of directivity amplitude pattern has shown that laser light of power density 10 MW cm^{-2}, when incident on a free surface of PVC, is the cause of formation of an acoustic source, mainly due to ablation mechanism and, to a small degree, to the thermoelastic mechanism.

Normalized results of the investigation of the directivity amplitude pattern by heads 1 MHz, 2.25 MHz and EA represented in polar coordinates differ negligibly from each other. In the range of angles $\alpha = \pm 55°$, the amplitude decreases by 6 dB. Investigation of the directivity frequency pattern have shown that the frequency of the disturbances measured is not constant, and changes non-uniformly as a function of angle α. This property of the analyzed acoustic source and visco-elastic properties of PVC are the reason that the results of measurements by the head 5 MHz are markedly different from those obtained by the other heads.

Supplement

$$g_L = \frac{2(S_L^2 + C_L^{-2})(2S_L^2 + C_S^{-2})}{(2S_L^2 + C_S^{-2})^2 - 4S_L^2(S_L^2 + C_L^{-2})^{1/2}(S_L^2 + C_S^{-2})^{1/2}} H\left(t - \frac{R}{C_L}\right)$$

$$g_S = \frac{-4S_S^2(S_S^2 + C_L^{-2})^{1/2}(S_S^2 + C_S^{-2})^{1/2}}{(2S_S^2 + C_S^{-2})^2 - 4S_S^2(S_S^2 + C_L^{-2})^{1/2}(S_S^2 + C_S^2)^{1/2}} H\left(t - \frac{R}{C_S}\right)$$

$$g_L^E = \frac{(S_L^2 + C_L^{-2})(2S_L^2 + C_S^{-2})^2}{[(2S_L^2 + C_S^{-2})^2 - 4S_L^2(S_L^2 + C_L^{-2})^{1/2}(S_L^2 + C_L^{-2})^{1/2}]^2} H\left(t - \frac{R}{C_L}\right)$$

$$g_S^E = \frac{-4S_S^2(S_S^2 + C_L^{-2})(S_S^2 + C_S^{-2})}{[(2S_S^2 + C_S^{-2})^2 - 4S_S^2(S_S^2 + C_L^{-2})^{1/2}(S_S^2 + C_S^{-2})^{1/2}]^2} H\left(t - \frac{R}{C_S}\right)$$

$$S_L^2 = \left(\frac{t^2}{R^2} - C_L^{-2}\right) \quad S_S^2 = \left(\frac{t^2}{R^2} - C_S^{-2}\right)$$

were C_L and C_S are velocities of longitudinal and shear waves respectively.

Acknowledgments

I am grateful to Dr E. NEUMANN and S. GRIPP of BAM in Berlin, Germany, for financial and scientific assistance during the investigations, as well as for discussion of the results. I am grateful to Professor J. OSIECKI for reading the manuscript and making numerous remarks.

References

[1] A. G. BELL, Phil. Mag., **11**, 510–528 (1881).
[2] V. J. DANILOWSKAYA, *Thermal stresses in an elastic half-space due to sudden heating on the surface*, J. Appl. Math. Mech., **14**, 316–318 (1950).
[3] R. M. WHITE, *Generation of elastic waves by transient surface heating*, J. Appl. Phys., **34**, 3559–3567 (1963).
[4] J. F. READY, *Effects due to absorption of laser radiation*, J. Appl. Phys., **36**, 462–468 (1965).
[5] J. C. BUSHNELL and D. J. MCCLOSKEY, *Thermoelastic stress production in solids*, J. Appl. Phys., **39**, 5541–5546 (1968).
[6] S. S. PENNER and O. P. SHARMA, J. Appl. Phys., **37**, 2304–2308 (1966).
[7] M. P. FELIX, *Laser-generated ultrasonic beams*, Review of Scientific Instruments, **45**, 1106–1108 (1974).
[8] R. E. LEE and R. M. WHITE, *Excitation of surface elastic waves by transient surface heating*, Appl. Phys. Lett., **12**, 12–14 (1968).
[9] H. M. LEDBETTER and J. C. MOULDER, J.A.S.A., *Laser-induced Rayleigh waves in aluminium*, **65**, 840–842 (1979).
[10] A. M. AINDOW *et al.*, *Laser-generated ultrasonic pulses at free metal surfaces*, J.A.S.A., **69**, 449–455 (1981).
[11] C. B. SCRUBY *et al.*, *Quantitative studies of thermally-generated elastic waves in laser-irradiated metals*, J. Appl. Phys., **51**, 6210–6216 (1980).
[12] C. B. SCRUBY *et al.*, *Laser generation of ultrasound in metals*, in "Research Techniques in Nondestructive Testing", (R. S. Sharpe, Ed.) p.p. 281–327, vol. 5, Ac. Press, London and New York (1982).
[13] R. J. DEWHURST *et al.*, *Quantitative measurements of laser-generated acoustic waveforms*, J. Appl. Phys., **53**, 4064–4071 (1982).
[14] L. R. F. ROSE, *Point-source representation for laser-generated ultrasound*, J.A.S.A., **75**, 723–732 (1984).
[15] H. N. G. WADLEY *et al.*, in "Review of Progress in QNDT" vol. 3b, (Ed. D. O. Thompson, D. E. Chimenti), New York, Plenum, p. 683 (1984).
[16] P. A. DOYLE, *On epicentral waveforms for laser-generated ultrasound*, J. Phys. D-Appl. Phys., **19**, 1613–1623 (1986).
[17] U. SCHLIECHERT, Dissertation, Universität-GH Kassel (1989).
[18] J. D. AUSSEL *et al.*, *Generating acoustic waves by laser: Theoretical and experimental study of the emission source*, Ultrasonics, 26, 245–255 (1988).
[19] R. J. CONANT and K. J. TELSCHOW, *Longitudinal wave precursor signal from an optically-penetrating thermoelastic source*, in: Rev. Prog. QNDT, vol. 8 (Ed. D. O. Thompson, D. E. Chimenti), New York, Plenum (1989).
[20] F. A. MCDONALD, *A practical, quantitative theory of pulsed photoacoustic generation*, Appl. Phys. Letter, **54**, 1504–1506 (1989).
[21] J. F. READY, *Effects of high-power laser radiation*, Ac. Press, NY, Ch. 3, 67–125 (1971).
[22] P. KREHL *et al.*, J. Appl. Phys., **46**, 4400–4406, (1975).
[23] D. A. HUTCHINS *et al.*, *Directivity patterns of laser-generated ultrasound in aluminium*,J.A.S.A., **70**, 1362–1369 (1981).

[24] J. A. COOPER, PhD thesis, Hull University (1985).
[25] C. B. SCRUBY and L. E. DRAIN, *Laser ultrasonics*, Adam Hilger, Bristol (1990).
[26] E. BOURKOFF and C. H. PALMER, *Low-energy optical generation and detection of acoustic pulses in metals and nonmetals*, Appl. Phys. Letters, **46**, 143–145 (1985).
[27] D. A. BUTTLE and C. B. SCRUBY, J. Acoust. Emission, **7**, 211 (1988).
[28] B. CASTAGNEDE *et all.*, *Determination of the elastic constants of anisotropic materials via laser-generated ultrasound*, Ultrasonic Int. 1989 Conf. Proc. (1989).
[29] G. S. TAYLOR *et al.*, TEA–CO_2 *laser generation of ultrasound in non-metals*, Ultrasonic, **28**, 343–349 (1990).
[30] B. F. POUET and N. J. P. RASOLOFOSAON, *Measurement of broadband intrinsic ultrasonic attenuation and dispersion in solids with laser techniques*, J.A.S.A., **93**, 1286–1292 (1993).
[31] C. CORBEL *et al.*, *Laser generated elastic waves in carbon-epoxy composite*, IEEE Transactions, October 1993, to be published.
[32] G. BIRNBAUM and G. S. WHITE, *Laser techniques in 'NDE*, in: "Research Techniques in NDT" vol. 7, 259–365, ed. Sharp R. S. Ac. Press (1984).
[33] J. SINCLAIR, *Epicentre solutions for point multipole sources in an elastic half-space*, J. Phys. D:Appl. Phys., **12**, 1309–1315 (1979).

ARCHIVES OF ACOUSTICS
19, 3, 395–404 (1994)

SIGNAL FILTRATION IN A PIEZOELECTRIC-SEMICONDUCTOR CONVOLVER WITH BROAD-BAND TRANSDUCERS

A. M. KAWALEC

Military University of Technology
(01-489 Warszawa ul. Kaliskiego 2)

The result of theoretical and experimental studies of a convolver in piezoelectric-semiconductor configuration (BGO-Si) are presented. Experimental results with using of the convolver for compression a signal with linear frequency modulation have been reported. Dispersive excitation transducers were used to improve the matching of the convolver inputs to the external sources of the signals in the pass band. A new measurement system for the amplitude characteristics of the convolver output has been proposed.

1. Introduction

Filtration of a signal in a filter with an acoustic surface wave SAW is performed by means of two co-operating interdigital transducers (Fig. 1a). The output signal is a convolution of an input signal $S_{\text{in}}(t)$ and a impulse response of the filter $h(t)$

$$S_{\text{out}}(t) = S_{\text{in}}(t) \otimes h(t). \tag{1.1}$$

The characteristic of such a filter is determined by the form of the transducers and the properties of the substrate, therefore it is invariable for a particular filter. Analogous filtration can be achieved by means of a convolver (Fig. 1b) except that, instead of the impulse response $h(t)$, the reference signal $S_{2\,\text{in}}(t)$ is used by applying it to the second input. The output signal $S_{\text{out}}(t)$ which is a result of nonlinear interaction of the acoustic signals moving in opposite directions is a convolution of the input signal $S_{1\,\text{in}}(t)$ and the reference signal $S_{2\,\text{in}}(t)$, that is

$$S_{\text{out}}(t) = S_{1\,\text{in}}(t) \otimes S_{2\,\text{in}}(t). \tag{1.2}$$

It follows that the reference signal replaces. In this case, the pulse response $h(t)$ of the filter with an acoustic surface wave cf. equation (1.1), therefore we can vary by simple change of the signal $S_{2\,\text{in}}(t)$, the characteristic of the convolver, which is decisive for its attraction for the signal processing and, in particular, the realization of matched filtering of signals.

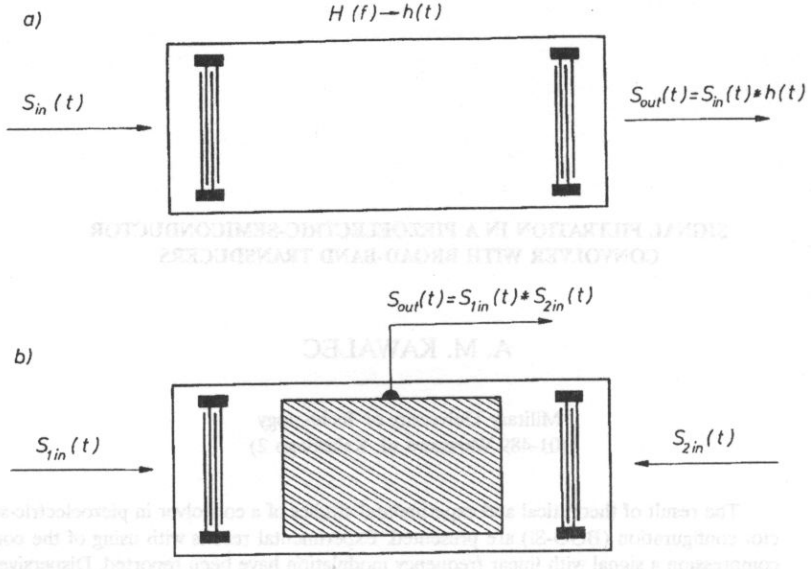

FIG. 1. a) A filter with an acoustic surface wave, b) A convolver with acoustic surface waves.

The nonlinear interaction of surface waves in a convolver can be made by making use of the mechanical nonlinearity of the material of the piezoelectric substrate [1] or electrical nonlinearity associated with the transport of electric charges in a piezoelectric semiconductor [2] or piezoelectric-semiconductor convolver system [3] as shown in Fig. 2. The transport of a charge is forced by an electric potential connected with a surface wave moving in the piezoelectric substrate and penetrating the semiconductor applied to the surface of the piezoelectric. For application, the convolver with charge nonlinearity appears to be better, owing to the effectiveness of the interaction of the surface waves being much higher.

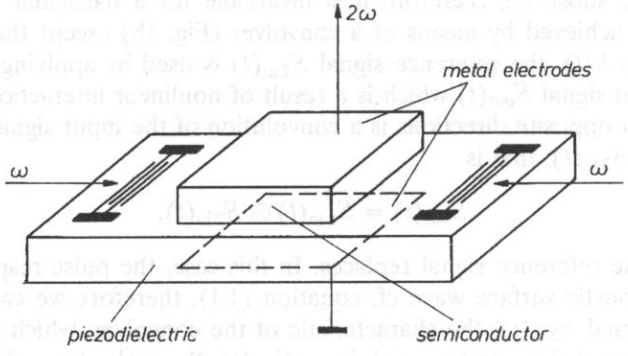

FIG. 2. Piezoelectric-semiconductor convolver.

2. The convolver with broad-band transducers

The source of a surfaces wave in a convolver are inter digital transducers. Common transducers contain a small number of electrodes in order to obtain a broad band operation. This is a consequence of the fact that the frequency band of a transducer structure is expressed by the formula

$$H_p(f) = \frac{\sin y}{y}, \tag{2.1}$$

where

$$y = \frac{N\pi(f - f_0)}{2f_0},$$

N is the number of electrodes of the transducer and f_0 — the middle frequency, the passband being, therefore, proportional to the number of electrodes. But transducers with a small number of electrodes are highly radiation resistivity, which makes impossible their being matched to the source of the electric signal. This in turn makes impossible generation of a surface wave with a sufficiently high amplitude such as is required for the nonlinear interaction of surface acoustic waves in a convolver.

The only effective method for generating broad-band signals is by using interdigital transducers with nonlinear phase characteristic [3], which makes possible considerable improvement of electric matching of convolver inputs.

In order to ensure that the convolver will be dispersionless two input transducers must be arranged as shown in Fig. 2. Then, their pulse responses will be $h_p(t)$ and $h_p(-t)$, which means that the spectra of their structures will be complex conjugate with each order.

$$H_p(\omega) = H_p^*(\omega) \tag{2.2}$$

In view of the form of the frequency characteristic and the dependence of the radiation

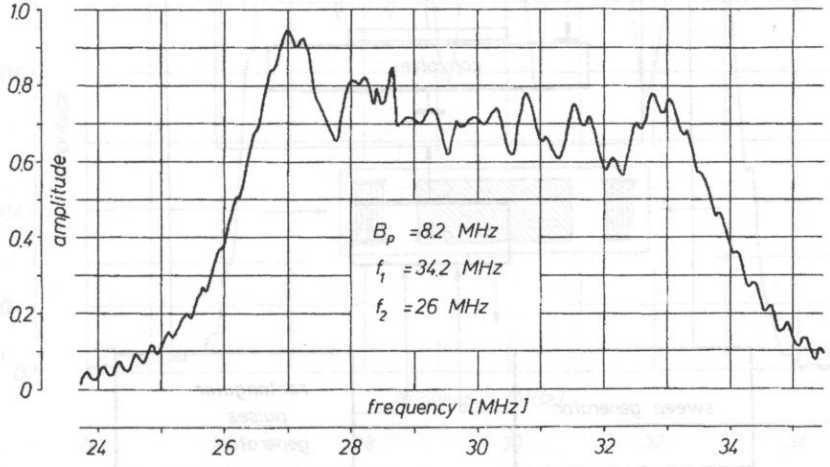

FIG. 3. The amplitude characteristic of a hyperbolic transducer

resistance of the frequency, it is advantagenous to apply hyperbolic dispersive transducers. The amplitude characteristic of such a transducer is shown in Fig. 3. The middle frequency of the transducer is $f_0 = 30$ MHz, the bandwidth — $B_p = 8.2$ MHz and the time duration of the impulse response — $T_p = 4$ μs.

3. The measurement of the frequency characteristic of the convolver

The insertion, loss which depend on the frequency transformed signal, are an important parameter of the convolver. The measurement of the frequency characteristic of the co-

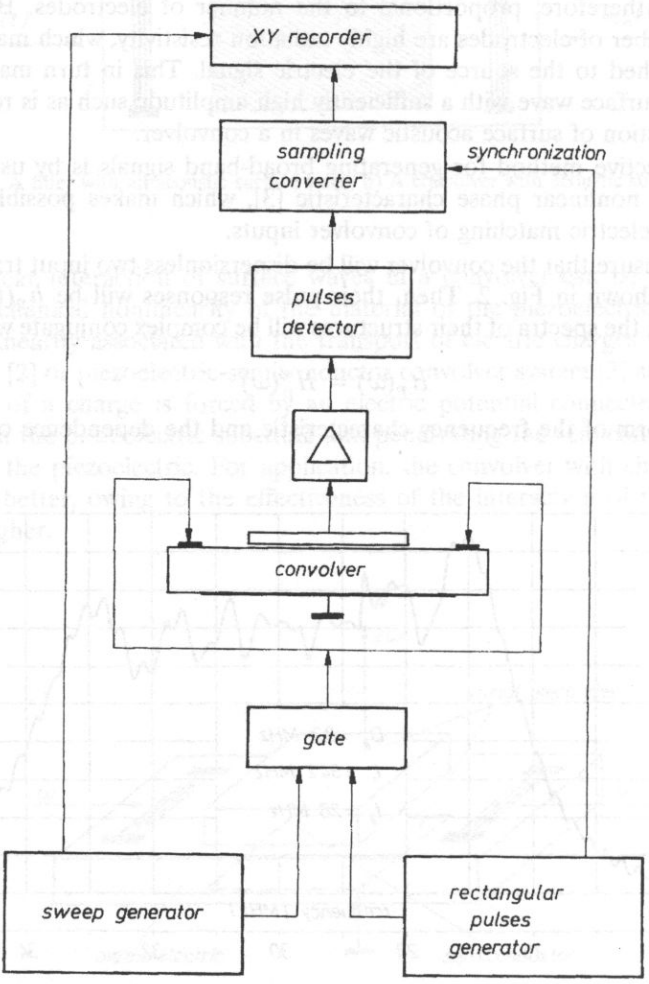

FIG. 4 A measuring set for the frequency characteristic of a convolver.

nvolver by means of continuous signals is difficult, the level of the electromagnetic signals between the interdigital transducers and the output electrode of the convolver being high. The measurement method which was used in the work reported here was of the pulse type, thus making possible separation of the useful output signal from false signals which usually are relatively strong. The proposed measurement system is illustrated in Fig. 4. The electrical signal produced by the generator, the frequency of which varies between the limits of 24 and 35 MHz is applied, in the form of rectangular pulses, to the input transducers of the convolver. After amplification and detection the output signal is transmitted to the input of the converter sampling. The investigated impulse is reproduced at the output of the converter in the form of samples. The sampling converter is able to move the sampling point of the signal, therefore other signal, delayed on each other, can also be analyzed, which is the greatest advantage of the system discussed. The amplitude characteristic of the convolver will depend on the frequency spectra $H_{p1}(\omega)$ and $H_{p2}(\omega)$ of the transducers generating surface waves, that is

$$|H(\omega)| = |H_{p1}(\omega)||H_{p2}(\omega)|. \tag{3.1}$$

Figure 5 shows the amplitude characteristic of the convolver output. Because the excitation transducers were identical (dispersive hyperbolic), the characteristic of the convolver output is the square of the spectrum of a single transducer. For the sake of comparison the amplitude characteristic was measured using the same measuring system, for two

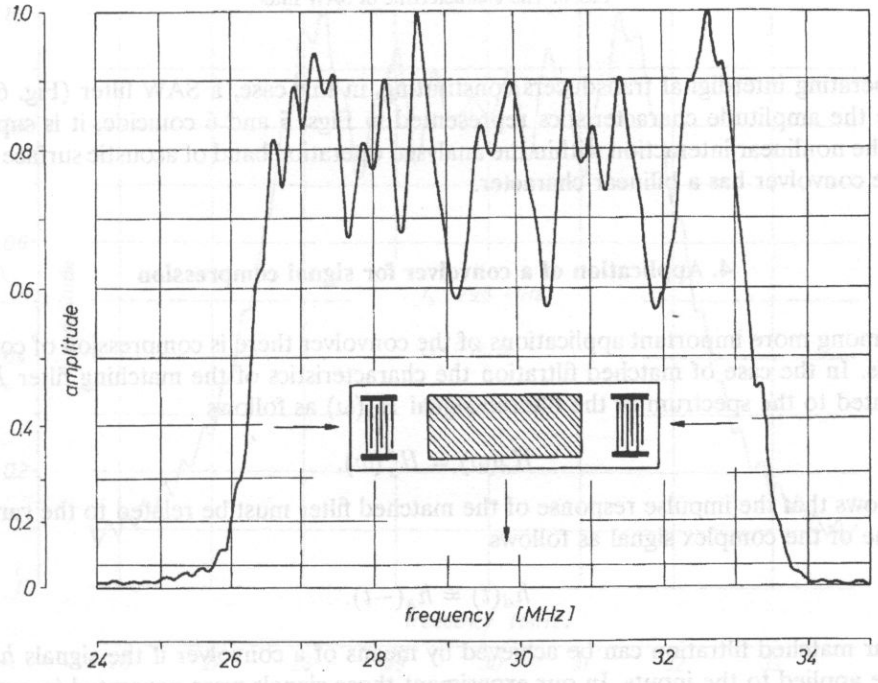

FIG. 5. The characteristic of a convolver output.

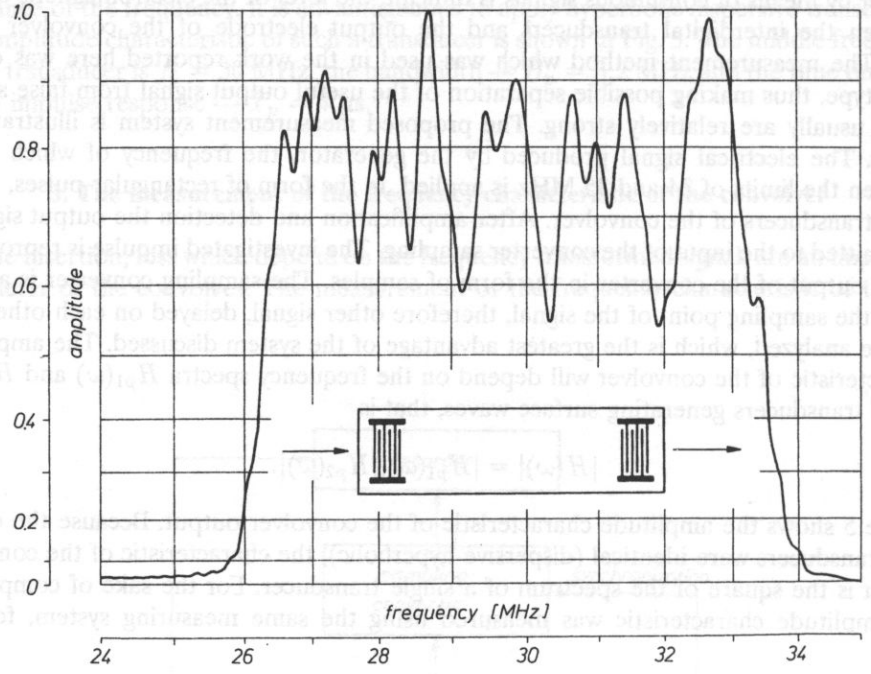

FIG. 6. The characteristic of SAW filter.

co-operating interdigital transducers constituting, in this case, a SAW filter (Fig. 6). Because the amplitude characteristics represented in Figs. 5 and 6 coincide, it is supposed that the nonlinear interaction within the analysed operation band of acoustic surface waves in the convolver has a bilinear character.

4. Application of a convolver for signal compression

Among more important applications of the convolver there is compression of complex signals. In the case of matched filtration the characteristics of the matching filter $H_d(\omega)$ is related to the spectrum of the filtered signal $H_s(\omega)$ as follows

$$H_d(\omega) = H_s^*(\omega). \tag{4.1}$$

It follows that the impulse response of the matched filter must be related to the variation in time of the complex signal as follows

$$h_d(t) = h_s(-t). \tag{4.2}$$

Similar matched filtration can be achieved by means of a convolver if the signals h_d and h_s are applied to the inputs. In our experiment those signals were generated in a system illustrated in Fig. 7. The middle transducer was excited with a short pulse. At the output

of the identical transduces located on both sides of the dispersive transducer the signals were obtained as described by the relation (4.2)

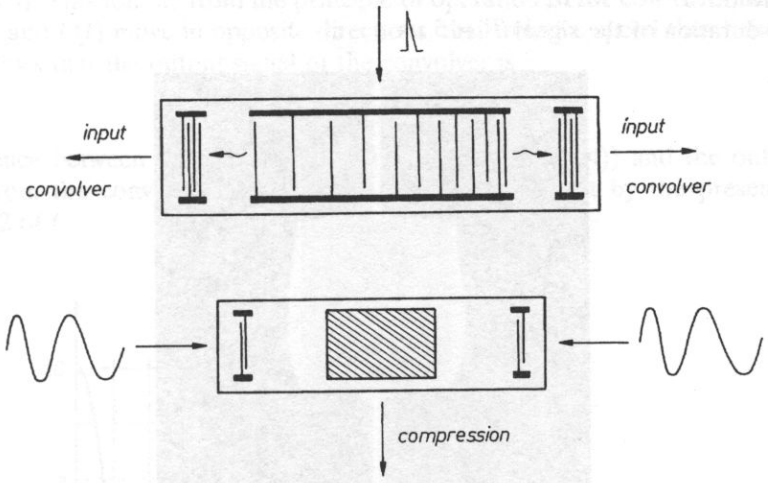

FIG. 7. A compressing set for a complex signal in convolver.

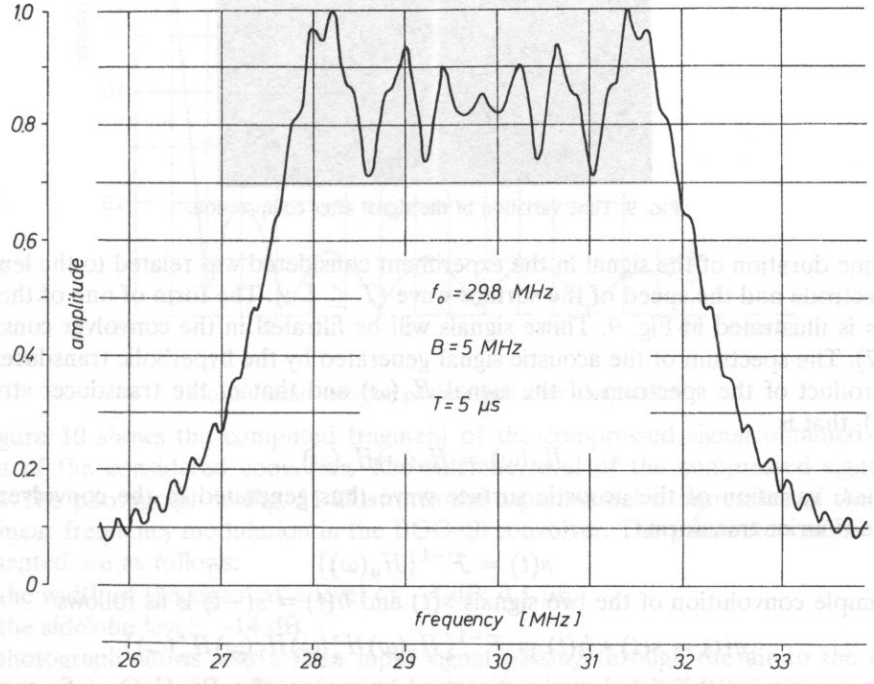

FIG. 8. The amplitude characteristic of a signal with L.f.m.

A signal with linear frequency modulation has been realized in practice, its amplitude spectrum being illustrated in Fig. 8. The parameters of the complex signal were as follows.

- middle frequency $f_0 = 29.8$ MHz,
- bandwidth $B = 5$ MHz,
- time-duration of the signal $T = 5$ μs

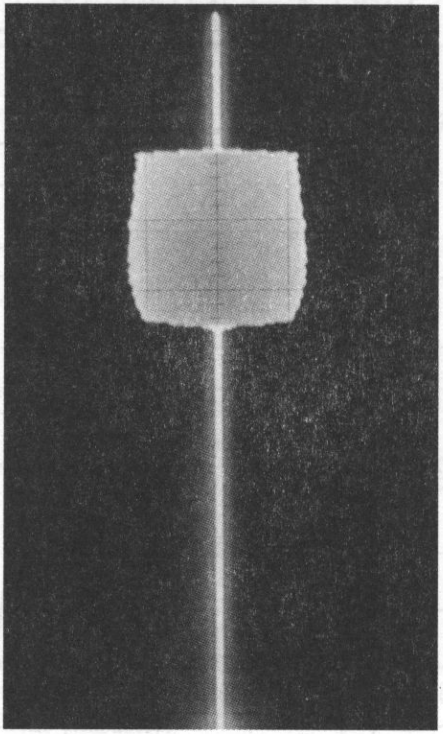

FIG. 9. Time variation of the signal after compression.

The time duration of the signal in the experiment considered was related to the length of the electrode and the speed of the surface wave ($T \leq Lv$). The form of one of the input signals is illustrated in Fig. 9. Those signals will be filtrated in the convolver considered (Fig. 7). The spectrum of the acoustic signal generated by the hyperbolic transduces used is a product of the spectrum of the signal $H_s(\omega)$ and that of the transducer structure $H_p(\omega)$, that is

$$H_a(\omega) = H_s(\omega)H_p(\omega) \tag{4.3}$$

The time variation of the acoustic surface wave thus generated in the convolver is an inverse Fourier transform

$$s(t) = \mathcal{F}^{-1}\{H_a(\omega)\} \tag{4.4}$$

The simple convolution of the two signals $s(t)$ and $h(t) = s(-t)$ is as follows

$$g(t) = s(t) * h(t) = \mathcal{F}^{-1}\{H_s(\omega)H_s^*(\omega)H_p(\omega)H_p^*(\omega)\} \tag{4.5}$$

In our experiment the signal was compressed by means of a $Bi_{12}GeO_{20}$—S_i convolver incorporating two identical hyperbolic transducers. The specific conductivity of Silicon

was $1.4.10^{-1}$ [$1/\Omega$m]. From the computation which was carried out according to the relation (4.5) it follows that the compressed out signal has 0.2 μs width.

The output signal of the convolver is $1/2$ the length of the signal described by the equation (4.5). This follows from the principle of operation of the convolver, in which the signals $s(t)$ and $h(t)$ move in opposite directions, their relative speed thus being twice as high. It follows that the output signal of the convolver is

$$g_k(t) = \int s(\tau)h(2t - \tau)\,d\tau \tag{4.6}$$

The difference between the simple convolution signal (cf. (4.4)) and the output signal obtained from the convolver (cf. (4.6)) is taken into account by the presence of the coefficient 2 of t.

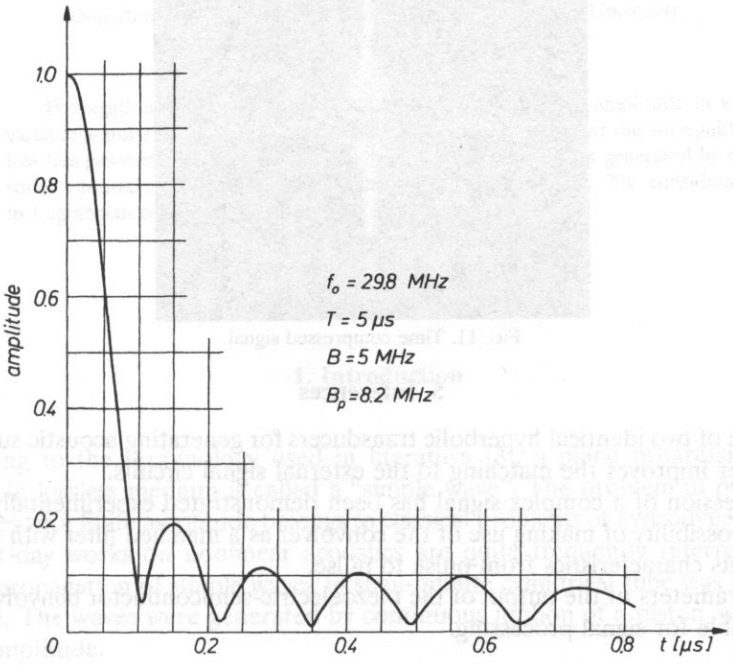

FIG. 10. Time variation of the signal after compression.

Figure 10 shows the computed fragment of the compressed signal obtained at the output of the considered convolver. The sidelobe level of the compressed signal is –14 dB. The photograph in Fig. 11 illustrates the experimental compression of the signal with linear frequency modulation in the BGO–Si convolver. The parameters of the signal represented are as follows:

- the width of the signal at a level of −4 dB: 0.1 μs,
- the sidelobe level: −14 dB.

The photograph shows also a false input signal passing through the air to the output electrode of the convolver. This signal presents a fundamental difficulty in measuring the frequency characteristic of the convolver output.

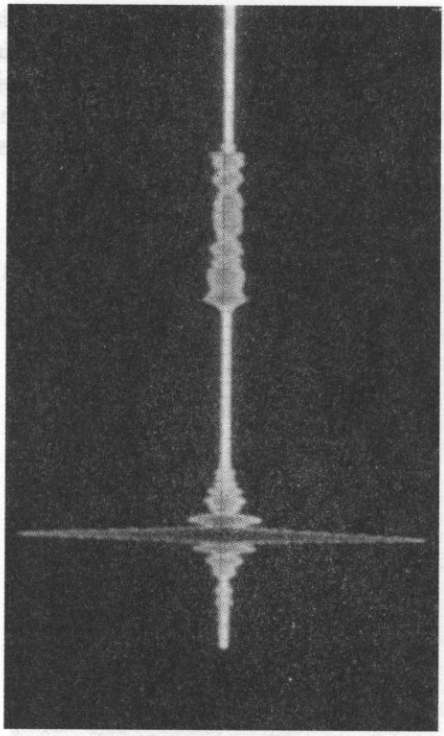

FIG. 11. Time compressed signal.

5. Inferences

- The use of two identical hyperbolic transducers for generating acoustic surface waves in a convolver improves the matching to the external signal circuits.
- Compression of a complex signal has been demonstrated experimentally, thus confirming the possibility of making use of the convolver as a matched filter with a possibility of changing its characteristics from pulse to pulse.
- The parameters of the output of the piezoelectric-semiconductor convolver BGO–Si make it suitable for signal processing.

Acknowledgement

The author wishes to express his gratitude to Professor Eugeniusz DANICKI for fruitful discussion and help in the realization of the experiment and the editorial work of the present paper.

References

[1] G. S. KINO, S. LUDVIK, H. J. SHAW, W. R. SHREVE, J. W. WHITE and D. K. WINSLOW, IEEE Trans. Sonics and Ultras., **SU-20**, 162 (1973).
[2] S. KALISKI, A. KAWALEC, Tringh DONGÁ and B. WĘCKI, Journal of Tech. Physics, **16**, 97 (1975).
[3] A. KAWALEC, Doctor's thesis (1980).

ARCHIVES OF ACOUSTICS
19, 3, 405–418 (1994)

SIMPLE WAVES WITH FINITE AMPLITUDE IN AXIALLY-SYMMETRICAL CHANNELS WITH ANNULAR CROSS-SECTION

T. ZAMORSKI

Department of Acoustic Institute of Physics Pedagogical University
(35-310 Rzeszów, ul. Rejtana 16a)

Propagation of a plane progressive sound wave with finite amplitude in a waveguide with variable annular cross-section was considered. It was assumed that this waveguide was filled with loss less gaseous medium and the wave with finite amplitude was generated by a annular piston, which vibrated in harmonic motion at the inlet of the waveguide. The considerations were done in Lagrangian coordinates.

1. Introduction

According to the terminology used in literature [3], a plane progressive wave that propagates in lossless medium is called a "simple wave". The problem of propagation of simple waves with finite amplitude belongs to classical problems of hydrodynamics to which the present-day works on nonlinear acoustics are quite frequently referred. Paper [1], where the propagation of simple waves in semi-infinite cylindrical tube was considered, is an example. The waves were generated by continuous motion of a piston, which vibrated at a high amplitude.

This paper presents an attempt of consideration of propagation of the wave with a finite amplitude in the axially-symmetrical waveguides with variable annular cross-section. This problem has direct practical implications, at least in two problems:

- analysis of sound waves in the inlet and outlet channels of axial compressors [13],
- optimization of a construction of strong acoustic field axial flow generators, in which the axially-symmetrical waveguides with ring-shaped cross-section and exponential or catenoidal expansion of walls are frequently used [2, 6, 7],

In spite of the fact that in both cases the acoustic waves with high intensity can occur, this problem, up to the present has been considered only in linear approximation [6, 7, 10, 13, 14].

2. Analysis of the wave propagation equation

The waveguide subject to our consideration is presented in longitudinal section in Fig. 1. It is assumed that the waveguide is filled with a loss less gaseous medium and the width of the annular channel is so small in comparison to the wavelength that the front of the wave can be assumed to be plane. Then the layer of acoustic particles with the Lagrangian coordinate a is enclosed between plane surfaces $S_{(a)}$ and $S_{(a+da)}$. As a result of the wave disturbance, this layer is moved to the position $a + \xi$ and its thickness is changed to the value $d(a + \xi) \equiv dx \equiv [1 + (\partial\xi/\partial a]\, da$. ξ is the displacement of the acoustic particle and x is the Eulerian coordinate.

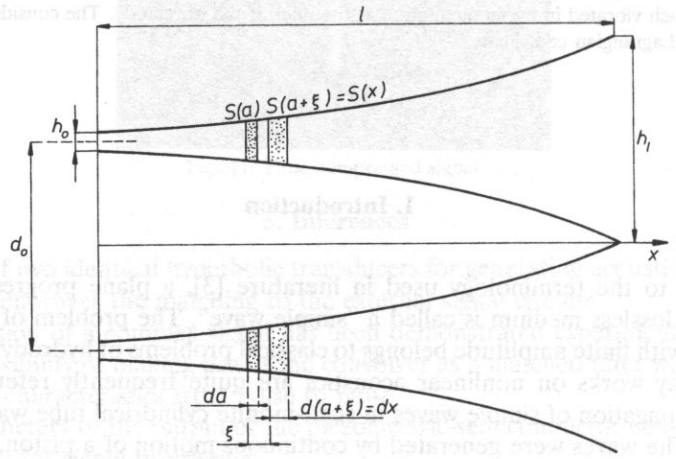

FIG. 1. The displacement of the medium layer in the waveguide.

The result of paper [8] will be a starting point for further considerations. In that paper it was shown, for the simplifying assumptions mentioned above, that the equation of propagation of the wave with finite amplitude in a waveguide with any geometry has the form

$$x'' + \frac{\zeta'}{\zeta} x' = \frac{\zeta^{\gamma-1}}{c^2} (x')^{\gamma+1} \cdot \frac{\partial^2 \xi}{\partial t^2}, \tag{2.1}$$

where

$$\zeta = \frac{S(a+\xi)}{S(a)}, \tag{2.2}$$

γ is the adiabatic exponent, c is the velocity of sound wave with infinitesimal amplitude and t is time. Commas in Eq. (2.1) denote differentiation with respect to the coordinate a.

It is assumed that the cross-section of the waveguide changes according to the formula

$$S = S_0\left[\cosh\left(\frac{x}{x_0}\right) + T\sinh\left(\frac{x}{x_0}\right)\right], \tag{2.3}$$

where $S_0 = \pi d_0 h_0$ is the surface of the inlet, x_0 is the coefficient of the wall expansion. The above formula defines the geometry of the so-called hyperbolic horns with annular section [14], which, among others, are applied to the construction of strong acoustic field flow generators. The waveguides with exponential ($T = 1$) and lately also catenoidal ($T = 0$) profiles are most frequently used. Thus these considerations are limited to the interval $T \in [0, 1]$. Then the formula (2.3) can be presented in a more compact form, which significantly simples further transformations:

$$S = \overline{S}_0 \cdot \cosh\left(\frac{x}{x_0} + \varepsilon\right), \tag{2.4}$$

where $T = \operatorname{tgh}\varepsilon$, $\overline{S}_0 = S_0/\cosh\varepsilon$. Then the value ζ in wave equation is equal to

$$\zeta = \frac{\cosh\left(\dfrac{a+\xi}{x_0} + \varepsilon\right)}{\cosh\left(\dfrac{a}{x_0} + \varepsilon\right)}. \tag{2.5}$$

Expanding the ζ and ζ' in to series, one can obtain

$$\zeta = 1 + \frac{\xi}{x_0}\operatorname{tgh}\left(\frac{a}{x_0} + \varepsilon\right) + \frac{\xi^2}{2x_0^2} + \ldots, \tag{2.6}$$

$$\zeta' = \frac{\xi'}{x_0}\operatorname{tgh}\left(\frac{a}{x_0} + \varepsilon\right) + \frac{\varepsilon}{x_0^2}\left[1 - \operatorname{tgh}^2\left(\frac{a}{x_0} + \varepsilon\right)\right] + \frac{\xi\xi'}{x_0^2} + \ldots \tag{2.7}$$

It is assumed that the hypothetical annular piston that vibrates in harmonic motion is a source of the wave at the inlet ($a = 0$)

$$\xi_{(0,t)} = k^{-1}A \cdot \cos\omega t, \tag{2.8}$$

where ω is the angular vibration frequency (pulsation), k is the wave number. $A = 2\pi B/\lambda$, where B is the vibration amplitude and λ is the wavelength. It is known from experiment that, even for relatively high intensity of the sound, the value of $M = B/\lambda$ is rarely higher than 10^{-2} for gases[1] [17].

Thus the dimensionless amplitude A is significantly less than unity. Therefore the solution of the wave equation is assumed in the form of power series of the amplitude a:

$$\xi_{a,t} = k^{-1}[A \cdot \varphi_{1(a,t)} + A^2 \cdot \varphi_{2(a,t)} + \ldots], \tag{2.9}$$

where the functions $\varphi_{1(a,t)}$, $\varphi_{2(a,t)}$ must fulfil the boundary condition (2.8) at the inlet of the horn:

$$\varphi_{1(0,t)} = \cos\omega t, \quad \varphi_{2(0,t)} = \varphi_{3(0,t)} = \ldots = 0. \tag{2.10}$$

[1] M is the so-called Mach acoustic number [17]

Since $A \ll 1$, further considerations will be done in the second-order approximation, i.e. the terms with orders higher than A^2 will be omited. The method of calculation applied here is analogical to that used in [16] for the Bessel horns: regarding the formula (2.9) and expansions (2.6) and (2.7) in Eq. (2.1) one can obtain the wave equation of the horn in the second-order approximation. This equation can be divided into two equations: the first one contains only terms with A, the second one — those with A^2. Each equation must be fulfilled for $A \neq 0$ separately. It is found that the first equation contains only the function φ_1:

$$\varphi_1'' + \frac{\operatorname{tgh}\left(\frac{a}{x_0} + \varepsilon\right)}{x_0}\varphi_1' + \frac{1 - \operatorname{tgh}^2\left(\frac{a}{x_0} + \varepsilon\right)}{x_0}\varphi_1 - \frac{1}{c^2}\ddot{\varphi}_1 = 0 \tag{2.11}$$

where the dots denote differentiation with respect to time. Second equation has the form:

$$\varphi_2'' + \frac{\operatorname{tgh}\left(\frac{a}{x_0} + \varepsilon\right)}{x_0}\varphi_2' + \frac{1 - \operatorname{tgh}^2\left(\frac{a}{x_0} + \varepsilon\right)}{x_0^2}\varphi_2 - \frac{1}{c^2}\ddot{\varphi}_2 = \psi_{(a,t)} \tag{2.12}$$

where

$$\Psi_{(a,t)} = \varphi_1\ddot{\varphi}_1\frac{\gamma - 1}{kx_0c^2}\operatorname{tgh}\left(\frac{a}{x_0} + \varepsilon\right) + \varphi_1'\ddot{\varphi}_1\frac{\gamma}{kc^2} + \frac{1}{k}\varphi_1'\varphi_1'' + \\ + \varphi_1^2\frac{\operatorname{tgh}\left(\frac{a}{x_0} + \varepsilon\right)\cdot\left[1 - \operatorname{tgh}^2\left(\frac{a}{x_0} + \varepsilon\right)\right]}{kx_0^3} - \varphi_1\varphi_1'\frac{1 - \operatorname{tgh}^2\left(\frac{a}{x_0} + \varepsilon\right)}{kx_0^2}. \tag{2.13}$$

Introducing to Eq. (2.11)

$$\varphi_{1(a,t)} = \Phi_{1(a)} \cdot e^{i\omega t}, \tag{2.14}$$

one obtains the propagation of the first harmonic wave:

$$\phi_1'' + \frac{\operatorname{tgh}\left(\frac{a}{x_0} + \varepsilon\right)}{x_0}\phi_1' + \left[1 - \frac{\operatorname{tgh}^2\left(\frac{a}{x_0} + \varepsilon\right)}{x_0} + k^2\right]\phi_1 = 0. \tag{2.15}$$

Substituting

$$\phi_{1(z)} = (\cosh z)^{-\frac{1}{2}} \cdot \eta_{(z)}, \tag{2.16}$$

where

$$z = \frac{a}{x_0} + \varepsilon, \tag{2.17}$$

the wave equation (2.15) can be transformed to the form

$$\eta'' + [\mu^2 - V_{(z)}]\eta = 0, \tag{2.18}$$

where

$$\mu = kx_0, \tag{2.19}$$

$$V_{(z)} = \frac{3}{4}\operatorname{tgh}^2 z - \frac{1}{2}, \tag{2.20}$$

and this time the commas denote differentiation with respect to the variable z.

The propagation equation of the first harmonic wave written in the form (2.18) is known in the linear theory of acoustic horns [11] and, therefore, it will not be considered here in details. It is known that, for the frequency higher than cut-off frequency of the horn, the solution of this equation can be presented in the form [15]

$$\eta = B_1 \cdot e^{i\bar{K}z} + B_2 \cdot e^{-i\bar{K}z}, \tag{2.21}$$

where

$$\bar{K} = \left\{ \frac{1}{z_1 - \varepsilon} \int_{\varepsilon}^{z_1} [\mu^2 - V_{(z)}] dz \right\}^{\frac{1}{2}} \tag{2.22}$$

$z_l = (l/x_0) + \varepsilon$, where l is the length of the horn. From that, on the basis Eqs. (2.19) and (2.20) one can obtain

$$\bar{K} = \left\{ k^2 x_0^2 - \frac{1}{4} + \frac{3x_0}{4l} \left[\operatorname{tgh} \varepsilon - \operatorname{tgh} \left(\frac{1}{x_0} + \varepsilon \right) \right] \right\}^{\frac{1}{2}}. \tag{2.23}$$

Subsequently, taking into account Eqs. (2.14), (2.16), (2.17) and considering only the real part of the solution, the following equation can be obtained for the wave running from the inlet to the outlet:

$$\varphi_{1(a,t)} = \frac{C_1}{\sqrt{\cosh(\frac{a}{x_0} + \varepsilon)}} \cos \left[\omega t - \bar{K} \left(\frac{a}{x_0} + \varepsilon \right) \right] - \frac{C_2}{\sqrt{\cosh(\frac{a}{x_0} + \varepsilon)}} \sin \left[\omega t - \bar{K} \left(\frac{a}{x_0} + \varepsilon \right) \right]. \tag{2.24}$$

The constants C_1 and C_2 can be calculated from the boundary condition (2.10)

$$C_1 = \sqrt{\cosh \varepsilon} \cdot \cos(\bar{K}\varepsilon), \tag{2.25}$$

$$C_2 = \sqrt{\cosh \varepsilon} \cdot \sin(\bar{K}\varepsilon) \tag{2.26}$$

and that allows us to write Eq. (2.24) in a more compact form:

$$\varphi_{1(a,t)} = \sqrt{\frac{\cosh \varepsilon}{\cosh(\frac{a}{x_0} + \varepsilon)}} \cdot \cos \left(\omega t - \bar{K} \frac{a}{x_0} \right). \tag{2.27}$$

The function $\varphi_{2(a,t)}$ that occurs in the second term of the solution (2.9) can be found from Eq. (2.12). This equation has a structure similar to Eq. (2.11) except that on the right-hand side the term $\Psi_{(a,t)}$ determined by the solution found in the first approximation see Eq. (2.13) appears. Applying Eqs. (2.24)–(2.26), this term can be presented in the form

$$\psi = \sigma_{(a)} \cdot \cos 2 \left(\omega t - \bar{K} \frac{a}{x_0} \right) + \delta_{(a)} \cdot \sin 2 \left(\omega t - \bar{K} \frac{a}{x_0} \right) + \Omega_{(a)}, \tag{2.28}$$

where

$$\sigma_{(a)} = \frac{-15 \operatorname{tgh}^3(\frac{a}{x_0} + \varepsilon) + [(2 - \gamma)4k^2 x_0^2 + 12\bar{K}^2 + 14] \operatorname{tgh}(\frac{a}{x_0} + \varepsilon)}{16kx_0^3 \cosh(\frac{a}{x_0} + \varepsilon)} \cosh \varepsilon, \tag{2.29}$$

$$\delta_{(a)} = \frac{18 \operatorname{tgh}^2(\frac{a}{x_0} + \varepsilon) - 8\bar{K}^2 - 8k^2 x_0^2 \gamma - 12}{16kx_0^3 \cosh(\frac{a}{x_0} + \varepsilon)} \bar{K} \cosh \varepsilon, \tag{2.30}$$

$$\Omega_{(a)} = \frac{-15\,\mathrm{tgh}^3(\frac{a}{x_0}+\varepsilon) + [(2-\gamma)4k^2x_0^2 - 4\overline{K}^2 + 14]\,\mathrm{tgh}(\frac{a}{x_0}+\varepsilon)}{16kx_0^3\cosh(\frac{a}{x_0}+\varepsilon)}\cosh\varepsilon. \quad (2.31)$$

The fact that the term Ψ is determined by the function $\varphi_{1(a,t)}$ reflects the fact that the second harmonic wave is generated as the result of a disturbance of a medium in the waveguide caused by waves with the fundamental frequency.

The function $\varphi_{2(a,t)}$, as an integral of Eq. (2.12), is a sum of two components [4]; the first one is the general solution of a homogeneous equation coupled with Eq. (2.12). This solution has a form similar to Eq. (2.24)

$$\varphi_{21} = \frac{C_3}{\sqrt{\cosh(\frac{a}{x_0}+\varepsilon)}}\cos[2\omega t - \overline{K}_1(\frac{a}{x_0}+\varepsilon)] + \\ - \frac{C_4}{\sqrt{\cosh(\frac{a}{x_0}+\varepsilon)}}\sin[2\omega t - \overline{K}_1(\frac{a}{x_0}+\varepsilon)], \quad (2.32)$$

where

$$\overline{K}_1 = \left\{4k^2x_0^2 - \frac{1}{4} + \frac{3x_0}{4l}\left[\mathrm{tgh}\,\varepsilon - \mathrm{tgh}\left(\frac{1}{x_0}+\varepsilon\right)\right]\right\}^{\frac{1}{2}}. \quad (2.33)$$

The second component is the singular of Eq. (2.12) and has the form which results from that of the free term of i.e.

$$\varphi_{22} = g_{(a)}\cos 2\omega t + f_{(a)}\cdot\sin 2\omega t + u_{(a)}. \quad (2.34)$$

Introducing φ_{22} in to Eq. (2.12), it is possible to find $g(a)$, $f(a)$ and $u(a)$, subsequently, for instance by the method of constant variations [4]. Finally, knowing $\varphi_{1(a,t)}$ and $\varphi_{2(a,t)}$, one can determine the particle displacement ξ in the waveguide in the second approximation on the basic of Eq. (2.9).

Determination of the particle velocity and acoustic pressure for the wave with finite amplitude will be the next step. So, the particle velocity of the medium in Lagrangian coordinates is obtained after differentiating Eq. (2.9) with respect to time

$$v_{(a,t)} = k^{-1}[A\cdot\dot{\varphi}_{1(a,t)} + A^2\cdot\dot{\varphi}_{2(a,t)} + \ldots]. \quad (2.35)$$

Using the relation between the Lagrangian and Eulerian coordinates [17], the vibration velocity at the point x can be determined

$$v_{(x,t)} = v_{(a,t)} - \frac{\partial v}{\partial a}\cdot\xi_{(a,t)} + \ldots \quad (2.36)$$

The acoustic pressure is a surplus of the pressure P in a vinicity of the particle a, over the so-called static pressure P_0 which occurs in the absence of a wave disturbance:

$$p = P_{(a+\xi)} - P_0. \quad (2.37)$$

To find a relation between the acoustic pressure p and the particle displacement ξ it is possible to use the equation of continuity:

$$S_{(a)}\cdot\varrho_0 = S_{(a+\xi)}\cdot(1+\xi')\cdot\varrho_{(a+\xi)}, \quad (2.38)$$

and the thermodynamic equation:

$$P_{(a+\xi)} = P_0\left[\frac{\varrho_{(a+\xi)}}{\varrho_0}\right]^{\gamma}, \tag{2.39}$$

where ρ denotes the medium density and, in particular, $\rho_{(a)} = \rho_0$ is the static density.

From Eq. (2.38) and (2.39) one obtains

$$P_{(a+\xi)} = P_0[\zeta(1+\xi')]^{-\gamma}. \tag{2.40}$$

From that, after using Eq. (2.37),

$$p = P_0\{[\zeta(1+\xi')]^{-\gamma} - 1\}, \tag{2.41}$$

A transformation into Eulerian coordinates is analogical to that in Eq. (2.36).

Now it is possible to analyze the first and second harmonic waves in a selected waveguide with the determined profile of walls.

3. The exponential waveguide with ring-shaped cross-section

Amond the considered wave guides with the ring-shaped cross-section those with exponential expansion of walls have been used most frequently. In this case $\varepsilon \to \infty$ $(T = 1)$, thus Eq. (2.4) take the form

$$S = S_0 \cdot e^{\frac{x}{x_0}}, \tag{2.42}$$

where e is the base of natural logarithms.

The function $\varphi_{1(a,t)}$, after taking into account $\varepsilon \to \infty$ in Eq. (2.27) assumes the form

$$\varphi_{1(a,t)} = e^{-\frac{a}{2x_0}} \cdot \cos\left(\omega t - \overline{K}\frac{a}{x_0}\right), \tag{2.43}$$

while $\overline{K}$ given by Eq. (2.23) is simplified to the form:

$$\overline{K} = \sqrt{\mu^2 - \frac{1}{4}}. \tag{2.44}$$

Equation (2.12) for the function $\varphi_{2(a,t)}$ is also simplified,

$$\varphi_2'' + \frac{1}{x_0}\varphi_2' - \frac{1}{c^2}\ddot{\varphi}_2 = \psi_{(a,t)} \tag{2.45}$$

where Eq. (2.28) for Ψ the limits of Eq. (2.29)–(2.31) for $\varepsilon \to \infty$ being accounted for, can be expressed as

$$\psi = e^{-\frac{a}{x_0}}\left\{\frac{(5-\gamma)\mu^2 - 1}{4kx_0^3}\cos 2\left(\omega t - \overline{K}\frac{a}{x_0}\right) + \right.$$
$$\left. + \sqrt{\mu^2 - \frac{1}{4}} \cdot \frac{1-(\gamma+1)\mu^2}{2kx_0^3}\sin 2\left(\omega t - \overline{K}\frac{a}{x_0}\right) + \frac{(1-\gamma)k}{4x_0}\right\}. \tag{2.46}$$

General solution of the homogeneous equation coupled with Eq. (2.45) for the pulsation 2ω has form

$$\varphi_{21} = e^{-\frac{a}{2x_0}}\left[C_3\cos\left(2\omega t - \overline{K}\frac{a}{x_0}\right) - C_4\sin\left(2\omega t - \overline{K}\frac{a}{x_0}\right)\right], \tag{2.47}$$

where (see Eq. (2.33))

$$\overline{K}_1 = \sqrt{4\mu^2 - \frac{1}{4}}. \tag{2.48}$$

The singular solution of Eq. (2.45) results from the formula for the agree term in Eq. (2.46)

$$\varphi_{22} = e^{-\frac{a}{x_0}}\left[Qa + L\cos 2\left(\omega t - \overline{K}\frac{a}{x_0}\right) + N\sin 2\left(\omega t - \overline{K}\frac{a}{x_0}\right)\right]. \tag{2.49}$$

The coefficient Q, L, N can be found by introducing φ_{22} into Eq. (2.45)

$$Q = \frac{\gamma - 1}{4}k, \tag{2.50}$$

$$L = \frac{\gamma + 1}{4}\mu - \frac{\gamma}{8\mu}, \tag{2.51}$$

$$N = \frac{2 - \gamma}{4\mu}\overline{K}. \tag{2.52}$$

Next, from the boundary condition (2.10), the constants C_3 and C_4 can be found. Thus, for $a = 0$ one gets.

$$\varphi_{2(0,t)} = \varphi_{12(0,t)} + \varphi_{22(0,t)} = 0. \tag{2.53}$$

This condition is fulfilled when

$$C_3 = -L, \quad C_4 = N. \tag{2.54}$$

Finally, Eq. (2.9) of the acoustic particle displacement takes the following form written in the second approximation:

$$\begin{aligned}\xi = k^{-1}\Bigg\{ & A \cdot e^{-\frac{a}{2x_0}} \cdot \cos\left(\omega t - \overline{K}\frac{a}{x_0}\right) + \\ & + A^2 \cdot e^{-\frac{a}{2x_0}}\left[- L\cos\left(2\omega t - \overline{K}_1\frac{a}{x_0}\right) - N\sin\left(2\omega t - \overline{K}_1\frac{a}{x_0}\right)\right] + \\ & + A^2 \cdot e^{-\frac{a}{x_0}}\left[Qa + L\cos 2\left(\omega t - \overline{K}\frac{a}{x_0}\right) + N\sin 2\left(\omega t - \overline{K}\frac{a}{x_0}\right)\right]\Bigg\}\end{aligned} \tag{2.55}$$

It can be noticed that in above equation the nonperiodic component equal to $k^{-1}A^2 \exp -a/x_0\, Qa$ occurs besides the periodic components, which corresponds to the first and second harmonic waves.

By differentiating Eq. (2.55) with respect to time, the expression for the vibration velocity of the particles in the Lagrangian coordinates can be obtained

$$\begin{aligned}v = & - Ace^{-\frac{a}{2x_0}} \cdot \sin\left(\omega t - \overline{K}\frac{a}{x_0}\right) + \\ & + 2cA^2\Bigg\{e^{-\frac{a}{2x_0}}\left[L\sin\left(2\omega t - \overline{K}_1\frac{a}{x_0}\right) + N\sin\left(2\omega t - \overline{K}_1\frac{a}{x_0}\right)\right] + \\ & + e^{-\frac{a}{x_0}}\left[- L\sin 2\left(\omega t - \overline{K}\frac{a}{x_0}\right) + N\cos 2\left(\omega t - \overline{K}\frac{a}{x_0}\right)\right]\Bigg\}.\end{aligned} \tag{2.56}$$

It is noticeable that in the second approximation, the term with frequency ω (first harmonic)

$$v_1 = -Ace^{-\frac{a}{2x_0}} \sin\left(\omega t - \overline{K}\frac{a}{x_0}\right) \tag{2.57}$$

is supplemented with the component of frequency 2ω (second harmonic). After transformations this component can be presented in the form

$$v_2 = 2cA^2 \cdot e^{-\frac{a}{2x_0}} D \cdot \sin(2\omega t + \alpha), \tag{2.58}$$

where

$$D = \sqrt{(L^2 + N^2)[1 + e^{-\frac{a}{x_0}} - 2e^{-\frac{a}{2x_0}} \cos(\overline{K}_1 - 2\overline{K})\frac{a}{x_0}}, \tag{2.59}$$

$$\operatorname{tg}\alpha = \frac{e^{-\frac{a}{2x_0}}(L\sin 2\overline{K}\frac{a}{x_0} + N\cos 2\overline{K}\frac{a}{x_0}) - (L\sin \overline{K}_1\frac{a}{x_0} + N\cos \overline{K}_1\frac{a}{x_0})}{L\cos \overline{K}_1\frac{a}{x_0} - N\sin \overline{K}_1\frac{a}{x_0} - e^{-\frac{a}{2x_0}}(L\cos 2\overline{K}\frac{a}{x_0} - N\sin 2\overline{K}\frac{a}{x_0})}. \tag{2.60}$$

The ratio of the velocity amplitudes of both harmonics is equal to

$$\frac{\hat{v}_2}{\hat{v}_1} = 2AD. \tag{2.61}$$

This acoustic pressure in the waveguide can be found from Eq. (2.41) and, on the basis of Eq. (2.2) and (2.42), for an exponential horn

$$\zeta = e^{\frac{\xi}{x_0}}. \tag{2.62}$$

From that it follows that

$$p = P_0[(1 + \xi')^{-\gamma} \cdot e^{\frac{-\gamma\xi}{x_0}} - 1]. \tag{2.63}$$

In the second approximation, when Eq. (2.9) is taken into account, the following relationship can be obtained:

$$p = P_0\left[\frac{-\gamma A}{kx_0}\varphi_1 - \frac{-\gamma A^2}{kx_0}\varphi_2 + \frac{\gamma^2}{2k^2x_0^2}A^2\varphi_1^2 - \frac{\gamma A}{k}\varphi_1' - \frac{\gamma A^2}{k}\varphi_2' + \right.$$
$$\left. + \frac{\gamma^2 A^2}{k^2 x_0}\varphi_1\varphi_1' + \frac{\gamma(\gamma+1)}{2k^2}A^2\varphi_1'^2\right]. \tag{2.64}$$

From that, finally, on the basis of Eqs. (2.43) and (2.45), one can get:

$$\frac{p}{P_0} = -\gamma Ae^{-\frac{a}{2x_0}} \sin\left(\omega t - \overline{K}\frac{a}{x_0} + \beta\right) + \frac{\gamma A^2}{2}e^{-\frac{a}{x_0}} + \gamma A^2 e^{-\frac{a}{2x_0}} G\sin(2\omega t + \Delta), \tag{2.65}$$

where

$$\operatorname{tg}\beta = \frac{1}{2\overline{K}}, \tag{2.66}$$

$$G = \left\{R^2 + W^2 + e^{-\frac{a}{x_0}}(X^2 + Z^2) + 2e^{-\frac{a}{2x_0}}\left[(RZ + WX)\cos(\overline{K}_1 - 2\overline{K})\frac{a}{x_0} + \right.\right.$$
$$\left.\left. + (RX - WZ)\sin(\overline{K}_1 - 2\overline{K})\frac{a}{x_0}\right]\right\}^{\frac{1}{2}}, \tag{2.67}$$

$$\operatorname{tg}\Delta = \frac{R\cos\overline{K}_1\frac{a}{x_0} - W\sin\overline{K}_1\frac{a}{x_0} + e^{-\frac{a}{x_0}}\left(Z\cos 2\overline{K}\frac{a}{x_0} - X\sin 2\overline{K}\frac{a}{x_0}\right)}{W\cos\overline{K}_1\frac{a}{x_0} + R\sin\overline{K}_1\frac{a}{x_0} + e^{-\frac{a}{2x_0}}\left(X\cos 2\overline{K}\frac{a}{x_0} + Z\sin 2\overline{K}\frac{a}{x_0}\right)} \tag{2.68}$$

and

$$R = \frac{4(\gamma-2)\overline{K}\,\overline{K}_1 - \gamma}{16\mu^2} + \frac{\gamma+1}{8}, \tag{2.69}$$

$$W = \left(\frac{\gamma+1}{4} - \frac{\gamma}{8\mu^2}\right)\overline{K}_1 + \frac{2-\gamma}{8\mu^2}\overline{K}, \tag{2.70}$$

$$X = \left(\frac{2\gamma-1}{4\mu^2} - \frac{\gamma+1}{2}\right)\overline{K}, \tag{2.71}$$

$$Z = \frac{2\gamma-1}{8\mu^2} - \frac{3}{4}(1-\gamma). \tag{2.72}$$

From Eq. (2.65) it results that the ratio of the pressure amplitudes of the second harmonic to the first one is given by

$$\frac{\widehat{p}_2}{\widehat{p}_1} = AG. \tag{2.73}$$

Furthermore, in Eq. (2.65) for the acoustic pressure, the component independent of time occurs

$$\overline{p} = \frac{1}{2}\gamma A^2 P_0 \cdot e^{-\frac{a}{x_0}}. \tag{2.74}$$

In the nonlinear theory of a plane wave in a lossless infinite medium, the component independent of time also occurs in the equation of the pressure, but in that case it is also independent of the position in the sounds wave. That is the so-called radiation stress [5]. It is seen that in the case of the waveguide considered this component decreases exponentially, like $\exp(-a/x_0)$, while the amplitude of the first harmonic decreases slower, like $\exp(-a/2x_0)$.

At the end, the exponential waveguide with typical dimensions for a construction of axial flow generators is taken into account in the numerical example:

- width of the channel at the inlet $h_0 = 1.5 \cdot 10^{-3}$ m,
- mean diameter of the annular channel $d_0 = 10^{-1}$ m,
- width of the channel at the outlet $h_l = 10^{-1}$ m,
- length of the waveguide $l = 1.5 \cdot 10^{-1}$ m.

The waveguide with these dimensions has the cut-off frequency $f_{\mathrm{gr}} = 760$ Hz.

On the basis of Eq. (2.57)–(2.59), the relations between the amplitude of the vibration velocities for the first ($n = 1$) and second ($n = 2$) harmonic and the particle displacement of the medium, in the waveguide, when the frequency of a piston that initiates the harmonic wave at the inlet is equal to $f = 3$ kHz, are presented in Fig. 2. The amplitudes of the vibration velocities are related to that of the piston $v_{10} = Ac$. Appearance of the second harmonic for $a > 0$ (it would be higher harmonics in subsequent approximations) is caused by nonlinear properties of the medium in the waveguide and explains the de-

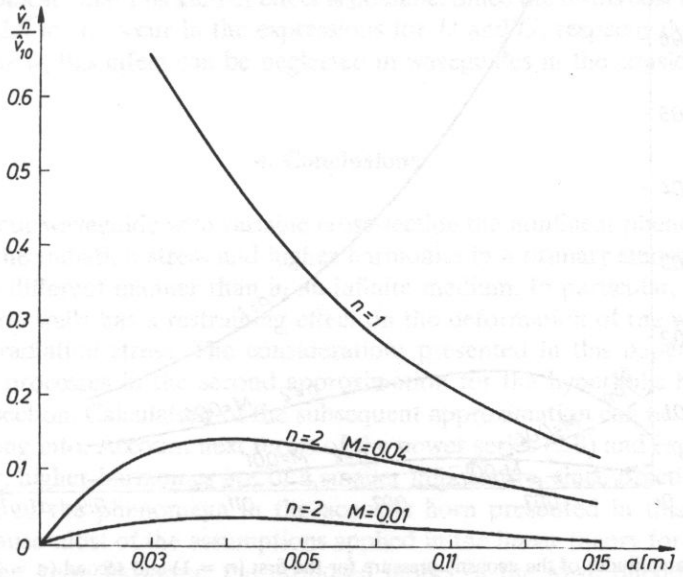

FIG. 2. The amplitudes of the particle velocities of the medium in the waveguide for the first ($n = 1$) and second ($n = 2$) harmonics. The generation frequency of the sinusoidal wave at the inlet is $f = 3$ kHz.

formation of the wave front when the wave moves along the horn. It can be seen that the second harmonic increases in the part near the inlet, and subsequently decreased as the walls of the waveguide expand. It means that deformation of the wave-front develops in the inlet part, and then it stops. So the course of the nonlinear phenomena is different than that in the case of propagation of a plane wave in a lossless infinite medium, or in a cylindrical tube when the wave deformation constantly increases and the amplitude of the second harmonic is proportional to the distance from a source [5].

It can be seen from the Fig. 3 that the plot of the acoustic pressure amplitudes for both harmonics (solid lines) is similar to that of the velocity amplitudes, as shown in Fig. 2. Furthermore, in Fig. 3, dashed line marks the course of the time-independent component $\overline{p}$ of the acoustic pressure. It appears that this component decreases significantly faster that the amplitude of the second harmonic pressure. it should be mentioned that the amplitude of both harmonics and the value of the component $\overline{p}$ are related here to pressure amplitude of the first harmonic at the inlet: $\hat{p}_{10} = \gamma A P_0$.

It is shown in Fig. 4 that, for a given layer of medium particles in the waveguide, the vibration velocity amplitude of the second harmonic increases compared with that of the first one when the frequency increases. This increase is faster when the amplitude of the piston which initiates the wave is greater. A similar conclusion can be formulated with respect to the harmonic components of the pressure; plot of $\hat{p}_2/\hat{p}_1$ as a function of the frequency has a similar course, as that of the vibration velocity, and therefore it is not presented here.

The medium in the acoustic horn is dispersive [11] and that can cause a characteristic pulsation of amplitudes of the higher harmonics [9]. Equation (2.58), (2.59) and

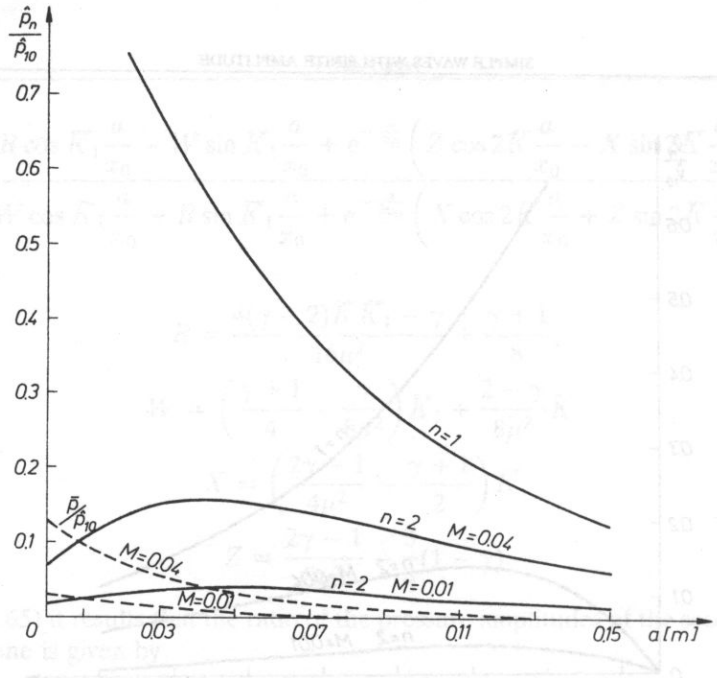

FIG. 3. The amplitudes of the acoustic pressure for the first ($n = 1$) and second ($n = 2$) harmonics (solid lines); the nonperiodic component of the acoustic pressure (dashed lines).

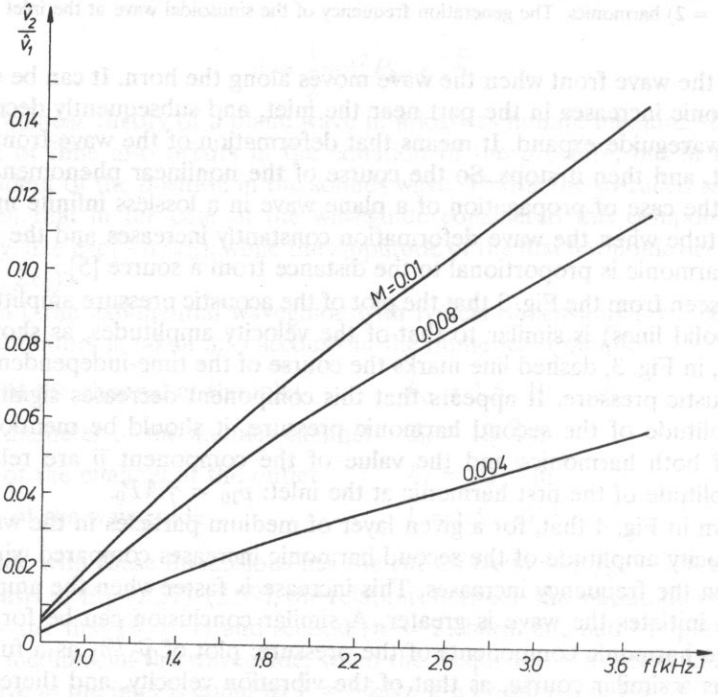

FIG. 4. The ratio of the vibration velocity amplitudes of the second harmonic to the first one for the layer of medium particles $a = 1.5 \cdot 10^{-1}$ m.

(2.65)–(2.67) indicate that this kind of effect is possible. Since the terms $\cos(\overline{K}_1 - 2\overline{K})a/x_0$ and $\sin(\overline{K}_1 - 2\overline{K})a/x_0$ occur in the expressions for D and G, respectively. However, as the Figs. 2–4 show, this effect can be neglected in waveguides in the considered range of frequencies.

4. Conclusions

In the acoustic waveguide with variable cross-section the nonlinear phenomena such as generation of the radiation stress and higher harmonics in a primary sinusoidal wave can take place in a different manner than in an infinite medium. In particular, the expansion of the waveguide walls has a restraining effect on the deformation of the wave-front and decreases the radiation stress. The considerations presented in this paper enable us to describe these processes in the second approximation for the hyperbolic horns with the annular cross-section. Calculation of the subsequent approximation can be done in a similar way by taking into. Account next terms of the power series (2.9) and expansions (2.6), (2.7). However, higher harmonics are of a smaller importance, since practically $|A| \ll 1$.

The course of the phenomena in the acoustic horn presented in this paper is still simplified, because most of the assumptions applied in the linear theory for infinitely long horns have been kept. However, the proposed model of the wave phenomena is more advanced than the linear one.

References

[1] D.T. Blackstock, *Propagation of plane sound waves of finite amplitude in nondissipative fluids*, JASA, 34, 1, 9–30 (1962).

[2] С.А. Цевилин, В.М. Цетлин, *Сирена для акустической коахулации аерозолей*, Акустич. Ж., **7**, 1, 78–86 (1961).

[3] R. Courant , K.O. Fredrischs, *Supersonic flow and shock waves*, Interscience Publishers, Inc. New York 1948.

[4] Е. Камке, *Справочник по обыкновенным дыфференцяльным уравненям, перевод с немецкого*, Изд. Инностр. Лит. Москва 1951.

[5] M. Kwiek, *Laboratory acoustics*, vol. 1, PWN, Poznań-Warszawa 1968.

[6] Е.Д. Медников, *Две конструкции экспериментальных звуковых сирен*, Акустич. Ж., **4** 1, 5–63 (1958).

[7] A. Puch, *Generalized model of axial dynamic generator*, Achives of Acoustics, **13**, 1, 17–34 (1978).

[8] Y. Rocard, *General dynamics of vibrations*, Unger, New York 1960 s. 467–479.

[9] О.Б. Руденко, С. Салуян, *Теоретические основы нелинейной акустики*, Изд. Наука, Москва 1975.

[10] R. Wyrzykowski, *Acoustic evaluation of a siren* (in Polish), Materiały I Konferencji Ultradźwiękowej PAN, PWN, Warszawa 1965.

[11] R. Wyrzykowski, *Linear theory of acoustic fields in gaseous media*, (in Polish), RTPN WSP Rzeszów 1972.

[12] R. Wyrzykowski and R. Hnatków, *Sirene mit hoher akustischer Leistung*, Acustica, 59, 225–229 (1986).

[13] K.W. Yeow, *Webster wave equation in two dimensions*, JASA, 56, 1, 19–21 (1974).

[14] T. Zamorski and R. Wyrzykowski, *Hyperbolic horns of annular cross-section*, (in Polish) Prace XXV OSA, 367–370, Poznań-Błażejewko 1978.

[15] T. Zamorski and R. Wyrzykowski, *Approximate methods for the solution of the equation of acoustic wave propagation in horns*, Achieves of Acoustics, **6**, 3, 237–285 (1981).

[16] T. Zamorski, *Waves with finite amplitude in Bessel horns*, Achives of Acoustics, **15**, 3–4, 531—542 (1990).

[17] Л.К. Заремво анд В.А. Красильников, *Введение в нелинейную акустику*, Изд. Наука, Москва 1966.

Notes for authors

ARCHIVES of ACOUSTICS is a quarterly journal in which original papers, both theoretical and experimental, concerning problems in acoustics and its application are published.

Each paper submitted to the Editorial Office is reviewed and the decision to accept is for publication is taken by the Editorial Board. The period from submission of the paper to its publication is usually not shorter than 6 months but can be minimized if intending authors will prepare their typescripts according to the following notes:

1. The papers should be typed on one side of size A4 paper, with double spacing, a margin of 4 cm at the left side and with serial numbering of the pages. Two copies should be submitted.

2. The author's first name and surname, the name of his place of work and its location should be typed under the title of the paper.

3. The paper should be divided into numbered sections, which should be given appropriate brief subheadings.

4. Enclosed with the paper, on a separate page of typescript, there should be a summary of up to 20 lines. It should contain information about the paper's purpose, the research methods applied and about the basic results. It is a good practise not to cite any references in the summary.

5. At the end to the paper it is necessary to state on a separate sheet the cited references, numbered and in alphabetical order, according to the following sequence:

(a) Papers appearing in journals and regular publications: author's initials and surname, full title of the paper, title of the publication or its abbreviation, volume number (underlined), number of publication, first and last pages of the paper, and year of publication in brackets.

For example: [7] A.S. Śliwiński, A.E. Brown, Ultrasonic light diffraction patterns in ethylene in the critical region, Acoustica, **16**, 5, 312–323 (1965/66).

(b) Books: author's initials and surname, chapter title (in collective works), book title, editor, publisher, place of publications, year of publication, pages.

For instance: [5] W.P. Mason, Piezoelectric crystals and their application to ultrasonics, Van Nostrand, New York 1960, p. 30.

In the text of the paper's reference should be cited by enclosing the appropriate number in square brackets.

6. Formulae and designation should be inscribed manually, very legibly, using only Latin and Greek letters. Indices should be written down distinctly and with particular care. All symbols occuring in the formulae should be explained in the text at the place where they appear for the first time. The formulae should be numbered at the right-hand side of the typescript page by numbers in round brackets. Formulae which can be easily found in the literature not be derived — it is sufficient to cite appropriate reference.

7. The International System of Units (SI) should be used throughout.

8. All drawings, diagrams and photos should be referred to in the text as figures (Fig.). They should be made on separate sheets (not smaller than A5) and at the very bottom (in the case of photos overleaf) the number on separate sheets (not smaller than A5) and at the very bottom (in the case of photos overleaf) the number of the figure, the author's name and the title of paper should be written. The figure number should be inscribed in the margin of the typescript at the place where the drawing should be included. The captions of the illustrations should be listed on separate sheets. Final execution of figures in undertaken by the Editorial Office.

9. Photos should be printed on high contrast gloss paper.

10. All tables, as figures, should be made on separate sheets and numbered in succession with Arabic numbers. At the top of each table an explanatory title should be given. A list of table captions should be enclosed on a separate sheet.

Authors are entitled to 25 free reprints. Additional copies can be ordered at their own expense.

The author of a paper accepted for publication will receive one proof should be corrected and returned within five days to the Editorial Office.

The papers submitted for publication in the journal should be written in English. No royalities are paid to the authors.